ISSN 2686-7575 (Online)

ТОНКИЕ ХИМИЧЕСКИЕ ТЕХНОЛОГИИ

Fine Chemical Technologies

- Theoretical Bases of Chemical Technology
- Chemistry and Technology of Organic Substances
- Chemistry and Technology of Medicinal Compounds and Biologically Active Substances
- Biochemistry and Biotechnology
- Synthesis and Processing of Polymers and Polymeric Composites
- Chemistry and Technology of Inorganic Materials
- Analytical Methods in Chemistry and Chemical Technology
- Mathematical Methods and Information Systems in Chemical Technology

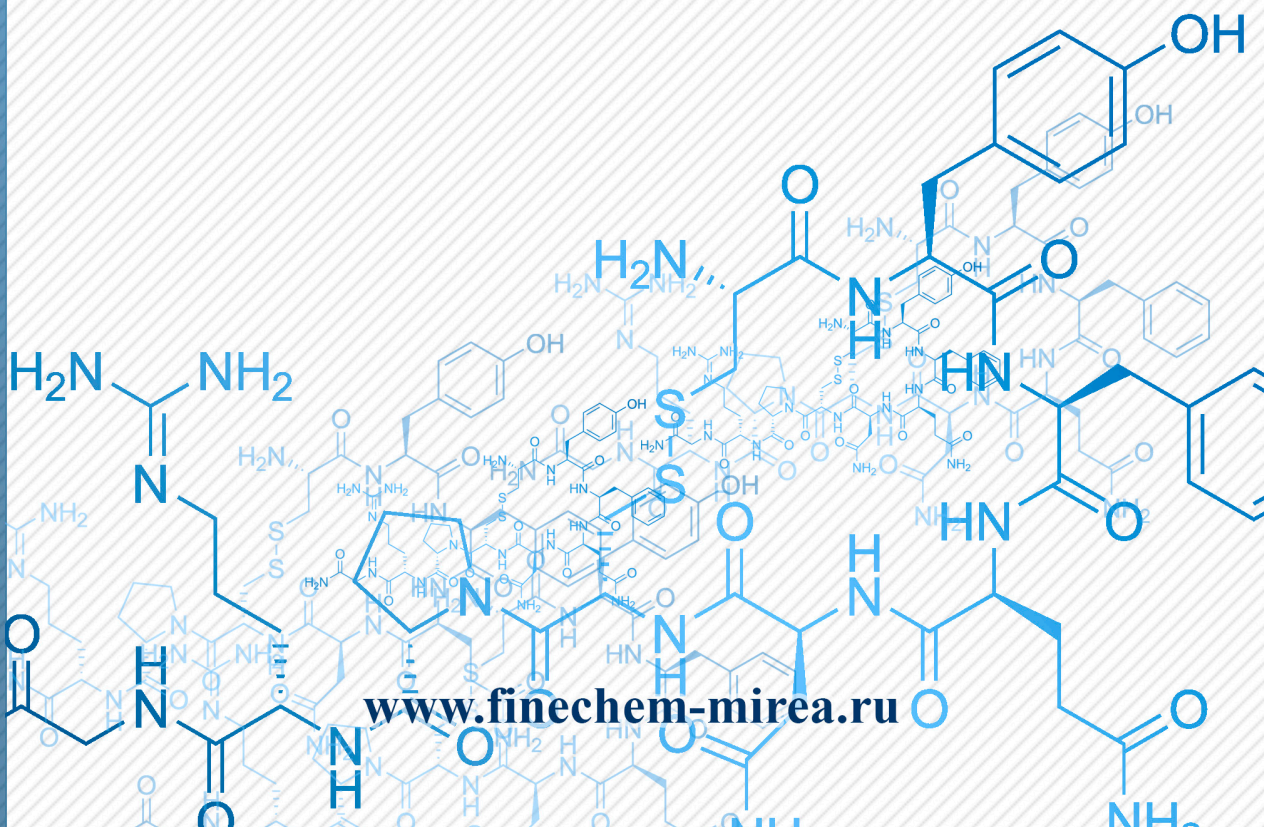

17(5)
2022

www.finechem-mirea.ru

ISSN 2686-7575 (Online)

ТОНКИЕ ХИМИЧЕСКИЕ ТЕХНОЛОГИИ

Fine Chemical Technologies

- Theoretical Bases of Chemical Technology
- Chemistry and Technology of Organic Substances
- Chemistry and Technology of Medicinal Compounds and Biologically Active Substances
- Biochemistry and Biotechnology
- Synthesis and Processing of Polymers and Polymeric Composites
- Chemistry and Technology of Inorganic Materials
- Analytical Methods in Chemistry and Chemical Technology
- Mathematical Methods and Information Systems in Chemical Technology

Tonkie Khimicheskie Tekhnologii = Fine Chemical Technologies
Vol. 17, No. 5, 2022

Тонкие химические технологии = Fine Chemical Technologies
Том 17, № 5, 2022

https://doi.org/10.32362/2410-6593-2022-17-5
www.finechem-mirea.ru

https://doi.org/10.32362/2410-6593 **ISSN 2686-7575 (Online)**

Tonkie Khimicheskie Tekhnologii = Fine Chemical Technologies 2022, vol. 17, no. 5

The peer-reviewed scientific and technical journal Fine Chemical Technologies highlights the modern achievements of fundamental and applied research in the field of fine chemical technologies, including theoretical bases of chemical technology, chemistry and technology of medicinal compounds and biologically active substances, organic substances and inorganic materials, biochemistry and biotechnology, synthesis and processing of polymers and polymeric composites, analytical and mathematical methods and information systems in chemistry and chemical technology.

Founder and Publisher

Federal State Budget
Educational Institution of Higher Education
"MIREA – Russian Technological University"
78, Vernadskogo pr., Moscow, 119454, Russian Federation.
Publication frequency: bimonthly.
The journal was founded in 2006. The name was Vestnik MITHT until 2015 (ISSN 1819-1487).

The journal is included into the List of peer-reviewed science press of the State Commission for Academic Degrees and Titles of the Russian Federation.
The journal is indexed:
SCOPUS, DOAJ, Chemical Abstracts, Science Index, RSCI, Ulrich's International Periodicals Directory

86, Vernadskogo pr., Moscow, 119571, Russian Federation.
Phone: +7(495) 246-05-55 (#2-88)
E-mail: *seredina@mirea.ru*

The registration number ПИ № ФС 77–74580 was issued in December 14, 2018 by the Federal Service for Supervision of Communications, Information Technology, and Mass Media of Russia.

The subscription index of *Pressa Rossii*: **36924**

Тонкие химические технологии = Fine Chemical Technologies 2022, том 17, № 5

Научно-технический рецензируемый журнал «Тонкие химические технологии» освещает современные достижения фундаментальных и прикладных исследований в области тонких химических технологий, включая теоретические основы химической технологии, химию и технологию лекарственных препаратов и биологически активных соединений, органических веществ и неорганических материалов, биохимию и биотехнологию, синтез и переработку полимеров и композитов на их основе, аналитические и математические методы и информационные системы в химии и химической технологии.

Учредитель и издатель

федеральное государственное бюджетное
образовательное учреждение высшего образования
«МИРЭА – Российский технологический университет»
119454, РФ, Москва, пр-кт Вернадского, д. 78.
Периодичность: один раз в два месяца.
Журнал основан в 2006 году. До 2015 года издавался под названием «Вестник МИТХТ» (ISSN 1819-1487).

Журнал входит в Перечень ведущих рецензируемых научных журналов ВАК РФ.
Индексируется:
SCOPUS, DOAJ, Chemical Abstracts, РИНЦ (Science Index), RSCI, Ulrich's International Periodicals Directory

119571, Москва, пр. Вернадского, 86, оф. Л-119.
Тел.: +7(495) 246-05-55 (#2-88)
E-mail: *seredina@mirea.ru*

Регистрационный номер и дата принятия решения о регистрации СМИ: ПИ № ФС 77-74580 от 14.12.2018 г. СМИ зарегистрировано Федеральной службой по надзору в сфере связи, информационных технологий и массовых коммуникаций (Роскомнадзор).

Индекс по Объединенному каталогу «Пресса России»: **36924**

Ivan A. Novakov – Academician at the RAS, Dr. Sci. (Chem.), Professor, President of the Volgograd State Technical University, Volgograd, Russian Federation.
Scopus Author ID 7003436556, ResearcherID I-4668-2015, http://orcid.org/0000-0002-0980-6591, *president@vstu.ru.*

Alexander N. Ozerin – Corresponding Member of the RAS, Dr. Sci. (Chem.), Professor, Enikolopov Institute of Synthetic Polymeric Materials of the RAS, Moscow, Russian Federation.
Scopus Author ID 7006188944, ResearcherID J-1866-2018, https://orcid.org/0000-0001-7505-6090, *ozerin@ispm.ru.*

Tapani A. Pakkanen – PhD, Professor, Department of Chemistry, University of Eastern Finland, Joensuu, Finland.
Scopus Author ID 7102310323, *tapani.pakkanen@uef.fi.*

Armando J.L. Pombeiro – Academician at the Academy of Sciences of Lisbon, PhD, Professor, President of the Center for Structural Chemistry of the Higher Technical Institute of the University of Lisbon, Lisbon, Portugal.
Scopus Author ID 7006067269, ResearcherID I-5945-2012, https://orcid.org/0000-0001-8323-888X, *pombeiro@ist.utl.pt.*

Dmitrii V. Pyshnyi – Corresponding Member of the RAS, Dr. Sci. (Chem.), Professor, Institute of Chemical Biologyand Fundamental Medicine, Siberian Branch of the RAS, Novosibirsk, Russian Federation.
Scopus Author ID 7006677629, ResearcherID F-4729-2013, https://orcid.org/0000-0002-2587-3719, *pyshnyi@niboch.nsc.ru.*

Alexander S. Sigov – Academician at the RAS, Dr. Sci. (Phys. and Math.), Professor, President of MIREA – Russian Technological University, Moscow, Russian Federation.
Scopus Author ID 35557510600, ResearcherID L-4103-2017, *sigov@mirea.ru.*

Alexander M. Toikka – Dr. Sci. (Chem.), Professor, Institute of Chemistry, Saint Petersburg State University, St. Petersburg, Russian Federation.
Scopus Author ID 6603464176, ResearcherI D A-5698-2010, http://orcid.org/0000-0002-1863-5528, *a.toikka@spbu.ru.*

Andrzej W. Trochimczuk – Dr. Sci. (Chem.), Professor, Faculty of Chemistry, Wrocław University of Science and Technology, Wrocław, Poland.
Scopus Author ID 7003604847, *andrzej.trochimczuk@pwr.edu.pl.*

Aslan Yu. Tsivadze – Academician at the RAS, Dr. Sci. (Chem.), Professor, A.N. Frumkin Institute of Physical Chemistry and Electrochemistry of the RAS, Moscow, Russian Federation.
Scopus Author ID 7004245066, ResearcherID G-7422-2014, *tsiv@phyche.ac.ru.*

Новаков Иван Александрович – академик РАН, д.х.н., профессор, президент Волгоградского государственного технического университета, Волгоград, Российская Федерация.
Scopus Author ID 7003436556, ResearcherID I-4668-2015, http://orcid.org/0000-0002-0980-6591, *president@vstu.ru.*

Озерин Александр Никифорович – член-корр. РАН, д.х.н., профессор, Институт синтетических полимерных материалов им. Н.С. Ениколопова РАН, Москва, Российская Федерация.
Scopus Author ID 7006188944, ResearcherID J-1866-2018, https://orcid.org/0000-0001-7505-6090, *ozerin@ispm.ru.*

Пакканен Тапани – PhD, профессор, Департамент химии, Университет Восточной Финляндии, Йоенсуу, Финляндия.
Scopus Author ID 7102310323, *tapani.pakkanen@uef.fi.*

Помбейро Армандо – академик Академии наук Лиссабона, PhD, профессор, президент Центра структурной химии Высшего технического института Университета Лиссабона, Португалия.
Scopus Author ID 7006067269, ResearcherID I-5945-2012, https://orcid.org/0000-0001-8323-888X, *pombeiro@ist.utl.pt.*

Пышный Дмитрий Владимирович – член-корр.РАН, д.х.н., профессор, Институт химической биологии и фундаментальной медицины Сибирского отделения РАН, Новосибирск, Российская Федерация.
Scopus Author ID 7006677629, ResearcherID F-4729-2013, https://orcid.org/0000-0002-2587-3719, *pyshnyi@niboch.nsc.ru.*

Сигов Александр Сергеевич – академик РАН, д.ф.-м.н., профессор, президент МИРЭА – Российского технологического университета, Москва, Российская Федерация.
Scopus Author ID 35557510600, ResearcherID L-4103-2017, *sigov@mirea.ru.*

Тойкка Александр Матвеевич – д.х.н., профессор, Институт химии, Санкт-Петербургский государственный университет, Санкт-Петербург, Российская Федерация.
Scopus Author ID 6603464176, Researcher ID A-5698-2010, http://orcid.org/0000-0002-1863-5528, *a.toikka@spbu.ru.*

Трохимчук Анджей – д.х.н., профессор, Химический факультет Вроцлавского политехнического университета, Вроцлав, Польша.
Scopus Author ID 7003604847, *andrzej.trochimczuk@pwr.edu.pl.*

Цивадзе Аслан Юсупович – академик РАН, д.х.н., профессор, Институт физической химии и электрохимии им. А.Н. Фрумкина РАН, Москва, Российская Федерация.
Scopus Author ID 7004245066, ResearcherID G-7422-2014, *tsiv@phyche.ac.ru.*

ТОНКИЕ ХИМИЧЕСКИЕ ТЕХНОЛОГИИ
Fine Chemical Technologies
17(5)
2022

CONTENTS

СОДЕРЖАНИЕ

CHEMISTRY AND TECHNOLOGY OF ORGANIC SUBSTANCES

ХИМИЯ И ТЕХНОЛОГИЯ ОРГАНИЧЕСКИХ ВЕЩЕСТВ

ISSN 2686-7575 (Online)

https://doi.org/10.32362/2410-6593-2022-17-5-377-383

UDC 547.245

RESEARCH ARTICLE

Behavior of morpholine and its trimethylsilyl derivative in reactions with trimethylsilyl isocyanate

Liya O. Belova[1], Nataliya A. Golub[1], Mariya V. Pletneva[1,✉], Nadezhda I. Kirilina[2], Alexey D. Kirilin[1]

[1]MIREA – Russian Technological University (M.V. Lomonosov Institute of Fine Chemical Technologies), Moscow, 119571 Russia

[2]State Research Institute of Chemistry and Technology of Organoelement Compounds, Moscow, 105118 Russia

✉Corresponding author, e-mail: pletneva@mirea.ru

Abstract

Objectives. *To study the patterns of behavior of morpholine and its trimethylsilyl derivative in reactions with trimethylsilyl isocyanate.*

Methods. *The study employed infrared and nuclear magnetic resonance spectroscopy, as well as elemental analysis.*

Results. *The formation of mixtures of tautomeric forms of silicon-containing urea—N-(trimethylsilyl)morpholine-4-carboxamide and trimethylsilylmorpholine-4-carboximidoate—was established.*

Conclusions. *It is shown that the composition and structure of the resulting products are determined both by the presence of a morpholine substituent at the nitrogen atom and by the type of isocyanate used. Unlike the trimethylsilyl derivative of morpholine, morpholine itself reacts with trimethylsilyl isocyanate to form a mixture of tautomeric forms.*

Keywords: *morpholine, trimethylsilyl isocyanate, silicon-containing ureas, tautomerism, amide-isoamide tautomerism, N-(trimethylsilyl)morpholine-4-carboxamide, trimethylsilylmorpholine-4-carboxyimidoate*

For citation: Belova L.O., Golub N.A., Pletneva M.V., Kirilina N.I., Kirilin A.D. Behavior of morpholine and its trimethylsilyl derivative in reactions with trimethylsilyl isocyanate. *Tonk. Khim. Tekhnol. = Fine Chem. Technol.* 2022;17(5):377–383 (Russ., Eng.). https://doi.org/10.32362/2410-6593-2022-17-5-377-383

НАУЧНАЯ СТАТЬЯ

Поведение морфолина и его триметилсилилпроизводного в реакциях с триметилсилилизоцианатом

Л.О. Белова[1], Н.А. Голуб[1], М.В. Плетнева[1,✉], Н.И. Кирилина[2], А.Д. Кирилин[1]

[1]МИРЭА – Российский технологический университет (Институт тонких химических технологий им. М. В. Ломоносова), Москва, 119571 Россия
[2]Государственный научно-исследовательский институт химии и технологии элементоорганических соединений (ГНИИХТЭОС), Москва, 105118 Россия
✉Автор для переписки, e-mail: pletneva@mirea.ru

Аннотация

Цели. *Изучить закономерности поведения морфолина и его триметилсилилпроизводного в реакциях с триметилсилилизоцианатом.*
Методы. *В исследовании использовались методы инфракрасной спектроскопии, спектроскопии ядерного магнитного резонанса и элементного анализа.*
Результаты. *Установлено образование смеси таутомерных форм кремнийсодержащей мочевины: N-(триметилсилил)морфолин-4-карбоксамида и триметилсилилморфолин-4-карбоксимидоата.*
Выводы. *Установлено, что состав и строение образующихся продуктов определяется как наличием заместителя при атоме азота морфолина, так и типом используемого изоцианата. Показано, что, в отличие от триметилсилильного производного морфолина, сам морфолин взаимодействует с триметилсилилизоцианатом с образованием смеси таутомерных форм.*

Ключевые слова: *морфолин, триметилсилилизоцианат, кремнийсодержащие мочевины, таутомерия, амид-изоамидная таутомерия, N-(триметилсилил)морфолин-4-карбоксамид, триметилсилилморфолин-4-карбоксимидоат*

Для цитирования: Белова Л.О., Голуб Н.А., Плетнева М.В., Кирилина Н.И., Кирилин А.Д. Поведение морфолина и его триметилсилилпроизводного в реакциях с триметилсилилизоцианатом. *Тонкие химические технологии*. 2022;17(5):377–383. https://doi.org/10.32362/2410-6593-2022-17-5-377-383

INTRODUCTION

The chemical study of organosilicon derivatives of morpholine began during the second half of the last century. The increase of research interest in this field of chemistry is due to the valuable properties of such compounds both from a practical and a theoretical point of view [1–8]. For example, due to their polarity and high selectivity, organosilicon morpholine derivatives have become widely applied as solvents. They are also used for the synthesis of enamines, which are synthons for the selective alkylation and acylation of carbonyl compounds [8]. It has been shown [7, 9, 10] that 4-(trimethylsilyl)morpholine, like silyl amines, interacts with organic isocyanates: the nature of the initial isocyanate determines the possibility of obtaining organosilicon ureas or organic ureas. Thus, as a result of the reaction

with *n*-butyl isocyanate, a stable urea containing a trimethylsilyl group was obtained [7]. Conversely, silicon-containing ureas were also initially obtained when using α-alkoxyalkyl isocyanates in this reaction; these can be easily hydrolyzed in air to form stable organic ureas [9]. However, all these studies were limited to investigated organic isocyanates or their analogs comprising carbofunctional organosilicon isocyanates [10] (Scheme 1).

It was also found that 4-phenyl-*N*-(trimethylsilyl)-4-morpholinecarboxamide **2** is a compound hydrolyzed by air moisture to form organic urea **2′** over time (Scheme 2).

Despite the availability of hydrolytically stable *N*-[3-(trimethylsilyl)propyl]-*N*-(trimethylsilyl)-4-morpholinecarboxamide **3** [11], the absence of any publications on the possibility of obtaining silicon-containing ureas using the functional silyl isocyanate trimethylsilyl isocyanatosilane has not yet been the topic of a detailed study. Thus, the continuation of research in this area of chemistry is an urgent task.

In addition, it should be noted that when using trimethylsilyl isocyanate in the reaction with 4-(trimethylsilyl)morpholine [10], the nature of the process does not change at the first stage: instead unstable (trimethylsilyl)urea **4** is formed. Subsequently, however, it can be easily induced to give up the trimethylsilyl group to transform into trimethylsilylmorpholine-4-carboximidoate **6** (Scheme 3).

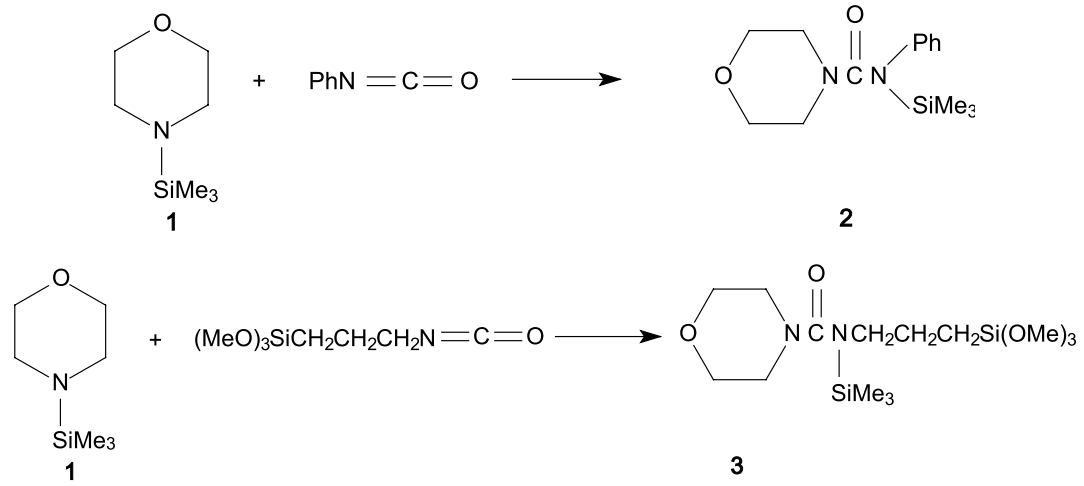

Scheme 1. Reactions of 4-(trimethylsilyl)morpholine with isocyanates.

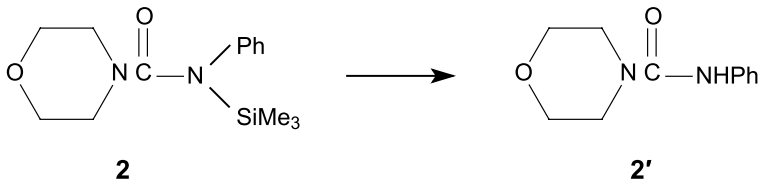

Scheme 2. Scheme of 4-phenyl-*N*-(trimethylsilyl)-4-morpholinecarboxamide **2** conversion to organic urea **2′**.

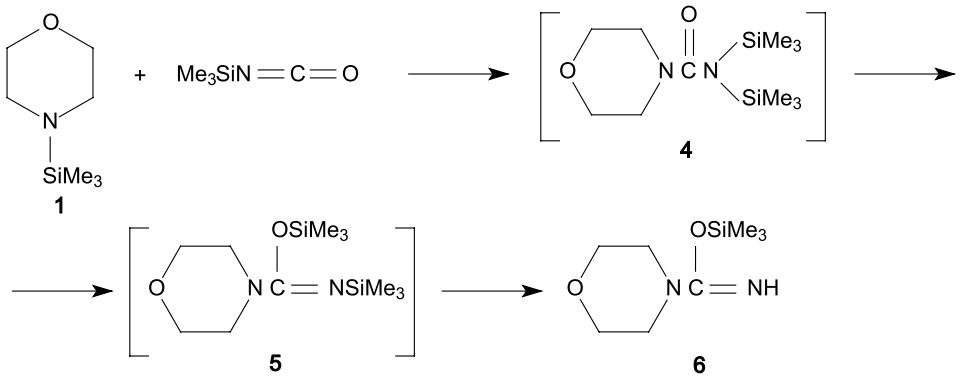

Scheme 3. Reaction of 4-(trimethylsilyl)morpholine with trimethylsilyl isocyanate.

EXPERIMENTAL

The infrared (IR) spectrum was recorded on a Nicolet 7600 spectrometer (*Thermo Fisher Scientific*, USA) in vaseline oil. The ^{1}H nuclear magnetic resonance (NMR) spectrum was recorded on a DRX400 instrument (*Bruker*, Germany) with an operating frequency of 400.13 MHz in $CDCl_3$. Chemical shifts are given in δ (ppm) scale relative to tetramethylsilane as an internal standard. The ^{29}Si NMR spectrum was recorded on an AVANCE AV-300 instrument (*Bruker*, Germany) with an operating frequency for silicon of 59.64 MHz. Elemental analysis was carried out on a FLASH EA 1112 instrument (*Thermo Finnigan Italia S.p.A.*, Italy). The melting point (m.p.) of the obtained compound was determined on a BUCHI Melting PointB-540 elemental analyzer (*BUCHI*, Switzerland).

All starting compounds were thoroughly dried before use and purified by distillation. Synthesis operations, isolation and sampling for the compounds analysis were carried out under an atmosphere of dry nitrogen.

Trimethylsilylmorpholine-4-carboximidoate (6) and *N*-(trimethylsilyl)-morpholine-4-carboxamide (6′)

Trimethylsilyl isocyanate (6.57 g, 0.057 mol) was added to morpholine (**7**) (4.96 g, 0.057 mol). The reaction mass was kept for 25 min, then evacuated at a pressure of 1 mmHg for 1 h to yield 10.37 g (90%) of compounds (**6** and **6′**), m.p. = 92.5–93.5°C. IR spectrum, ṽ, cm^{-1}: 3365 (NH), 1666 (C=O), 1609 (C=N). ^{1}H NMR spectrum, ppm: 0.03 s (9H, $SiMe_3$), 0.21 s (9H, $Si(CH_3)_3$), 2.84 t (4H, CH_2NCH_2), 3.34 q (4H, CH_2NCH_2), 3.65 t (8H, CH_2OCH_2). ^{29}Si NMR spectrum, ppm: 5.96 s, 7.34 s. Elemental analysis, found, %: C 47.65; H 8.85; N 13.91. $C_8H_{18}O_2N_2Si$; calculated, %: C 47.49; H 8.97; N 13.85.

RESULTS AND DISCUSSION

It was found that morpholine **7**, along with its trimethylsilyl derivative **1**, reacts with trimethylsilyl isocyanate without heating. However, the reaction product is a mixture of tautomeric forms of silicon-containing urea: trimethylsilylmorpholine-4-carboximidoate **6** (*O*-form) and *N*-(trimethylsilyl)morpholine-4-carboxamide **6′** (*N*-form) (Scheme 4).

The existence of such isomerism is evidenced by the results of physicochemical studies. In the IR spectrum of compounds **6** and **6′** (Fig. 1), the intense absorption band recorded i n the region of 3365 cm^{-1} corresponds to vibrations of the NH group bond. An intense absorption band in the region of 1666 cm^{-1} corresponds to vibrations of the C=O group bond. An intense absorptionband in the region of 1609 cm^{-1} corresponds to vibrations of the C=N group bond.

In the ^{1}H NMR spectrum (Fig. 2), two signals of the Me_3Si group protons were recorded in the region of 0.03 ppm. and 0.21 ppm. These are characteristic of the protons of the trimethylsilyl group at the nitrogen atom and those of the trimethylsilyl group at the oxygen atom, respectively. The signals of the protons of the CH_2N and CH_2O groups of the morpholine fragment were also recorded in their characteristic regions; here, a doubling of the proton signals of the methylene groups at the nitrogen atom in the region of 2.84 ppm and 3.34 ppm is observed.

The ^{29}Si NMR spectrum (Fig. 3) also contains two silicon signals in the region of 5.96 ppm and 7.34 ppm corresponding to the $NSiMe_3$ and $OSiMe_3$ groups.

Thus, the difference between the interaction of trimethylsilyl isocyanate with 4-(trimethylsilyl) morpholine from its reaction with morpholine

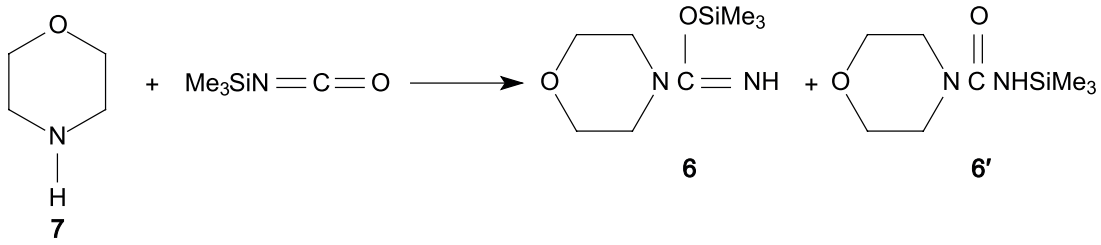

Scheme 4. Reaction of morpholine with trimethylsilyl isocyanate.

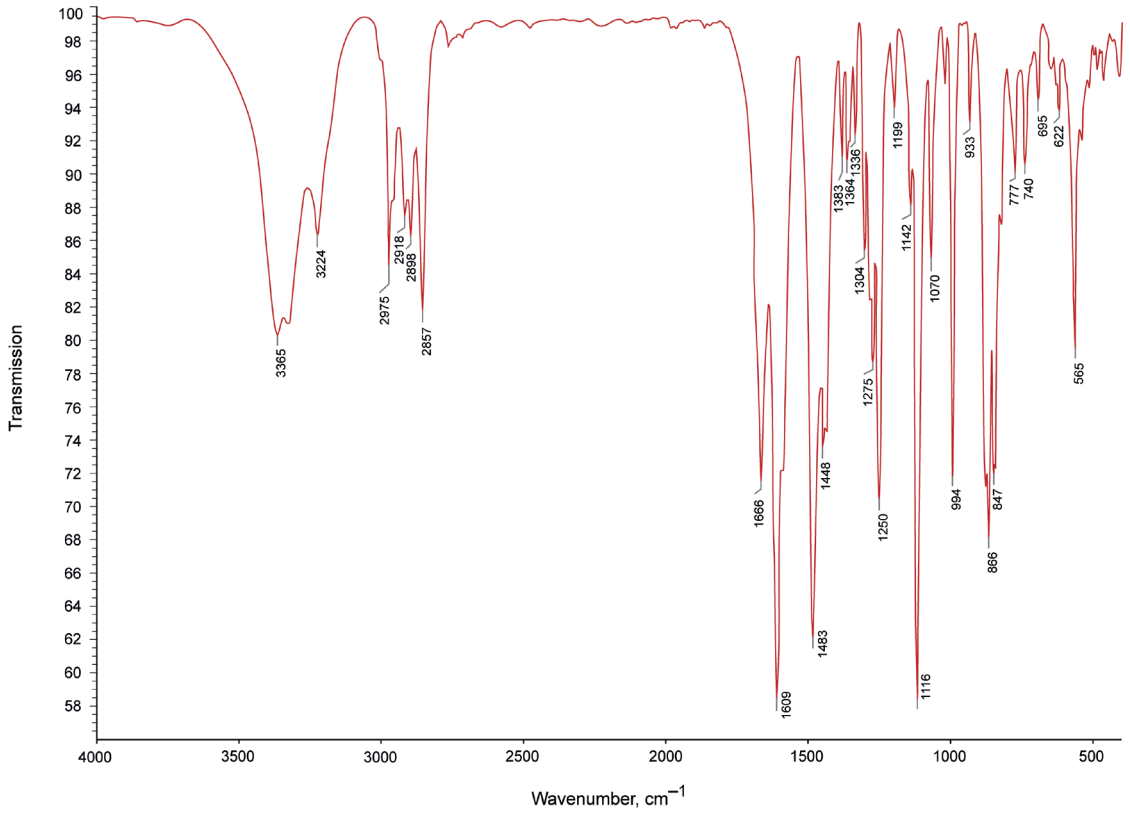

Fig. 1. IR spectrum of trimethylsilylmorpholine-4-carboxyimidoate **6** and *N*-(trimethylsilyl)morpholine-4-carboxamide **6′**.

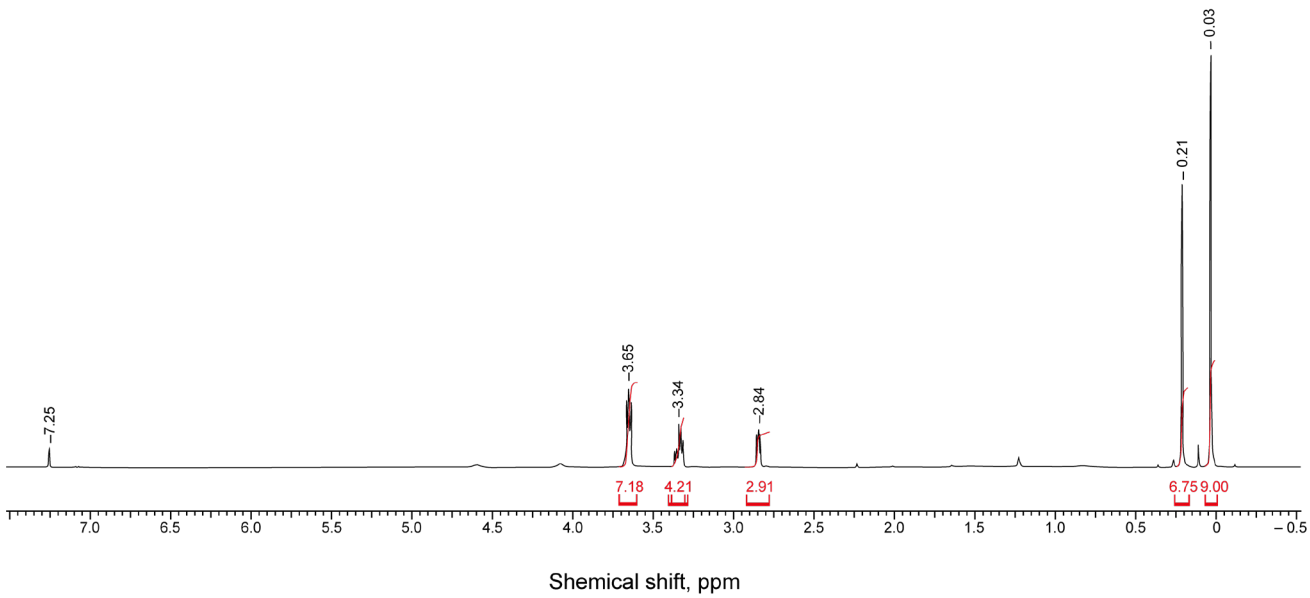

Fig. 2. [1]H NMR spectrum of trimethylsilylmorpholine-4-carboxyimidoate **6** and *N*-(trimethylsilyl)morpholine-4-carboxamide **6′**.

is the formation in the second case of *N*-(trimethylsilyl)morpholine-4-carboxamide, i.e., trimethylsilylurea. The formation of a mixture of tautomeric forms (Scheme 5) is known to be typical of the latter compound. The existence of such amide-isoamide tautomerism involving the Me_3Si group in silicon-containing ureas was previously assumed by J.F. Klebe *et al*. [12].

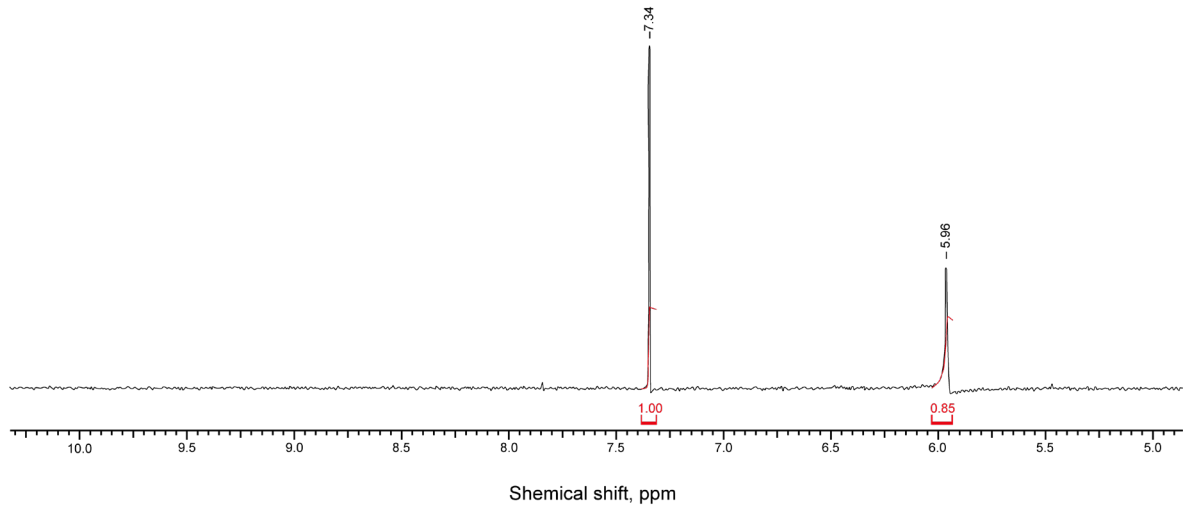

Fig. 3. ^{29}Si NMR spectrum of trimethylsilylmorpholine-4-carboxyimidoate **6** and *N*-(trimethylsilyl)morpholine-4-carboxamide **6′**.

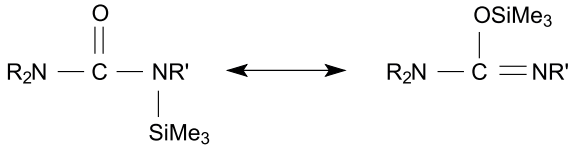

N-form *O*-form

Scheme 5. Amide-isoamide tautomerism involving the Me_3Si group for silicon-containing ureas.

CONCLUSIONS

The study of morpholine derivatives in reactions with isocyanates establishes that the composition and structure of the resulting products are determined both by the presence of a substituent at the nitrogen atom of morpholine and by the type of isocyanate used. It is shown that, unlike the trimethylsilyl derivative of morpholine, morpholine itself reacts with trimethylsilyl isocyanate to form a mixture of tautomeric forms.

Authors' contributions

A.D. Kirilin – idea of the study and general management;

L.O. Belova, N.I. Kirilina – writing the text of the article and the analysis of the obtained results;

N.A. Golub, M.V. Pletneva – conducting the experiments.

The authors declare no conflict of interest.

REFERENCES

1. Rakhlin V.I., Tsyrendorzhieva I.P., Sysoev S.V., Rumyantsev Yu.M., Maslova O.V., Kosinova M.L. 4-(Trimethylsilyl)-morpholine: synthesis, characterization, and prospects of use in film deposition processes. *Russ. Chem. Bull.* 2017;66(12):2283–2289. https://doi.org/10.1007/s11172-017-2015-1

[Rakhlin V.I., Tsyrendorzhieva I.P., Sysoev S.V., Rumyantsev Yu.M., Maslova O.V., Kosinova M.L. 4-(Trimethylsilyl)-morpholine: synthesis, characterization, and prospects of use in film deposition processes. *Izvestiya Akademii Nauk. Seriya Khimicheskaya.* 2017;(12):2283–2289 (in Russ.).]

2. Yoshida K., Liu Q., Yasue R., Wada S., Kimura R., Konishi T., Ogasawara M. Versatile and Enantioselective Preparation of Planar-Chiral Metallocene-Fused 4-Dialkylaminopyridines and Their Application in Asymmetric Organocatalysis. *ACS Catalysis*. 2020;10(1):292–301. https://doi.org/10.1021/acscatal.9b04438

3. Zhong W., Xu W., Yang Q., Kato T., Liu Y., Maruoka K. A new approach for the copper-catalyzed functionalization of alkyl hydroperoxides with organosilicon compounds via *in-situ*-generated alkylsilyl peroxides. *Tetrahedron*. 2022;112:132627. https://doi.org/10.1016/j.tet.2021.132627

4. Zasukha S., Khairulin A., Shermolovich Y. The reactions of *N*-trimethylsilyl substituted ethers of α- and β-amino acids with sulfur tetrafluoride and morpholinosulfur trifluoride. *J. Sulfur Chem*. 2021;42(5):477–489. https://doi.org/10.1080/17415993.2021.1912045

5. Yang J., Shkrob I., Liu K., Connell J., Dietz-Rado N.L., Zhang Z., Liao C. 4-(Trimethylsilyl) Morpholine as a Multifunctional Electrolyte Additive in High Voltage Lithium Ion Batteries. *J. Electrochem. Soc*. 2020;167(7):070533. https://doi.org/10.1149/1945-7111/ab7a9e

6. Herbig M., Kroke E. Low cost apparatus for rapid boiling point determination of small air sensitive samples under inert atmosphere. *Thermochimica Acta*. 2017;654:81–84. https://doi.org/10.1016/j.tca.2017.05.005

7. Herbig M., Böhme U., Kroke E. Insertion of CO_2 and related heteroallenes into the Si-N-bond of methyl(*N*-morpholino)silanes. *Inorg. Chim. Acta.* 2018;73:20–28. https://doi.org/10.1016/j.ica.2017.12.020

8. Jahn U.A., Schroth W. Novel and simple method for the preparation of imivium salts. *Tetrahedron Lett.* 1993;34(37):5863–5866. https://doi.org/10.1016/S0040-4039(00)73799-3

9. Sinitsa A.D., Parkhomenko N.A., Stukalo E.A. Reactions of trimethylsilylamines with α-substituted alkyl isocyanates. *Zhurnal Obshchei Khimii.* 1977;47(9):2077–2081 (in Russ.).

10. Belova L.O., Golub N.A., Storozhenko P.A., Kirilin A.D. Unusual Behavior of Nitrogen-Containing Organosilicon Compounds in the Reactions with Isocyanates. *Russ. J. Gen. Chem.* 2021;91(5):820–827. https://doi.org/10.1134/S1070363221050108

11. Kozyukov V.P., Sheludyakov V.D., Mironov V.F. Silicon-containing isocyanates. *Russ. Chem. Rev.* 1973;42(8):662–667. https://doi.org/10.1070/RC1973v042n08ABEH002704

[Original Russian Text: Kozyukov V.P., Sheludyakov V.D., Mironov V.F. Silicon-containing isocyanates. *Uspekhi Khimii.* 1973;42(8):1451–1480 (in Russ.).]

12. Klebe J.F., Bush J.B., Lyon, J.E. The Addition of Silylamines and Silazanes to Isocyanates *J. Am. Chem. Soc.* 1964;86(20):4400–4406. https://doi.org/10.1021/ja01074a035

About the authors:

Liya O. Belova, Dr. Sci. (Chem.), Professor, K.A. Andrianov Department of Chemistry and Technology of Organoelement Compounds, M.V. Lomonosov Institute of Fine Chemical Technologies, MIREA – Russian Technological University (86, Vernadskogo pr., Moscow, 119571, Russia). E-mail: belova@mirea.ru. Scopus Author ID 7102282244, RSCI SPIN-code 3499-7697, https://orcid.org/0000-0002-3920-2908

Nataliya A. Golub, Cand. Sci. (Chem.) Associate Professor, K.A. Andrianov Department of Chemistry and Technology of Organoelement Compounds, M.V. Lomonosov Institute of Fine Chemical Technologies, MIREA – Russian Technological University (86, Vernadskogo pr., Moscow, 119571, Russia). E-mail: golub@mirea.ru. Scopus Author ID 56084643600, RSCI SPIN-code 4240-3509, https://orcid.org/0000-0001-9932-7588

Mariya V. Pletneva, Cand. Sci. (Chem.) Associate Professor, K.A. Andrianov Department of Chemistry and Technology of Organoelement Compounds, M.V. Lomonosov Institute of Fine Chemical Technologies, MIREA – Russian Technological University (86, Vernadskogo pr., Moscow, 119571, Russia). E-mail: pletneva@mirea.ru. Scopus Author ID 37104888400, RSCI SPIN-code 9399-0150, https://orcid.org/0000-0002-4940-292X

Nadezhda I. Kirilina, Cand. Sci. (Chem.), Leading Engineer, State Scientific Research Institute of Chemistry and Technology of Organoelement Compounds (38, Entuziastov shosse, Moscow, 111123, Russia). E-mail: ous@eos.su. Scopus Author ID 57193056863, RSCI SPIN-code 4549-8907, https://orcid.org/0000-0001-9932-7588

Alexey D. Kirilin, Dr. Sci. (Chem.), Professor, Head of the K.A. Andrianov Department of Chemistry and Technology of Organoelement Compounds, M.V. Lomonosov Institute of Fine Chemical Technologies, MIREA – Russian Technological University (86, Vernadskogo pr., Moscow, 119571, Russia). E-mail: kirilin@mirea.ru. Scopus Author ID 6603604447, ResearcherID O-9744-215, RSCI SPIN-code 5500-5030, https://orcid.org/0000-0001-9225-9551

Об авторах:

Белова Лия Олеговна, д.х.н., профессор кафедры химии и технологии элементоорганических соединений им. К.А. Андрианова Института тонких химических технологий им. М.В. Ломоносова ФГБОУ ВО «МИРЭА – Российский технологический университет» (119571, Россия, Москва, пр-т Вернадского, д. 86). E-mail: belova@mirea.ru. Scopus Author ID 7102282244, SPIN-код РИНЦ 3499-7697, https://orcid.org/0000-0002-3920-2908

Голуб Наталия Александровна, к.х.н., доцент кафедры химии и технологии элементоорганических соединений им. К.А. Андрианова Института тонких химических технологий им. М.В. Ломоносова ФГБОУ ВО «МИРЭА – Российский технологический университет» (119571, Россия, Москва, пр-т Вернадского, д. 86). E-mail: golub@mirea.ru. Scopus Author ID 56084643600, SPIN-код РИНЦ 4240-3509, https://orcid.org/0000-0001-9932-7588

Плетнева Мария Владимировна, к.х.н., доцент кафедры химии и технологии элементоорганических соединений им. К.А. Андрианова Института тонких химических технологий им. М.В. Ломоносова ФГБОУ ВО «МИРЭА – Российский технологический университет» (119571, Россия, Москва, пр-т Вернадского, д. 86). E-mail: pletneva@mirea.ru. Scopus Author ID 37104888400, SPIN-код РИНЦ 9399-0150, https://orcid.org/0000-0002-4940-292X

Кирилина Надежда Ивановна, к.х.н., ведущий инженер, ГНЦ РФ АО «Государственный научно-исследовательский институт химии и технологии элементоорганических соединений» (111123, Россия, Москва, шоссе Энтузиастов, д. 38). E-mail: ous@eos.su. Scopus Author ID 57193056863, SPIN-код РИНЦ 4549-8907, https://orcid.org/0000-0001-9932-7588

Кирилин Алексей Дмитриевич, д.х.н., профессор, заведующий кафедрой химии и технологии элементоорганических соединений им. К.А. Андрианова Института тонких химических технологий им. М.В. Ломоносова ФГБОУ ВО «МИРЭА – Российский технологический университет» (119571, Россия, Москва, пр-т Вернадского, д. 86). E-mail: kirilin@mirea.ru, Scopus Author ID 6603604447, ResearcherID O-9744-215, SPIN-код РИНЦ 5500-5030, https://orcid.org/0000-0001-9225-9551

The article was submitted: April 08, 2022; approved after reviewing: May 25, 2022; accepted for publication: September 26, 2022.

Translated from Russian into English by M. Povorin
Edited for English language and spelling by Thomas Beavitt

BIOCHEMISTRY AND BIOTECHNOLOGY

БИОХИМИЯ И БИОТЕХНОЛОГИЯ

ISSN 2686-7575 (Online)

https://doi.org/10.32362/2410-6593-2022-17-5-384-393

UDC 615.275.2

RESEARCH ARTICLE

Effect of antiviral siRNAs on the production of cytokines *in vitro*

Anastasia V. Pak[1], Evgeny A. Pashkov[1,2,✉], Natalia D. Abramova[2], Alexander V. Poddubikov[2], Firaya G. Nagieva[2], Ekaterina A. Bogdanova[1], Evgeny P. Pashkov[1], Oxana A. Svitich[1,2], Vitaliy V. Zverev[1,2]

[1]I.M. Sechenov First Moscow State Medical University (Sechenov University), Moscow, 119991 Russia
[2]I. Mechnikov Research Institute of Vaccines and Sera, Moscow, 105064 Russia
✉Corresponding author, e-mail: pashckov.j@yandex.ru

Abstract

Objectives. *To evaluate the dynamics of the expression level of IL-1β and IL-28β (IFN-λ3) genes as a result of complex knockdown of some cellular genes, whose expression products play an important role in the reproduction of the influenza virus.*

Methods. *Following the collection of virus-containing liquid and cell lysate within three days from the moment of transfection and infection, the intensity of viral reproduction was assessed using the cytopathic effect titration method. The concentration of viral ribonucleic acid (vRNA) and change in the expression of IL-1β and IL-28β (IFN-λ3) were determined by real-time reverse transcription quantitative polymerase chain reaction (real-time RT-qPCR). The nonparametric Mann–Whitney test was used to statistically calculate significant differences between groups.*

Results. *The use of each small interfering ribonucleic acid (siRNA) complex led to a decrease in viral reproduction on the first day at the multiplicity of infection (MOI) of 0.001. The use of complex A (FLT4.2 + Nup98.1) and D (FLT4.2 + Nup98.1 + Nup205) led to a decrease in viral titer by 2.8 lg$TCID_{50}$/mL and by 2.1 lg$TCID_{50}$/mL relative to the use of nonspecific L2 siRNA and viral control ($p \le 0.05$). Transfection of complexes B (Nup98.1 + Nup205) and C (FLT4.2 + Nup205) also reduced the viral titer by 1.5 lg$TCID_{50}$/mL and 1.8 lg$TCID_{50}$/mL relative to nonspecific L2 siRNA and viral control ($p \le 0.05$). When conducting real-time RT-qPCR, a significant decrease in the concentration of viral RNA was also noted. When using complexes B, C, and D, the concentration of vRNA decreased on the first day by 14.5, 4.1, and 15 times, respectively. On the second*

day, a decrease in vRNA was observed in cells with B and D complexes by 17.1 and 18.3 times (p ≤ 0.05). Along with a decrease in the viral titer and vRNA, an increase in the expression of the IL-1β and IL-28β genes was observed on the first day when using all siRNA complexes relative to nonspecific and viral controls (p ≤ 0.05). On the second day, an increase was also observed in cells with A and D complexes, while on the third day, there was an increase in the expression of these genes in cells with complex D (p ≤ 0.05).

Conclusions. *The use of siRNA complexes is shown to have a pronounced antiviral effect while simultaneously suppressing the activity of cellular genes (FLT4, Nup98 and Nup205). In parallel, the transfection of complexes that block the formation of expression products necessary for viral reproduction is demonstrated to lead to an increase in the level of expression of the IL-1β and IL-28β genes. These results indicate not only that the use of siRNA has antiviral activity, but also immunomodulatory activity, which can contribute to a more effective immune response of the body.*

Keywords: *RNA interference, IL-1β, influenza A virus, IFN-λ3, gene expression, siRNA, pro-inflammatory cytokines, IL-28β, viral RNA*

For citation: Pak A.V., Pashkov E.A., Abramova N.D., Poddubikov A.V., Nagieva F.G., Bogdanova E.A., Pashkov E.P., Svitich O.A., Zverev V.V. Effect of antiviral siRNAs on the production of cytokines *in vitro*. *Tonk. Khim. Tekhnol. = Fine Chem. Technol.* 2022;17(5):384–393 (Russ., Eng.). https://doi.org/10.32362/2410-6593-2022-17-5-384-393

НАУЧНАЯ СТАТЬЯ

Действие противовирусных миРНК на выработку цитокинов *in vitro*

А.В. Пак[1], Е.А. Пашков[1,2,✉], Н.Д. Абрамова[2], А.В. Поддубиков[2], Ф.Г. Нагиева[2], Е.А. Богданова[1], Е.П. Пашков[1], О.А. Свитич[1,2], В.В. Зверев[1,2]

[1]Первый Московский государственный медицинский университет им. И.М. Сеченова Минздрава России (Сеченовский Университет), Москва, 119991 Россия
[2]Научно-исследовательский институт вакцин и сывороток им. И.И. Мечникова Минздрава России, Москва, 105064 Россия
✉ Автор для переписки, e-mail: pashckov.j@yandex.ru

Аннотация

Цели. *Оценить динамику уровня экспрессии генов IL-1β и IL-28β (IFN-λ3) в результате комплексного нокдауна некоторых клеточных генов, чьи продукты экспрессии играют важную роль в репродукции вируса гриппа.*

Методы. *Вируссодержащую жидкость и клеточный лизат отбирали в течение 3-х дней с момента трансфекции и заражения и оценивали интенсивность вирусной репродукции методами титрования по цитопатическому действию. Концентрацию вирусной рибонуклеиновой кислоты (вРНК) и изменение экспрессии IL-1β и IL-28β (IFN-λ3) определяли*

методом обратной транскрипции и полимеразной цепной реакции в режиме реального времени (ОТ-ПЦР-РВ). Для вычисления статистически значимых различий между группами использовали непараметрический критерий Манна-Уитни.

Результаты. *Использование каждого комплекса малых интерферирующих РНК (миРНК) приводило к снижению вирусной репродукции на 1-е сутки при множественности заражения 0.001. Применение комплексов A (FLT4.2 + Nup98.1) и D (FLT4.2 + Nup98.1 + Nup205) приводило к снижению вирусного титра на 2.8 lgТЦД$_{50}$/мл и на 2.1 lgТЦД$_{50}$/мл относительно применения неспецифической миРНК L2 и вирусного контроля ($p \le 0.05$). В результате трансфекции комплексов B (Nup98.1 + Nup205) и C (FLT4.2 + Nup205) вирусный титр также снижался на 1.5 lgТЦД$_{50}$/мл и 1.8 lgТЦД$_{50}$/мл соответственно относительно неспецифической миРНК L2 и вирусного контроля ($p \le 0.05$). При проведении ОТ-ПЦР-РВ также было отмечено достоверное уменьшение концентрации вРНК. При использовании комплексов B, C и D концентрация вРНК снижалась на 1-е сутки в 14.5, 4.1 и 15.0 раз соответственно. На 2-е сутки в клетках с комплексами B и D наблюдалось уменьшение концентрации вРНК в 17.1 и 18.3 раз ($p \le 0.05$). Наряду со снижением вирусного титра и вРНК наблюдалось повышение экспрессии генов IL-1β и IL-28β на 1-е сутки при использовании всех комплексов миРНК относительно неспецифического и вирусного контроля ($p \le 0.05$). На 2-е сутки также наблюдалось повышение экспрессии в клетках с комплексами A и D, а на третьи – в клетках с комплексом D ($p \le 0.05$).*

Выводы. *Исследование показало, что применение комплексов миРНК приводит к выраженному противовирусному эффекту при одновременном подавлении активности клеточных генов (FLT4, Nup98 и Nup205). Параллельно с этим было выявлено, что при трансфекции комплексов, блокирующих образование продуктов экспрессии, необходимых для вирусной репродукции, повышается уровень экспрессии генов IL-1β и IL-28β. Данные результаты свидетельствуют о том, что используемые миРНК обладают не только противовирусной, но также и иммуномодулирующей активностью, что способствует более эффективному иммунному ответу организма.*

Ключевые слова: *РНК-интерференция, IL-1β, вирус гриппа А, IFN-λ3, экспрессия генов, миРНК, провоспалительные цитокины, IL-28β, вирусная РНК*

Для цитирования: Пак А.В., Пашков Е.А., Абрамова Н.Д., Поддубиков А.В., Нагиева Ф.Г., Богданова Е.А., Пашков Е.П., Свитич О.А., Зверев В.В. Действие противовирусных миРНК на выработку цитокинов *in vitro*. *Тонкие химические технологии*. 2022;17(5):384–393. https://doi.org/10.32362/2410-6593-2022-17-5-384-393

INTRODUCTION

The present work continues research on the creation of a universal platform for the rapid development of cost-effective and safe treatments for viral infections, which was launched in 2021 by a group of scientists from the I.I. Mechnikov Research Institute of Vaccines and Serums (Russia) [1, 2].

Today, respiratory viral infections have become one of the most pressing global problems, having severe social and economic consequences. For example, the COVID-19 pandemic caused by the SARS-CoV-2 virus has claimed the lives of more than 6.3 mln people worldwide since 2019[1], and influenza ended almost 650000 lives in 2021 alone[2]. Viral infections affect not

[1] https://coronavirus-graph.ru/mir, accessed June 20, 2022.

[2] https://www.euro.who.int/ru/media-centre/events/events/2021/10/flu-awareness-campaign-2021, accessed June 20, 2022.

only the respiratory, but also central nervous, genitourinary, cardiovascular and immune systems, as well as leading to the development of bacterial and fungal complications [3–6].

Influenza viruses have proteins with immunomodulatory properties, which can trigger secondary immunodeficiencies. Among these, the best-studied protein is NS-1 (nonstructural protein-1), one of whose main functions is to disrupt the functioning of interferon-mediated defense mechanisms of the body, reducing the production of pro-inflammatory cytokines known as interleukins, which in turn leads to a lack of immune response [7].

To date, there are a number of etiotropic, pathogenetic, symptomatic, and immunomodulatory drugs used for the treatment of influenza. However, achieving a full therapeutic effect from the use of these drugs is prevented by the emergence of new resistant forms of the influenza virus, the development of allergic reactions to drugs, and the need for their individual selection [8–11]. The question of the use of immunomodulatory drugs also remains open, since the effect of their use is limited, and in some cases can lead to serious consequences for the patient himself [12–14]. The use of anti-influenza drugs also has certain limitations [15]. To overcome these problems, the design and development of fundamentally new antiviral drugs is required. One of the promising new technologies for creating specific antiviral drugs is based on the mechanism of RNA interference [16–18].

Previously, we have demonstrated a pronounced antiviral effect from the use of small interfering RNAs (siRNAs) directed to one, two, or more cellular genes simultaneously, whose expression products are important in viral reproduction. However, in earlier works, we did not evaluate changes in the expression of some pro-inflammatory cytokines role in the formation of antiviral immunity [1, 2, 19]. *IL-1β* is involved in increased expression of the MCP-1 and MCP-3 genes and functional maturation of tissue macrophages and dendritic cells [20, 21]. This leads to increased inflammatory response and activation of an efficient antigen presentation system. *IFN-λ3*, which are formed earlier than other types of interferons, demonstrate a powerful protective function at early stages of infection. The use of siRNAs in relation to cellular genes involved in the reproduction of the influenza virus can reduce viral activity *in vitro* and promote a more effective immune response [18].

Based on the foregoing, the aim of the present study is to evaluate the dynamics of the expression level of *IL-1β* and *IL-28β* (*IFN-λ3*) genes as a result of complex knockdown of some cellular genes, whose expression products play an important role in the reproduction of the influenza virus.

MATERIALS AND METHODS

Methods used in the present work included selection of siRNAs, oligonucleotides, sequences of siRNAs used, information about the influenza A/WSN/33 (**H1N1**) virus used, cell cultures, method for assessing the cytotoxicity of siRNA complexes, method for transfection of siRNA cells with subsequent infection, siRNA complexes used. The used virus titration method on the end point of cytopathic action was as presented in our earlier studies [1, 2, 19]. The expression of *IL-1β* and *IFN-λ3* genes was studied by real-time reverse transcription polymerase chain reaction (real-time RT-PCR).

Detection of viral RNA

Total RNA was isolated from the cell lysate using the ExtractRNA kit (*Evrogen*, Russia). The OT-1 reagent kit (*Syntol*, Russia) was used to set up the reverse transcription reaction. Changes in the concentration of viral RNA (vRNA) were monitored using quantitative real-time RT-PCR with a set of primers and probes for the influenza A M gene [22]. To assess the expression of *IL-1β* and *IFN-λ3*, real-time RT-PCR and the expression evaluation criterion $2^{-\Delta\Delta Ct}$ were used.

For real-time PCR, a set of reagents in the presence of EVA Green dye and reference dye ROX (*Syntol*) and a 2.5-fold reaction mixture for real-time PCR (*Syntol*) were used. The working concentration of primers and probes was 10 pmol/μL and 5 pmol/μL, respectively. The real-time PCR reaction was carried out in a DT-96 amplifier (*DNA-technology*, Russia). The temperature-time regime was 95°C and 5 min (1 cycle), 62°C and 40 s, 95°C and 15 s (40 cycles). Primers and probes were synthesized by *Syntol* and presented in [2].

Statistical data processing

The statistical significance of the results obtained was determined using the Mann–Whitney U test. The difference was considered significant at a statistical significance level of $0.01 \leq p \leq 0.05$. Reliability indicators were calculated using the Minitab software[3].

[3] https://www.minitab.com/en-us/, accessed June 08, 2022.

RESULTS

Assessment of cytotoxicity

Previously, similar siRNA sequences were used in a study to evaluate the antiviral effect against the influenza virus. Detailed results of the cytotoxicity evaluation are presented in the study [2].

Influence of siRNA complexes on virus titer

To assess the effectiveness of the antiviral action of siRNA in reducing viral activity, titration of the virus-containing liquid was performed on a Madin-Darby Canine Kidney cell culture, which was taken at 24, 48, and 72 h from the moment of transfection of the siRNA complexes into the A549 cell culture. In contrast to our previous study [1], in this work, the multiplicity of infection (MOI) was 0.001. It was found that the use of all siRNA complexes at a given MOI directed to cellular genes leads to a significant decrease in viral reproduction on the first day after infection. The obtained data shown in Fig. 1 indicate the ability of siRNA to reduce viral activity *in vitro*. Upon transfection of the A complex directed to the *FLT4* + *Nup98* genes, a significant decrease in the viral titer was observed compared to the nonspecific control by 2.8 $lgTCID_{50}$/mL ($p \leq 0.05$). Upon transfection of the B complex (*Nup98* + Nup205 genes), the corresponding increase was 1.5 $lgTCID_{50}$/mL ($p \leq 0.05$). The use of complexes C (*FLT4* + *Nup205* genes) and D (*FLT4* + *Nup98* + *Nup205* genes) led to a significant decrease in viral titer compared with nonspecific control by 1.8 and 2.1 $lgTCID_{50}$/mL, respectively ($p \leq 0.05$).

Influence of siRNA on vRNA concentration

Figure 2 shows the change in *in vitro* vRNA concentration resulting from siRNA transfection as assessed using real-time RT-PCR. At MOI = 0.001, the use of B, C, and D complexes led to a significant decrease in vRNA on the first day as compared with nonspecific control by 14.5, 4.1, and 15 times, respectively ($p \leq 0.05$). On the second day, a decrease in vRNA was observed when using B and D complexes by 17.1 and 18.3 times, respectively ($p \leq 0.05$).

Expression dynamics of IL-1β and IFN-λ3

Expression of *IL-1β* and *IFN-λ3* was assessed using real-time RT-PCR and the expression evaluation criterion $2^{-\Delta\Delta Ct}$. Figure 3 shows the results of the evaluation of the expression of *IL-1β*. At MOI = 0.001, a significant increase in *IL-1β* expression by 18% relative to nonspecific control was observed on day 1 when complex A was used. When transfecting B, C, and D complexes, a significant increase in *IL-1β* expression was also

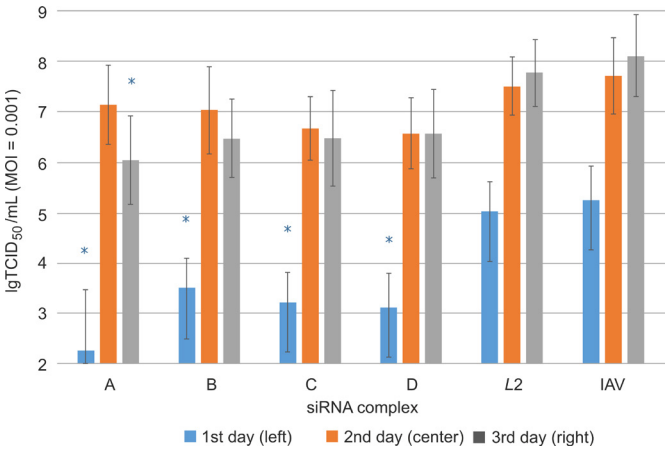

Fig. 1. Influence of siRNAs complexes (A: *FLT4* + *Nup98*; B: *Nup98* + *Nup205*; C: *FLT4* + *Nup205*; D: *FLT4* + *Nup98* + *Nup205*) directed to the *FLT4, Nup98*, and *Nup205* genes on the reproduction of the influenza virus ($p \leq 0.05$). IAV—influenza A virus. The ordinate indicates the change in virus titer in $lgTCD_{50}$/mL. The abscissa shows siRNA complexes.

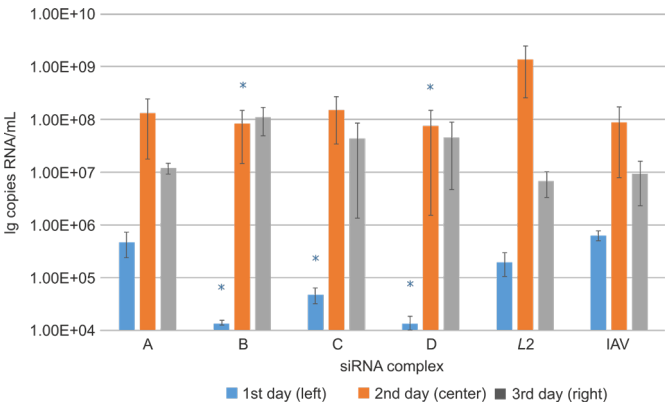

Fig. 2. Effect of siRNA complexes (A: *FLT4* + *Nup98*; B: *Nup98* + *Nup205*; C: *FLT4* + *Nup205*; D: *FLT4* + *Nup98* + *Nup205*) on the concentration of viral RNA. (On the graph, the data are given in log_{10}, in the text the decrease is indicated in the number of times) ($p \leq 0.05$). IAV—influenza A virus. The ordinate indicates the change for vRNA in log_{10}. The abscissa shows siRNA complexes.

noted on days 10, 17, and 25%, respectively ($p \leq 0.05$). On the second day, the expression level of *IL-1β* increased in cells transfected with A and D complexes by 118 and 90% ($p \leq 0.05$) as compared with the nonspecific control, which also exceeded the expression level in uninfected cells by 45 and 17%, respectively. On the third day, an increase in *IL-1β* expression by 47% was noted in cells transfected with complex D ($p \leq 0.05$). Figure 4 shows data on the change in the expression of *IFN-λ3* within three days from the moment of transfection and infection. A significant increase inexpression relative to nonspecific control was noted only on the second day when using A and C complexes by 10 and 24%, respectively ($p \leq 0.05$).

DISCUSSION

The present work evaluates the effect of siRNAs on the induction of *IL-1β* and *IFN-λ3* production and the concomitant decrease in viral activity. A series of experiments was carried out to assess changes in the expression of the level of *IL-1β* and *IFN-λ3* during suppression of the expression of cellular genes *FLT4*, *Nup98* and *Nup205*, which are important for the reproduction of the influenza virus using siRNA. To evaluate the effectiveness of cytokine expression and decrease in viral activity, two mutually-compatible methodological approaches were used: virus titration by cytopathic effect and real-time RT-PCR. The use of siRNA was shown to lead to a pronounced antiviral effect: the obtained data indicated a dependent relationship between a decrease in viral titer, a change in the amount of vRNA, and increased levels of *IL-1β* and *IFN-λ3*. Earlier results demonstrated the low cytotoxicity of siRNA complexes, allowing significant disturbances in cell vital activity following knockdown of one or several genes to be avoided [2].

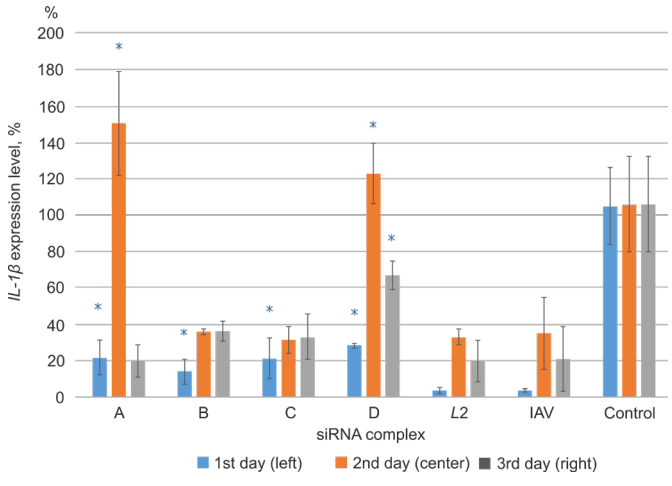

Fig. 3. Effect of siRNA complexes (A: *FLT4* + *Nup98*; B: *Nup98* + *Nup205*; C: *FLT4* + *Nup205*; D: *FLT4* + *Nup98* + *Nup205*) on changes in *IL-1β* expression ($p \leq 0.05$). IAV—influenza A virus. The ordinate shows the change in the expression level of *IL-1β*. The abscissa shows siRNA complexes.

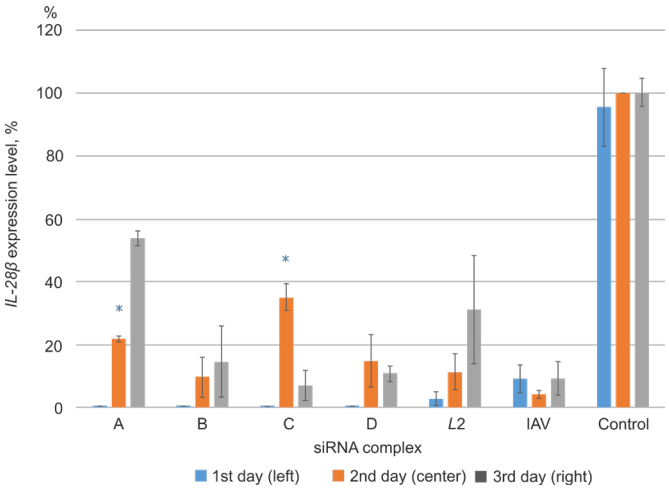

Fig. 4. Effect of siRNA complexes (A: *FLT4* + *Nup98*; B: *Nup98* + *Nup205*; C: *FLT4* + *Nup205*; D: *FLT4* + *Nup98* + *Nup205*) on changes in *IFN-λ3* expression ($p \leq 0.05$). IAV—influenza A virus. The ordinate shows the change in the expression level of *IFN-λ3*. The abscissa shows siRNA complexes.

When the virus was titrated against cytopathic effect, each siRNA complex was shown to lead to a decrease in viral activity on the first day following infection. Table 1 shows that at MOI = 0.001, the viral titer in cells treated with A and D complexes decreased by 2.8 $lgTCID_{50}$/mL and by 2.1 $lgTCID_{50}$/mL, respectively, relative to nonspecific *L2* siRNA ($p \leq 0.05$). Upon transfection of B and C complexes, the respective decreases in viral titer were 1.5 $lgTCID_{50}$/mL and 1.8 $lgTCID_{50}$/mL as compared with the nonspecific control *L2* ($p \leq 0.05$).

According to the results of RT-PCR, there was a decrease in the amount of vRNA in the cells treated with the complexes as compared to nonspecific and viral controls. The use of complexes B, C, and D led to a significant decrease in vRNA on the first day compared to si*L2* siRNA by factors of 14.5, 4.1, and 15, respectively ($p \leq 0.05$). When using the B and D complexes, the vRNA concentration on the

second day was observed to decrease by 17.1 and 18.3 times, respectively ($p \leq 0.05$). It is significant that, when using complex A, despite a pronounced observed decrease in viral titer, there was no decrease in the concentration of vRNA. This result is likely due to the combination of complex A directed to the *FLT4* and *Nup98* genes leading to partial synthesis of vRNA. Nevertheless, there was limited assembly and release of the virion from the cell, while the remaining complexes, apparently, completely blocked the synthesis of vRNA, the assembly and release of the virion. Similar results are noted in the work of J. Piasecka *et al*., where the antiviral effect of siRNAs is also assessed [23].

Expression of *IL-1β* and *IFN-λ3* was assessed using real-time RT-PCR and the expression evaluation criterion $2^{-\Delta\Delta Ct}$. Figures 3 and 4 show data on the dynamics of *IL-1β* and *IFN-λ3* expression within three days from the moment of transfection and infection. The most effective increase in *IL-1β* expression is observed when using A and D complexes. In relation to the nonspecific control *L2* ($p \leq 0.05$), the increase in expression on the first and second days following transfection was 18/118% for complex A and 25/90% for complex D, respectively, as well as exceeding the expression level in uninfected cells by 45% and 17% on the second day. On the third day, an increased expression was also noted when the complex D was used by 47%. When using B and C complexes, an increase in expression was noted only on the first day by 10% and 17%, respectively ($p \leq 0.05$). When assessing the increase in the expression level of *IFN-λ3*, an increase was observed only on the second day when using A and C complexes by 10% and 24%, respectively, relative to the nonspecific control ($p \leq 0.05$). This result of a heterogeneous increase in the expression of *IL-1β* and *IFN-λ3* is apparently due to different siRNA nucleotide sequences differently inducing the production of pro-inflammatory cytokines and interferons through Toll-like receptors.

CONCLUSIONS

The challenge of developing medicines for the prevention and treatment of highly contagious respiratory infections is currently of particular relevance. It is necessary that such medicinal substances be safe, non-toxic for the patient, as well as having a low spectrum of contraindications. In addition, such drugs should offer a clear therapeutic and prophylactic effect despite the drug resistance of the pathogen. The present study provides evidence that the simultaneous knockdown of several cellular genes that play an important role in viral reproduction by means of siRNA complexes significantly reduced influenza viral activity *in vitro*. Despite the ability of the influenza virus to exert an immunosuppressive effect, a pronounced decrease in vRNA and increase in the expression level of IL-1β and IFN-λ3 was observed. The results indicate that siRNAs used in the work have not only antiviral but also immunomodulatory activity, which contributes to a more effective immune response. Additionally, these results represent the development of principles for the rapid design and creation of specific antiviral agents designed to protect against existing and emerging pathogenic viruses, ensure the anti-epidemic safety of various population groups, and effectively respond to the emergence of pandemics and possible cases of bioterrorism.

Acknowledgments

The study was carried out using the scientific equipment of the Center for Collective Use of the I. Mechnikov Research Institute of Vaccines and Sera, and supported by the Ministry of Science and Higher Education of the Russian Federation, Agreement No. 075-15-2021-676 dated July 28, 2021.

Authors' contributions

A.V. Pak, E.A. Pashkov, N.D. Abramova – conducting the experiments;

E.A. Pashkov, E.A. Bogdanova – writing the text of the article and the analysis of the obtained results;

A.V. Poddubikov, F.G. Nagieva – scientific editing;

E.P. Pashkov, O.A. Svitich, V.V. Zverev – idea of the study, summary, and general management.

The authors declare no obvious and potential conflicts of interest related to the publication of this article.

REFERENCES

1. Pashkov E.A., Korotysheva M.O., Pak A.V., Faizuloev E.B., Sidorov A.V., Poddubikov A.V., Bystritskaya E.P., Dronina Y.E., Solntseva V.K., Zaiceva T.A., Pashkov E.P., Bykov A.S., Svitich O.A., Zverev V.V. Investigation of the anti-influenza activity of siRNA complexes against the cellular genes *FLT4*, *Nup98*, and *Nup205 in vitro*. *Tonk. Khim. Tekhnol. = Fine Chem. Technol*. 2022;17(2):140–151 (in Russ.). https://doi.org/10.32362/2410-6593-2022-17-2-140-151

2. Pashkov E.A., Faizuloev E.B., Korchevaya E.R., Rtishchev A.A., Cherepovich B.S., Sidorov A.V., Poddubikov A.V., Bystritskaya E.P., Dronina Yu.E., Bykov A.S., Svitich O.A., Zverev V.V. Knockdown of *FLT4*, *Nup98*, and *Nup205* cellular genes as a suppressor for the viral activity of Influenza A/WSN/33 (H1N1) in A549 cell culture. *Tonk. Khim. Tekhnol. = Fine Chem. Technol*. 2021;16(6):476–489 (in Russ.). https://doi.org/10.32362/2410-6593-2021-16-6-476-489

3. Sellers S.A., Hagan R.S., Hayden F.G., Fischer W.A. II. The hidden burden of influenza: A review of the extra-pulmonary complications of influenza infection. *Influenza Other Respir. Viruses*. 2017;11(5):372–393. https://doi.org/10.1111/irv.12470

4. Koehler P., Bassetti M., Kochanek M., Shimabukuro-Vornhagen A., Cornely O.A. Intensive care management of influenza-associated pulmonary aspergillosis. *Clin. Microbiol. Infect*. 2019;25(12):1501–1509. https://doi.org/10.1016/j.cmi.2019.04.031

5. Radzišauskienė D., Vitkauskaitė M., Žvinytė K., Mameniškienė R. Neurological complications of pandemic A(H1N1)2009pdm, postpandemic A(H1N1)v, and seasonal influenza A. *Brain Behav*. 2021;11(1):e01916. https://doi.org/10.1002/brb3.1916

6. Kalil A.C., Thomas P.G. Influenza virus-related critical illness: pathophysiology and epidemiology. *Crit. Care*. 2019;23(1):258. https://doi.org/10.1186/s13054-019-2539-x

7. Plotnikova M.A., Klotchenko S.A., Vasin A.V. Development of a multiplex quantitative PCR assay for the analysis of human cytokine gene expression in influenza A virus-infected cells. *J. Immunol. Methods*. 2016;430:51–55. https://doi.org/10.1016/j.jim.2016.01.005

8. Wang J., Wu Y., Ma C., Fiorin G., Wang J., Pinto L.H., *et al*. Structure and inhibition of the drug-resistant S31N mutant of the M2 ion channel of influenza A virus. *Proc. Natl. Acad. Sci. USA*. 2013;110(4):1315–1320. https://doi.org/10.1073/pnas.1216526110

9. Lampejo T. Influenza and antiviral resistance: an overview. *Eur. J. Clin. Microβiol. Infect. Dis*. 2020;39(7):1201–1208. https://doi.org/10.1007/s10096-020-03840-9

10. Leneva I.A., Russell R.J., Boriskin Y.S., Hay A.J. Characteristics of arbidol-resistant mutants of influenza virus: Implications for the mechanism of anti-influenza action of arbidol. *Antiviral Res*. 2009;81(2):132–140. https://doi.org/10.1016/j.antiviral.2008.10.009

11. Goldhill D.H., Te Velthuis A.J.W., Fletcher R.A., Langat P., Zambon M., Lackenby A., Barclay W.S. The mechanism of resistance to favipiravir in influenza. *Proc. Natl. Acad. Sci. USA*. 2018;115(45):11613–11618. https://doi.org/10.1073/pnas.1811345115

12. Yang H., Winkler W., Wu X. Interferon Inducer IFI35 regulates RIG-I-mediated innate antiviral response through mutual antagonism with Influenza protein NS1. *J. Virol.* 2021;95(11):e00283–21. https://doi.org/10.1128/jvi.00283-21

13. Sa Ribero M., Jouvenet N., Dreux M., Nisole S. Interplay between SARS-CoV-2 and the type I interferon response. *PLoS Pathog*. 2020;16(7):e1008737. https://doi.org/10.1371/journal.ppat.1008737

14. Hauser P., Khosla J., Aurora H., Laurin J., Kling M.A., Hill J., Gulati M., Thornton A.J., Schultz R.L., Valentine A.D., Meyers C.A., Howell C.D. A prospective study of the incidence and open-label treatment of interferon-induced major depressive disorder in patients with hepatitis C. *Mol. Psychiatry*. 2002;7(9):942–947. https://doi.org/10.1038/sj.mp.4001119

15. Han J., Perez J., Schafer A., Cheng H., Peet N., Rong L., *et al*. Influenza virus: small molecule therapeutics and mechanisms of antiviral resistance. *Curr. Med. Chem*. 2018;25(38):5115–5127. https://doi.org/10.2174/0929867324666170920165926

16. Fire A.Z. Gene silencing by double-stranded RNA. *Cell Death Differ*. 2007;14(12):1998–2012. https://doi.org/10.1038/sj.cdd.4402253

17. Fire A., Xu S.Q., Montgomery M.K., Kostas S.A., Driver S.E., Mell C.C. Potent and specific genetic interference by double-stranded RNA in Caenorhabditis elegans. *Nature*. 1998;391(6669):806–811. https://doi.org/10.1038/35888

18. Estrin M.A., Hussein I.T.M., Puryear W.B., Kuan A.C., Artim S.C., Runstadler J.A. Host-directed combinatorial RNAi improves inhibition of diverse strains of influenza A virus in human respiratory epithelial cells. *PLoS One.* 2018;13(5):e0197246. https://doi.org/10.1371/journal.pone.0197246

19. Pashkov E.A., Korchevaya E.R., Faizuloev E.B., Pashkov E.P., Zvereva T.A. Rtishchev A.A., Poddubikov A.V., Svitich O.A., Zverev V.V. Creation of model for studying the antiviral effect of small interfering RNAs *in vitro*. *Sanitarnyi vrach*. 2022;1 (in Russ.). https://doi.org/10.33920/med-08-2201-07

20. Park H.S., Liu G., Thulasi Raman S.N., Landreth S.L., Liu Q., Zhou Y. NS1 Protein of 2009 Pandemic Influenza A Virus Inhibits Porcine NLRP3 Inflammasome-Mediated Interleukin-1 Beta Production by Suppressing ASC Uβiquitination. *J. Virol.* 201828;92(8):e00022–18. https://doi.org/10.1128/JVI.00022-18

21. Julkunen I., Melén K., Nyqvist M., Pirhonen J., Sareneva T., Matikainen S. Inflammatory responses in influenza A virus infection. *Vaccine*. 2000;19(Suppl. 1):S32–S37. https://doi.org/10.1016/S0264-410X(00)00275-9

22. Lee H.K, Loh T.P., Lee C.K., Tang J.W., Chiu L., Koay E.S. A universal influenza A and B duplex real-time RT-PCR assay. *J. Med. Virol*. 2012;84(10):1646–1651. https://doi.org/10.1002/jmv.23375

23. Piasecka J., Lenartowicz E., Soszynska-Jozwiak M., Szutkowska B., Kierzek R., Kierzek E. RNA Secondary Structure Motifs of the Influenza A Virus as Targets for siRNA-Mediated RNA Interference. *Mol. Ther. Nucleic Acids.* 2020;19:627–642. https://doi.org/10.1016/j.omtn.2019.12.018

About the authors:

Anastasia V. Pak, Student, Institute of Clinical Medicine, I.M. Sechenov First Moscow State Medical University (Sechenov University) (8, Trubetskaya ul., Moscow, 119991, Russia). E-mail: dcnnpk@gmail.com. https://orcid.org/0000-0003-4295-7858

Evgeny A. Pashkov, Postgraduate Student, A.A. Vorobiev Department of Microbiology, Virology and Immunology, I.M. Sechenov First Moscow State Medical University (Sechenov University) (8, Trubetskaya ul., Moscow, 119991, Russia); Junior Researcher, Laboratory of Molecular Immunology, Federal State Budgetary Scientific Institution "I. Mechnikov Research Institute of Vaccines and Sera" (5A, Malyi Kazennyi pereulok, Moscow, 105064, Russia). E-mail: pashckov.j@yandex.ru. RSCI SPIN-code 4933-1128, https://orcid.org/0000-0002-5682-4581

Natalia D. Abramova, Junior Researcher, Laboratory of Molecular Immunology, Federal State Budgetary Scientific Institution "I. Mechnikov Research Institute of Vaccines and Sera" (5A, Malyi Kazennyi pereulok, Moscow, 105064, Russia). E-mail: and960911@gmail.com. RSCI SPIN-code 1763-8942, https://orcid.org/0000-0002-7307-0515

Alexander A. Poddubikov, Cand. Sci. (Biol.), Head of the Laboratory of Microbiology of Opportunistic Pathogenic Bacteria, Federal State Budgetary Scientific Institution "I. Mechnikov Research Institute of Vaccines and Sera" (5A, Malyi Kazennyi pereulok, Moscow, 105064, Russia). E-mail: poddubikov@yandex.ru. RSCI SPIN-code 9658-1553, https://orcid.org/0000-0001-8962-4765

Firaya G. Nagieva, Dr. Sci. (Med.), Associate Professor, Head of the Laboratory of Hybrid Cell Cultures, Federal State Budgetary Scientific Institution "I. Mechnikov Research Institute of Vaccines and Sera" (5A, Malyi Kazennyi pereulok, Moscow, 105064, Russia). E-mail: fgn42@yandex.ru. RSCI SPIN-code 5897-3591, https://orcid.org/0000-0001-8204-4899

Ekaterina A. Bogdanova, Cand. Sci. (Med.), Associate Professor, A.A. Vorobiev Department of Microbiology, Virology and Immunology, I.M. Sechenov First Moscow State Medical University (Sechenov University) (8, Trubetskaya ul., Moscow, 119991, Russia). E-mail: bogdekaterin@yandex.ru. RSCI SPIN-code 7250-5808, https://orcid.org/0000-0002-5620-1843

Evgeny P. Pashkov, Dr. Sci. (Med.), Professor, A.A. Vorobiev Department of Microbiology, Virology and Immunology, I.M. Sechenov First Moscow State Medical University (Sechenov University) (8, Trubetskaya ul., Moscow, 119991, Russia). E-mail: 9153183256@mail.ru. https://orcid.org/0000-0002-4963-5053

Oxana A. Svitich, Corresponding Member of the Russian Academy of Sciences, Dr. Sci. (Med.), Head of the Federal State Budgetary Scientific Institution "I. Mechnikov Research Institute of Vaccines and Sera," Head of the Laboratory of Molecular Immunology, Federal State Budgetary Scientific Institution "I. Mechnikov Research Institute of Vaccines and Sera" (5A, Malyi Kazennyi pereulok, Moscow, 105064, Russia); Professor, A.A. Vorobiev Department of Microbiology, Virology and Immunology, I.M. Sechenov First Moscow State Medical University (Sechenov University) (8, Trubetskaya ul., Moscow, 119991, Russia). E-mail: svitichoa@yandex.ru. RSCI SPIN-code 8802-5569, https://orcid.org/0000-0003-1757-8389

Vitaliy V. Zverev, Full Member of the Russian Academy of Sciences, Dr. Sci. (Biol.), Scientific Director of the Federal State Budgetary Scientific Institution "I. Mechnikov Research Institute of Vaccines and Sera" (5A, Malyi Kazennyi pereulok, Moscow, 105064, Russia); Head of the A.A. Vorobiev Department of Microbiology, Virology and Immunology, I.M. Sechenov First Moscow State Medical University (Sechenov University) (8, Trubetskaya ul., Moscow, 119991, Russia). E-mail: vitalyzverev@outlook.com. RSCI SPIN-code 2122-1808, https://orcid.org/0000-0002-0017-1892

Об авторах:

Пак Анастасия Витальевна, студент, Институт клинической медицины им. Н.В. Склифосовского, Первый Московский государственный медицинский университет им. И.М. Сеченова Минздрава России (Сеченовский Университет) (119991, Россия, Москва, ул. Трубецкая, д. 8, с. 2). E-mail: dcnnpk@gmail.com. https://orcid.org/0000-0003-4295-7858

Пашков Евгений Алексеевич, аспирант, кафедра микробиологии, вирусологии и иммунологии им. академика А.А. Воробьева, Первый Московский государственный медицинский университет им. И.М. Сеченова Минздрава России (Сеченовский Университет) (119991, Россия, Москва, ул. Трубецкая, д. 8, с. 2); младший научный сотрудник, лаборатория молекулярной иммунологии, Научно-исследовательский институт вакцин и сывороток им. И.И. Мечникова (105064, Россия, Москва, Малый Казенный переулок, д. 5А). E-mail: pashckov.j@yandex.ru. SPIN-код РИНЦ 4933-1128, https://orcid.org/0000-0002-5682-4581

Абрамова Наталья Дмитриевна, младший научный сотрудник, лаборатория молекулярной иммунологии, Научно-исследовательский институт вакцин и сывороток им. И.И. Мечникова (105064, Россия, Москва, Малый Казенный переулок, д. 5А). E-mail: and960911@gmail.com. SPIN-код РИНЦ 1763-8942, https://orcid.org/0000-0002-7307-0515

Поддубиков Александр Владимирович, к.б.н., заведующий лабораторией микробиологии условно-патогенных бактерий, Научно-исследовательский институт вакцин и сывороток им. И.И. Мечникова (105064, Россия, Москва, Малый Казенный переулок, д. 5А). E-mail: poddubikov@yandex.ru. SPIN-код РИНЦ 9658-1553, https://orcid.org/0000-0001-8962-4765

Нагиева Фирая Галиевна, д.м.н., доцент, заведующий лабораторией гибридных клеточных культур, Научно-исследовательский институт вакцин и сывороток им. И.И. Мечникова (105064, Россия, Москва, Малый Казенный переулок, д. 5А). E-mail: fgn42@yandex.ru. SPIN-код РИНЦ 5897-3591, https://orcid.org/0000-0001-8204-4899

Богданова Екатерина Александровна, к.м.н., доцент кафедры микробиологии, вирусологии и иммунологии им. академика А.А. Воробьева, Первый Московский государственный медицинский университет им. И.М. Сеченова Минздрава России (Сеченовский Университет) (119991, Россия, Москва, ул. Трубецкая, д. 8, с. 2). E-mail: bogdekaterin@yandex.ru. SPIN-код РИНЦ 7250-5808, https://orcid.org/0000-0002-5620-1843

Пашков Евгений Петрович, д.м.н., профессор кафедры микробиологии, вирусологии и иммунологии им. академика А.А. Воробьева, Первый Московский государственный медицинский университет им. И.М. Сеченова Минздрава России (Сеченовский Университет) (119991, Россия, Москва, ул. Трубецкая, д. 8, с. 2). E-mail: 9153183256@mail.ru. https://orcid.org/0000-0002-4963-5053

Свитич Оксана Анатольевна, чл.-корр. Российской академии наук, д.м.н., директор, заведующий лабораторией молекулярной иммунологии, Научно-исследовательский институт вакцин и сывороток им. И.И. Мечникова (105064, Россия, Москва, Малый Казенный переулок, д. 5А); профессор кафедры микробиологии, вирусологии и иммунологии им. академика А.А. Воробьева, Первый Московский государственный медицинский университет им. И.М. Сеченова Минздрава России (Сеченовский Университет) (119991, Россия, Москва, ул. Трубецкая, д. 8, с. 2). E-mail: svitichoa@yandex.ru. SPIN-код РИНЦ 8802-5569, https://orcid.org/0000-0003-1757-8389

Зверев Виталий Васильевич, академик РАН, д.б.н., профессор, научный руководитель Научно-исследовательского института вакцин и сывороток им. И.И. Мечникова (105064, Россия, Москва, Малый Казенный переулок, д. 5А); заведующий кафедрой микробиологии, вирусологии и иммунологии им. академика А.А. Воробьева, Первый Московский государственный медицинский университет им. И.М. Сеченова Минздрава России (Сеченовский Университет) (119991, Россия, Москва, ул. Трубецкая, д. 8, с. 2). E-mail: vitalyzverev@outlook.com. SPIN-код РИНЦ 2122-1808, https://orcid.org/0000-0002-0017-1892

The article was submitted: July 19, 2022; approved after reviewing: August 30, 2022; accepted for publication: September 20, 2022.

Translated from Russian into English by H. Moshkov
Edited for English language and spelling by Thomas Beavitt

BIOCHEMISTRY AND BIOTECHNOLOGY

БИОХИМИЯ И БИОТЕХНОЛОГИЯ

ISSN 2686-7575 (Online)

https://doi.org/10.32362/2410-6593-2022-17-5-394-409

UDC 577.151.042; 546.23

RESEARCH ARTICLE

Thiol-dependent mechanisms of selenium-containing preparations and thiolylfluanide effect on electrolytes leaching and peroxidase activity in *Zea mays* L.

Pavel A. Poluboyarinov[1,✉], Natalia V. Shchetinina[1], Inessa Ya. Moiseeva[1], Nadezhda I. Mikulyak[1], Nadezhda A. Golubkina[2], Alexander P. Kaplun[3]

[1]Penza State University, Penza, 440026 Russia
[2]Federal Scientific Center of Vegetable Production, VNIISSOK, Moscow oblast, 143072 Russia
[3]MIREA – Russian Technological University (M.V. Lomonosov Institute of Fine Chemical Technologies), Moscow, 119571 Russia
[✉]Corresponding author, e-mail: poluboyarinovpavel@yandex.ru

Abstract

Objectives. *While organic and inorganic derivatives of selenium like thiol poisons are known to activate enzymes in cells of different organisms, the mechanism of enzyme activity induction is poorly studied. Therefore, the aim of the study was to investigate the effect of selenium compounds on peroxidase activity induction in maize tissues.*

Methods. *Mechanism of sulfhydryl groups blocking in selenium derivatives was studied on maize in comparison with fungicide tolylfluanid—a typical thiol poison. Electrolytes leakage was determined using conductometry and capillary electrophoresis, protein fractions—by the Ermakov–Durinina method, protein concentration—according to Bradford protein essay, and peroxidase activity—by the Boyarkin method.*

Results. *Diacetophenolylselenide (DAPS-25) was shown to react with SH-groups similarly with tolylfluanid fungicide. DAPS-25 increased K^+ and NH_4^+ leakage by 58 and 14 times, while appropriate increases for tolylfluanid were 4.4 and 1.5 times as compared to control. Increased*

total protein content—especially albumins—was due to electrolyte leakage from maize cells. DAPS-25 increased albumins concentration by 2.4–4.5 times, and tolylfluanid application by 2 times. Similar increase of peroxidase activity in maize roots and sprouts as a result of DAPS-25 (by 63% and 112%) and tolylfluanid (by 73% and 63%) application indicates close mechanism of their effect. Under DAPS-25 loading L-cysteine decreases peroxidase activity, which records the removal of SH-groups blockage. A less intensive effect was registered for sodium selenite and L-selenocystin, also capable of reacting with SH-groups. L-cysteine supplementation to DAPS-25 solution decreases selenium concentration in maize, indicating the decrease of selenium bioavailability.

Conclusions. *The results indicated that selenium containing compounds react with SH-groups of maize cells increasing electrolytes leakage, protein content and especially albumins resulting in the increase of peroxidase activity.*

Keywords: *diacetophenonyl selenide, tolylfluanid, Zea mays, peroxidase, electrolytes, proteins*

For citation: Poluboyarinov P.A., Shchetinina N.V., Moiseeva I.Ya., Mikulyak N.I., Golubkina N.A., Kaplun A.P. Thiol-dependent mechanisms of selenium-containing preparations and thiolylfluanide effect on electrolytes leaching and peroxidase activity in *Zea mays* L. *Tonk. Khim. Tekhnol. = Fine Chem. Technol*. 2022;17(5):394–409 (Russ., Eng.). https://doi.org/10.32362/2410-6593-2022-17-5-394-409

НАУЧНАЯ СТАТЬЯ

Тиолзависимые механизмы действия селеносодержащих препаратов и толилфлуанида на истечение электролитов и активность пероксидазы в растениях кукурузы (*Zea mays* L.)

П.А. Полубояринов[1,✉], Н.И. Щетинина[1], И.Я. Моисеева[1], Н.И. Микуляк[1], Н.А. Голубкина[2], А.П. Каплун[3]

[1]Пензенский государственный университет, Пенза, 440026 Россия
[2]Федеральный научный центр овощеводства, ВНИИССОК, Московская обл., 143086 Россия
[3]МИРЭА – Российский технологический университет (Институт тонких химических технологий им. М.В. Ломоносова), Москва, 119571 Россия
✉ *Автор для переписки, e-mail: poluboyarinovpavel@yandex.ru*

Аннотация

Цели. *Неорганические и органические соединения селена, как и ряд других тиоловых ядов, активируют ферменты в клетках разных организмов, однако механизм индукции ферментативной активности малоизучен, в связи с этим целью настоящей работы стало изучение механизма влияния соединений селена на индукцию активности фермента пероксидазы в тканях растений кукурузы.*

Методы. *Механизм блокирования сульфгидрильных групп (SH-групп) соединений селена исследовали на растениях кукурузы в сравнении с фунгицидом толилфлуанидом – классическим тиоловым ядом. Истечение электролитов определяли методом кондуктометрии и капиллярного электрофореза, фракции белков по методу Ермакова–Дурыниной, их концентрацию по Брэдфорду, активность пероксидазы по методу Бояркина.*

Результаты. *Было установлено, что диацетофенонилселенид (ДАФС-25) взаимодействовал с SH-групами, как и фунгицид толилфуанид, который является классическим органическим тиоловым ядом. ДАФС-25 стимулирует истечение катионов калия и аммония в 58 и 14 раз, а толилфлуанид в 4.4 и 1.5 раз в сравнении с контролем. Истечение электролитов из клеток растений кукурузы приводит к увеличению концентрации общего белка и особенно альбуминов. Концентрация альбуминов с ДАФС-25 возрастала в 2.4–4.5 раза, а с толилфлуанидом – в 2 раза. ДАФС-25 активировал фермент пероксидазу в корнях и надземной части кукурузы на 63% и 112%, а толилфлуанид на 73% и 63%, что говорит о схожем механизме их действия. L-цистеин снижает активность пероксидазы от действия ДАФС-25, т.е. снимает блокирование SH-групп. Слабее активируют пероксидазу Na_2SeO_3 и L-селеноцистин, которые также взаимодействуют с SH-группами. Содержание селена в растениях кукурузы уменьшается при добавлении L-цистеина в раствор с ДАФС-25, что говорит о снижении его поступления в растения.*

Выводы. *Исследования показали, что селенсодержащие вещества взаимодействуют с SH-группами клеток растений кукурузы, усиливая истечение электролитов и повышая концентрацию белков в тканях, особенно альбуминов, а, следовательно, увеличивая активность фермента пероксидазы.*

Ключевые слова: *диацетофенонилселенид, толилфлуанид, кукуруза, пероксидаза, электролиты, белки*

Для цитирования: Полубояринов П.А., Щетинина Н.И., Моисеева И.Я., Микуляк Н.И., Голубкина Н.А., Каплун А.П. Тиолзависимые механизмы действия селеносодержащих препаратов и толилфлуанида на истечение электролитов и активность пероксидазы в растениях кукурузы (*Zea mays* L.). *Тонкие химические технологии*. 2022;17(5):394–409. https://doi.org/10.32362/2410-6593-2022-17-5-394-409

INTRODUCTION

In recent years, the catalytic functions of the trace element selenium, which forms the active selenol sites of antioxidant enzymes—in the first place, four selenium-dependent glutathione peroxidases, selenium-containing peptides and proteins—have been widely studied [1].

Inorganic salts of selenium (sodium selenate and selenite) and organic selenium compounds: ebselen, 2-phenylbenzoselenazol-1,2-3(2n)-one)[2], selenopyran, 9-phenyl-sym-nona-hydro-10-selenaanthracene[1], diacetophenonyl selenide (DAPS-25), 1,5-diphenyl-3-selenapentadione-1,5 [3], (**I**), have an activating effect on a number of enzymes: catalase, peroxidase, superoxide dismutase, glutathione peroxidase (GPx) in plants [4–7], bacteria [8], insects [9], crustaceans [10], farm animals and birds [11, 12]. It should be especially noted that out of 27 organic selenium compounds and their 16 sulfur-containing analogs, the highest activity of phase **II** enzymes—quinone reductase (EC 1.6.5.5) and glutathione-S-transferase (EC 2.5.1.18)—was induced by 9 selenium-containing compounds: dimethyl diselenide, dibenzyl diselenide, diphenyl diselenide, benzyl selenol, benzene selenic acid, ebselen, 2,5-diphenyl selenophen, triphenylselenonium chloride, i.e., mainly those drugs that interact with sulfhydryl groups of mouse hepatoma cells (Hepa-1c1c7) with the formation of selenosulfide bonds [13]. However, the mechanisms of metabolism of organoselenium xenobiotics in biological media and their effect on the induction of enzyme activity are not well understood. It is known that at high concentrations, inorganic selenium compounds: selenite, sodium selenate, selenium oxide, act as thiol poisons to block the sulfhydryl groups of proteins [14, 15]. Such poisons acting in this way also include certain heavy metals: mercury, cadmium, and lead.

[1] Blinokhvatov A.F. *9-R-sim-nonahydro-10-oxa (chalcogen) anthracene and 9-R-sim-octahydro-10-oxonium (chalcogenonia) anthracene salts*. Dr. Sci. Thesis (Chem.). Saratov: SGU; 1993.

A relationship between electrolyte leakage in wheat root cell membrane damage by mercury chloride ($HgCI_2$) was shown to involve an increase in the concentration of malondialdehyde (MDA), along with activation of catalase, superoxide dismutase, peroxidase, and ascorbate peroxidase [16]. In contrast to plants not treated with selenium, where the level of enzyme activity is lower, rapeseed plants treated with sodium selenite demonstrated an increase in the activity of catalase and ascorbate peroxidase under stress and drought conditions [17].

The method of inhibitors is widely used to determine the mechanism of action of various drugs. The classic thiol poison is tolylfluanid (**IV**) (fungicide Euparen Multi 500 g/kg), which does not contain selenium. Regarding the mechanisms of action, it is known that it nonspecifically inhibits biochemical processes in which enzymes and coenzymes containing sulfhydryl groups and thiol-containing cellular components take part [18]. Like all thiol poisons, it increases the permeability of cell membranes and promotes the "leakage" of potassium ions from the cell [19].

The mechanism of increased activity of enzymes may be due to the synthesis of *de novo* isoenzymes, a change in the conformation of the enzyme molecule or prosthetic group under the influence of an inhibitor, or the catalytic effect of the trace element selenium on selenium-dependent enzymes. However, antioxidant defense enzymes (catalase, peroxidase, superoxide dismutase), which utilize peroxides and free radicals, do not belong to selenium-dependent enzymes. In most scientific studies, there is a relationship between the action of thiol poisons—heavy metal ions, selenium preparations—and the induction of the activity of various enzymes. This may be due to the leakage of electrolytes, i.e., modification of ion channels, aquaporins, and lead to an increase in protein concentration in the biomass, and, as a result, an increase in enzyme activity.

In connection with the above, the aim of the present study is to study the mechanism of the effect of selenium compounds on the induction of peroxidase enzyme activity in corn seedlings (*Zea mays* L.).

MATERIALS AND METHODS

Reagents and equipment

The following reagents were used in the work: hydrogen peroxide 30%, benzidine, L-cysteine hydrochloride, acetone (*Vekton*, Russia), DAPS-25 (*Sulfat*, Russia), tolylfluanid—Euparen Multi fungicide (*BASF*, Germany). The organoselenium xenobiotic DAPS-25 and tolylfluanid were dissolved in acetone and added to the Knop's solution[2]. Sodium selenite and L-selenocystin were dissolved in 0.1 M HCI (*Vekton*, Russia). Solvents—acetone (chemically pure) and hydrochloric acid (chemically pure) (*Vekton*, Russia)—were added to the control variants.

Determination of the electrical conductivity of distilled water and solutions was carried out on the conductometer Expert-002-2-6 (*AnalitPromPribor*, Russia) according to GOST 6709-72[3].

Determination of inorganic cations in water was carried out according to the M 01-31-2011[4] method using a Capel 105M capillary electrophoresis system (*LUMEX Group of Companies*, Russia).

Peroxidase activity was determined using a KFK-3 photometer (*ZOMZ*, Russia).

The study of the anatomy of corn root cells was carried out under a Levenhuk D320L microscope (*Levenhuk*, Russia).

Germination of corn seeds

Seeds of corn (*Zea mays* L.) varieties *Krasnodarsky 291 AMV* (*Gavrish*, Russia) and *Utrennyaya Pesnya* (*Gavrish*, Russia) were germinated for 3 days in a thermostat at a temperature of 25–26°C [20]. For experiments, seedlings with a root length of 1–2 cm were used. The roots of control seedlings were immersed in a Knop's solution or distilled water through a perforated plastic plate, while the experimental seedlings were immersed in a solution with the addition of preparations. The roots of the seedlings were kept either in the Knop's solution or distilled water during the entire time of the experiment (3 days).

To determine protein fractions (albumins, globulins, prolamins, and glutelins) and peroxidase activity, unseparated corn roots were immersed in Knop's solutions containing selenium-containing preparations and tolylfluanid in various concentrations for 3 days. Next, the seedling samples were divided into roots and aerial parts (hereinafter referred to as seedlings), crushed, ground, and centrifuged. Proteins were extracted according to the Ermakov–Durynina method [21]. The content of individual protein fractions was determined by the Bradford method [22]. The control was corn

[2] Chesnokov V.A., Bazyrina E.N., Bushueva T.M., Il'inskaya N.L. *Growing plants without soil*. Leningrad: Izd. Leningrad. Univ.; 1960. 170 p.

[3] GOST 6709-72. Interstate Standard. Distilled water. Specifications. Moscow: Standartinform; 2010.

[4] https://www.lumex.ru/complete_solutions/11ar03_01_02_1.php. Accessed April 18, 2020.

seedlings whose roots were in the Knop's solution without the addition of biologically active substances.

Peroxidase activity was determined by the Boyarkin method at a wavelength of 610 nm. This method is based on measuring the time during which a certain optical density is reached in an experimental solution (E = 0.250). The change in optical density for 1 s per 1 g of raw tissue was calculated. Benzidine was used as a substrate, the oxidation of which results in the formation of a blue compound [23].

The presence of elemental selenium was determined by a qualitative reaction according to Feigley and West [24]. The total selenium content in the roots and seedlings of corn was determined by the fluorimetric method with diaminonaphthalene.[5]

Statistical analysis was carried out using the Duncan test and the computer statistical program Excel.

RESULTS AND DISCUSSION

Influence of DAPS-25 and tolylfluanid on the outflow of electrolytes from the cells of the roots of corn plants

When DAPS-25 is added to the Knop's solution, a reaction occurs on the roots of corn seedlings with the formation of a red modification of elemental selenium (Fig. 1a). The formation of elemental selenium granules and strong plasmolysis revealed under microscopic examination indicates an increase in the permeability of cell membranes and the outflow of electrolytes from root cells. An increase in the permeability of cell membranes is characteristic of some thiol poisons [19].

Plasmolysis of maize root cells was also noted in the variant with tolylfluanid (Fig. 1b). Thus, the separation of the protoplast from the cell wall of the corn root is related to the presence of thiol poison in the Knop's solution.

Thiol poisons can disrupt the functioning of potassium channels [19] to cause the outflow of electrolytes from cells. To determine the outflow of electrolytes from root cells, distilled water was used as a nutrient solution instead of Knop's solution (Table 1).

Thus, according to Table 1, it can be judged that DAPS-25 promotes the outflow of electrolytes from root cells, increasing the permeability of cell membranes, causing plasmolysis. Determination of cations by capillary electrophoresis showed the presence of ammonium, potassium, sodium, magnesium and calcium ions (Table 2).

Analysis of electropherogram data and those given in Table 2 indicates that DAPS-25 stimulates the outflow from root cells mainly of potassium cations, as well as ammonium cations, whose similarity in terms of ionic radius to potassium ions [25] indicates a probable modification of the potassium ion channels of DAPS-25. Residues of the amino acid cysteine contained in potassium ion channels and aquaporins [26] increase sensitivity to the effects of thiol poisons such as mercury [27] and silver [28] ions, as well as to subsequent blocking of ion channels.

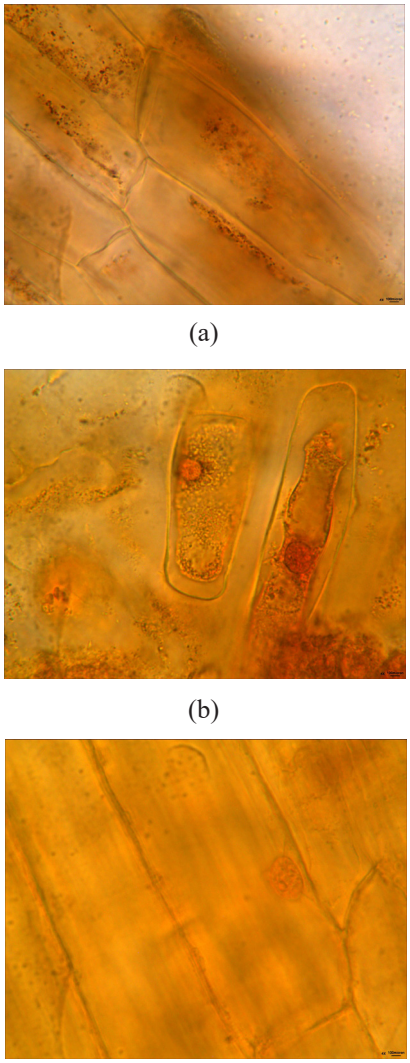

(a)

(b)

(c)

Fig. 1. Maize roots with 100× magnification: (a) DAPS-25 in Knop's solution (0.025 mg Se/L, 0.16 mM/L), (b) tolylfluanide (0.16 mM/L), (c) control.

[5] MUK 4.1.033-95. *Methods of control. Chemical factors. Determination of selenium in food. Methodical instructions*. Moscow: Inform.-izd. Tsentr Goskomsanepidemnadzora Rossii; 1995.

Table 1. Electrical conductivity of solution from roots of maize, *Krasnodarsky 291 AMV* (μS/cm^2)*

Days	Control, μS/cm	DAPS-25, 0.025 mg Se/L, μS/cm
3	2.13 ± 0.17 a	2.04 ± 0.14 a
4	13.61 ± 0.54 b	70.24 ± 3.51 b
6	12.97 ± 0.65 b	265.20 ± 26.52 c

*Values in columns with the same letters are not statistically different according to Duncan's test with a significance value of $p < 0.05$.

Table 2. Cations of solutions from roots of maize, *Krasnodarsky 291 AMV* (mg/L)*

Variants	Cations				
	NH_4^+	K^+	Na^+	Mg^{2+}	Ca^{2+}
Control	0.34 ± 0.01 a	3.57 ± 0.04 a	1.82 ± 0.04 a	0.37 ± 0.01 a	0.96 ± 0.013 a
DAPS-25	19.72 ± 0.78 b	52.17 ± 1.56 b	4.69 ± 0.15 b	7.22 ± 0.02 b	4.84 ± 0.17 b
Multiplicity of increase in the expiration of cations, DAPS-25, times	58.0	14.6	2.6	19.5	5.0

*Values in columns with different letters are significantly different at $p < 0.001$.

The outflow of electrolytes from the root cells occurred similarly in the experiment with another variety of corn with the addition of DAPS-25 and tolylfluanid (Table 3).

The outflow of electrolytes in this experiment was most active in the variant with DAPS-25 and to a much lesser extent in the variant with tolylfluanid. Capillary electrophoresis analysis also demonstrated the presence of ammonium, potassium, sodium, magnesium and calcium ions (Table 4).

The outflow of ammonium ions from the cells of corn roots is 42 and 1.5 times higher than the control in the variants with DAPS-25 and tolylfluanid, while the outflow of potassium ions is 16.7 and 4.4 times higher, respectively. The outflow of sodium and calcium ions is 3.6 and 1.9 times higher in the

Table 3. Electrical conductivity of solution from roots of maize, *Utrennyaya Pesnya* (μS/cm^2)*

Days	Control	DAPS-25, 0.025 mg Se/L, 0.16 mmol/L	Tolylfluanid, 0.16 mmol/L
3	2.047 ± 0.08	1.890 ± 0.1	1.789 ± 0.05
6	6.12 ± 0.36	101.7 ± 6.1	21.79 ± 1.1

*Values with the same indices do not differ statistically according to the Duncan's test at $p < 0.05$.

Table 4. Electrolyte cations of solution from roots of maize, *Utrennyaya Pesnya* (mg/L)*

Variants	Cations				
	NH_4^+	K^+	Na^+	Mg^{2+}	Ca^{2+}
Control	0.164 ± 0.01 a	1.16 ± 0.04 a	0.268 ± 0.04 a	0.41 ± 0.01 a	1.76 ± 0.01 a
DAPS-25	6.90 ± 0.78 b	19.36 ± 1.56 b	0.96 ± 0.15 b	3.58 ± 0.02 b	3.39 ± 0.17 b
Tolylfluanid	0.25 ± 0.03 c	5.10 ± 0.15 c	0.56 ± 0.01 c	0.77 ± 0.02 c	2.26 ± 0.05 c
Multiplicity increase in the expiration of cations, DAPS-25/tolylfluanid, times	42.0/1.52	16.7/4.4	3.56/2.0	8.7/1.88	1.9/1.3

*Values in columns with different letters are statistically different according to Duncan's test at $p < 0.05$.

variants with DAPS-25 and tolylfluanid. The concentration of magnesium ions in the solution is 8.7 and 1.9 times higher in the variants with DAPS-25 and tolylfluanid compared to the control. In general, tolylfluanid is more ion channel selective than DAPS-25 and promotes efflux mainly of potassium cations. The absence of protein in the studied solutions indicates that the cell walls of the plant roots have remained intact.

In our studies, DAPS-25 (**I**) interacts with reduced glutathione and L-cysteine to form elemental selenium and acetophenone (**II**) [29–31]. As a result of the first reaction, acetophenone and S-(acetophenylselenyl) cysteine (**III**) are formed (Fig. 2). This selenosulfide compound (**III**) is detected by high performance liquid chromatography. A similar substance—S-(acetophenylselenyl)glutathione—is formed by the interaction of reduced glutathione and DAPS-25.

It is possible that DAPS-25 interacts with cysteine residues in aquaporins and potassium channels, increasing the water permeability of corn root cell membranes (Fig. 3a).

The outflow of electrolytes from plant cells and their plasmolysis upon the addition of

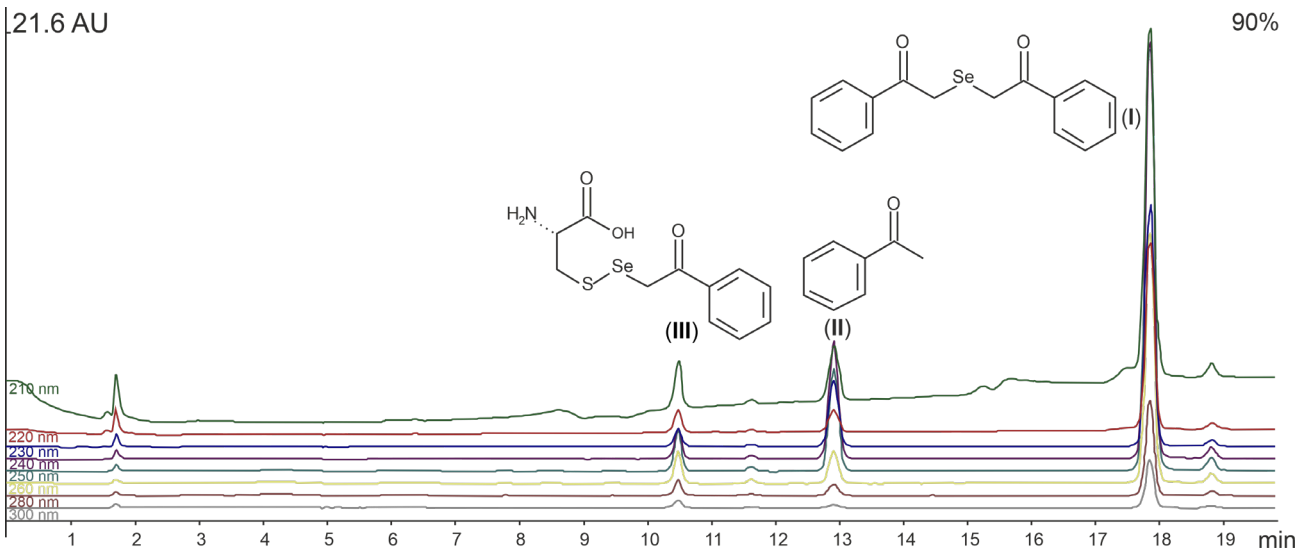

Fig. 2. Chromatogram of a reaction mixture obtained in DAPS-25 and cysteine interaction (molar ratio 1:1, pH 7.0).

tolylfluanid (**IV**) additionally indicates the general mechanism of action of both substances in the modification of ion channels (Fig. 3b).

Influence of DAPS-25 and tolylfluanid on the content and fractions of proteins in corn plants

With the loss of electrolytes and dehydration of the body, an increase in the concentration of proteins and, first of all, albumins is observed [32]. It is known that the total protein of plants includes albumins and prolamins—mainly low molecular weight, water-soluble and alcohol-soluble proteins, as well as globulins—proteins soluble in salt solutions. The last group of so-called storage high-molecular proteins are alkali-soluble proteins—glutelins.

The outflow of electrolytes from the cells of corn plants causes their dehydration and increases the concentration of proteins in them (Fig. 4).

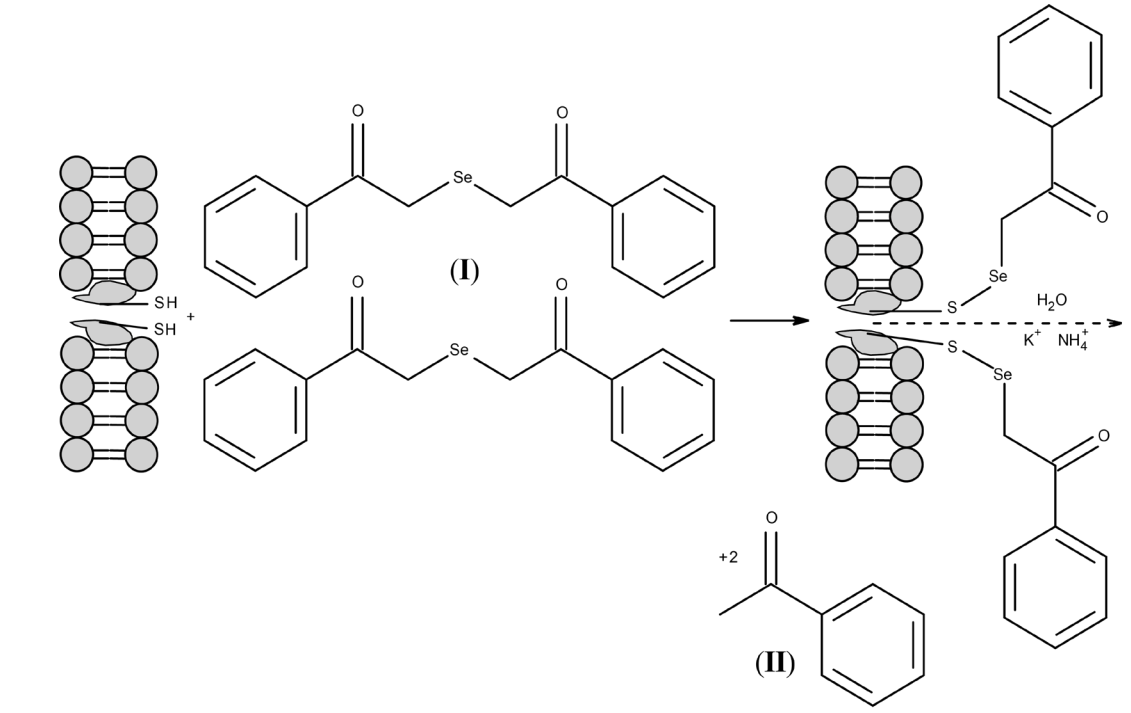

(a)

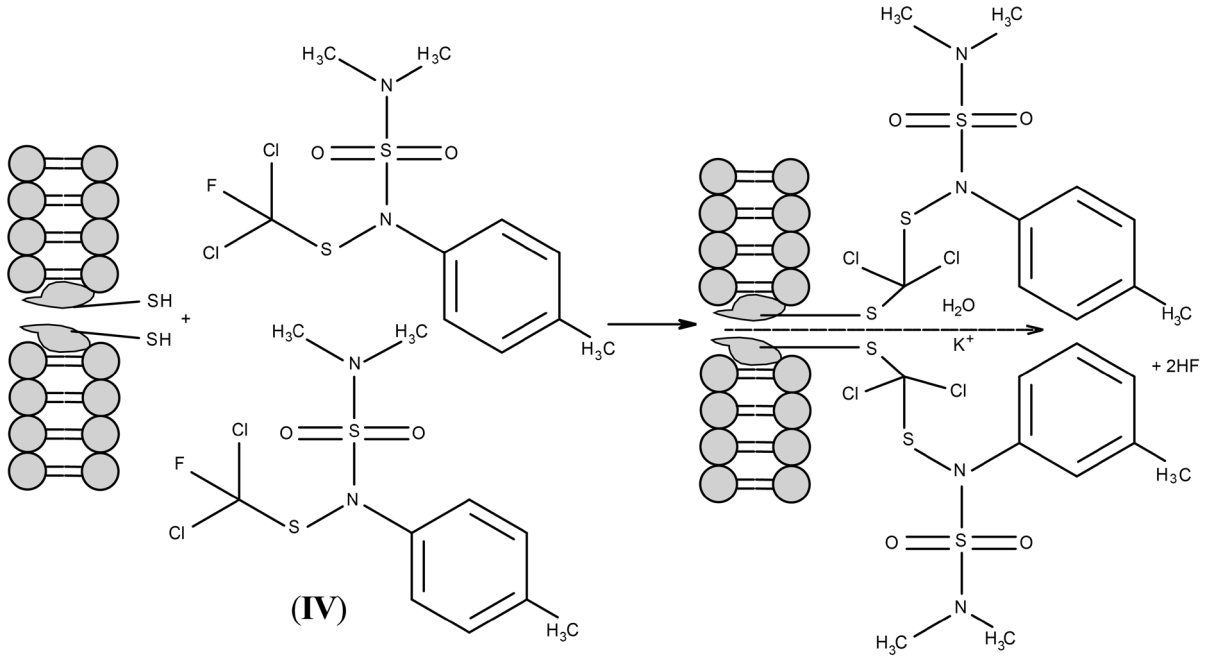

(b)

Fig. 3. Interaction of DAPS-25 (a) and tolylfluanide (b) with sulfhydryl groups in ionic channels of maize cells.

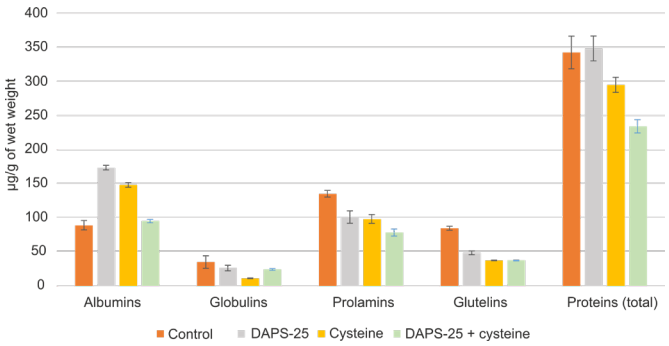

(a)

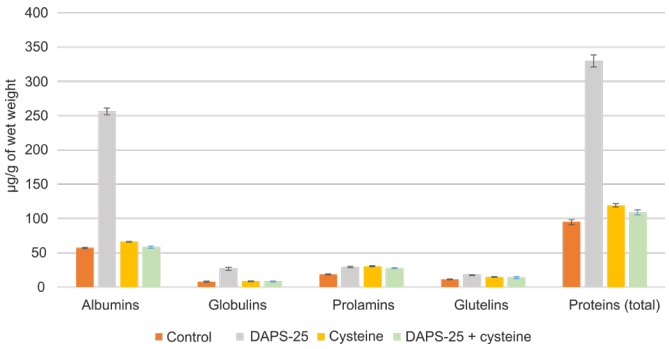

(b)

Fig. 4. Effect of DAPS-25, cysteine, and their mixture on quantitative composition of protein fractions in roots (a) and sprouts (b) of maize seedlings (*Krasnodarsky 291 AMV*).

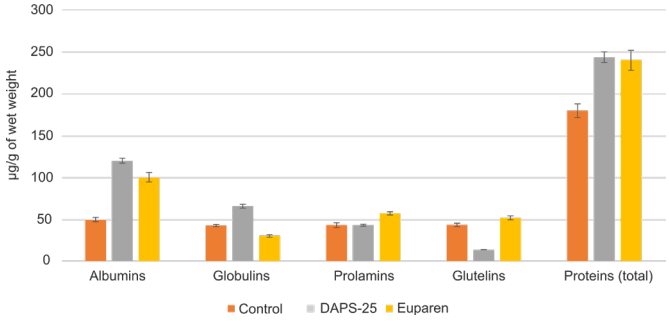

(a)

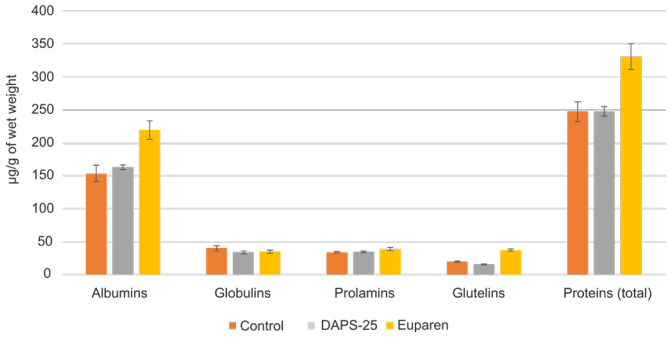

(b)

Fig. 5. Effect of DAPS-25 and tolylfluanide on quantitative composition of protein fractions in roots (a) and sprouts (b) of maize seedlings (*Utrennyaya Pesnya*).

DAPS-25 increased the content of albumins in the aerial part by 4.5 times, globulins by 3.5 times, prolamins and glutelins by 1.5 times, and total protein by 3.5 times. Apparently, DAPS-25 causes dehydration of corn root cells due to the loss of electrolytes, which leads to an increase in the concentration of proteins. In another experiment, with tolylfluanid and DAPS-25, there was also an increase in the albumin fraction and the concentration of total protein in the roots and aerial parts of corn seedlings (Fig. 5).

As in the previous study, the content of albumin in the roots in the variant with DAPS-25 increased by 2.4 times, with tolylfluanid by 2 times. In the aerial part, the content of albumins changed less significantly: in the variant with DAPS-25 it increased by 6%, with tolylfluanid by 1.4 times. The concentration of other protein fractions changes less significantly.

Thus, in the variants with thiol poisons—DAPS-25 and tolylfluanid—the content of the albumin fraction and total protein increased both in the roots and in the above-ground mass of plants, which indicates their dehydration.

The antidote of thiol poisons is the amino acid L-cysteine, which contains a sulfhydryl group. The addition of L-cysteine to a Knop's solution containing DAPS-25 showed that the content of the albumin fraction and total protein in corn plants differed from the control by no more than 10–20%. L-cysteine leveled the effect of DAPS-25 (Fig. 5), i.e., was its antidote.

Effect of DAPS-25 and tolylfluanid on peroxidase activity in corn plants

An increase in the protein content in plant tissues due to the loss of electrolytes under the influence of thiol poisons should also lead to a higher enzyme protein content, and, as a result, an increase in their activity. DAPS-25 had a significant effect on peroxidase activity in both roots and seedlings of corn (Figs. 6a and 6b).

DAPS-25 sharply stimulated the activity of the enzyme in almost all concentrations. The most significant increase in peroxidase activity was observed on the first day under the action of the highest concentration of DAPS-25, 0.025 mg Se/L (63% in the roots and 112% in the aerial part), a less significant increase was observed at a concentration

of 0.0025 mg Se/L (29% in the roots and 57% in the aerial part). At the conclusion of the experiment, DAPS-25 at a concentration of 0.00025 mg Se/L had a stimulating effect on peroxidase activity in the variant with roots, 29% (Fig. 7a), but a weakly inhibitory effect in seedlings, 8.6% (Fig. 7b). In the control, during the experiment, peroxidase activity in seedlings changed little, but slightly increased in the roots.

Similarly to the other maize variety, an increase in peroxidase activity in the variant with DAPS-25 was noted as compared to the control (Figs. 7c and 7d). In corn roots, peroxidase activity in the variant with tolylfluanid is 73% higher, while with DAPS-25, it is 36% higher than the control. In the aerial part variant at the beginning of the experiment, peroxidase activity is higher with tolylfluanid by 60%, while at the end of the experiment in the variant with DAPS-25 it is 95% higher. Thus, tolylfluanid, having a similar mechanism of action to that of DAPS-25, increases the activity of peroxidase.

It is known that thiol-dependent redox mechanisms can modulate the activity of the adenosine triphosphate-dependent K^+ channel in the pancreatic beta cell [33]. Oxidation of sulfhydryl groups with mercury-containing thimerosal and 2,2'-dithio-bis-(5-nitropyridine) (DTBNP) at micromolar concentrations causes rapid blocking of the channel, which is reversible by thiols, dithiothreitol and cysteine. Moreover, an excess of thiols restores the functioning of aquaporins blocked by ions of mercury, silver, and other heavy metals [26–28]. Apparently, DAPS-25, interacting with sulfhydryl groups, blocks ion channels, leading to the outflow of electrolytes from the cell (Tables 2 and 4) and consequent increase in protein concentration (Figs. 5 and 6) and activity peroxidase (Fig. 7). Accordingly, an excess of L-cysteine should restore the functioning of ion channels to prevent the outflow of electrolytes from the cell, reducing the concentration of proteins almost to control values along with the peroxidase activity.

In our study, the amino acid L-cysteine reduces the activity of peroxidase both in the roots and in the aerial parts of corn (Figs. 7a and 7b).

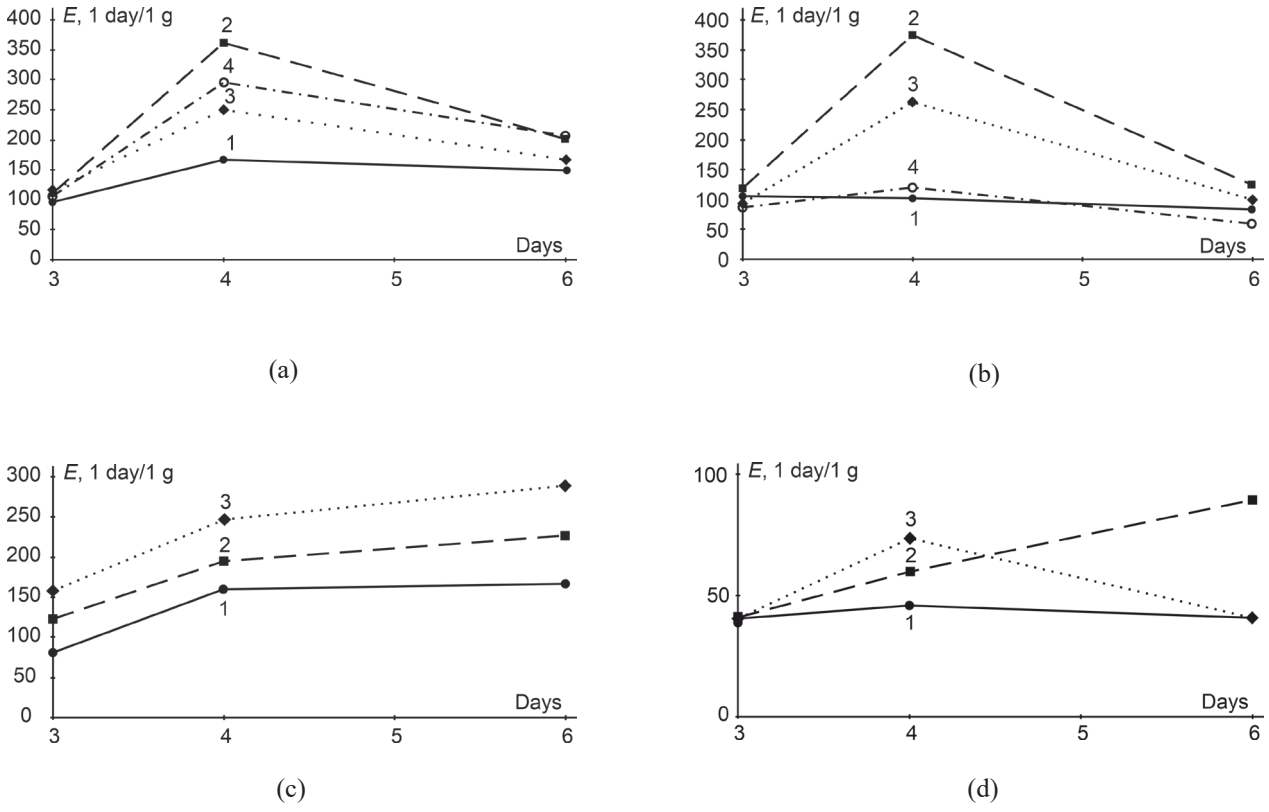

Fig. 6. Effect of DAPS-25 on peroxidase activity in roots (a) and sprouts (b) on maize seedlings (*Krasnodarsky 291 AMV*). 1 – Control; 2 – 0.025 mg Se/L; 3 – 0.0025 mg Se/L; 4 – 0.00025 mg Se/L. Effect of DAPS-24 and tolylfluanides on peroxidase activity in roots (c) and sprouts (d) of maize seedlings (*Utrennyaya Pesnya*). 1 – Control; 2 – DAPS-25 (0.025 mg Se/L); 3 – tolylfluanide. The ordinate is the change in optical density (E_{610}); the abscissa axis is the processing time, starting from 3 days from the moment of the beginning of the corn germination.

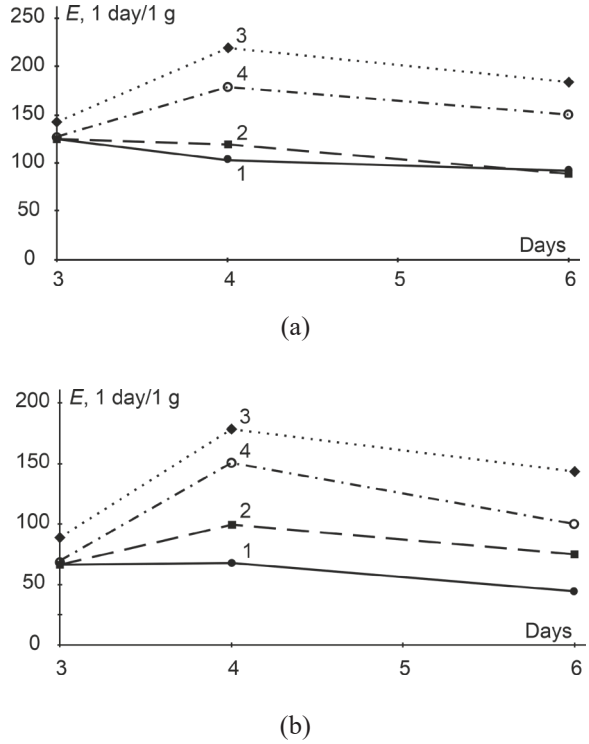

Fig. 7. Changes in peroxidase activity in roots (a) and sprouts (b) of maize seedlings treated with DAPS-25 and L-cysteine. The ordinate is the change in optical density (E_{610}); the abscissa axis is the processing time, starting from 3 days from the moment of the beginning of the corn germination. 1 – Control; 2 – 0.1% L-cysteine; 3 – 0.025 mg Se/L DAPS-25; 4 – 0.025 mg Se/L DAPS-25 + 0.1% L-cysteine.

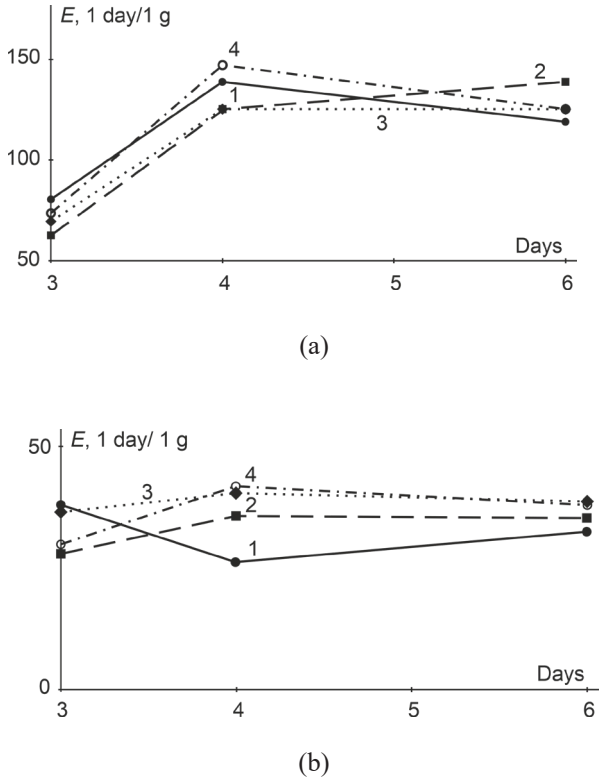

Fig. 8. Effect of sodium selenite Na_2SeO_3 on peroxidase activity in roots (a) and sprouts (b) of maize seedlings. The ordinate is the change in optical density (E_{610}); the abscissa axis is the processing time, starting from 3 days from the moment of the beginning of the corn germination. 1 – Control; 2 – 0.025 mg Se/L; 3 – 0.0025 mg Se/L; 4 – 0.00025 mg Se/L.

In this experiment, peroxidase showed the highest activity on the first day in the variant with DAPS-25 at a concentration of 0.025 mg Se/L; this was true both of the roots and the aerial parts (exceeding the control by 69% and 129%, respectively). In a mixture of DAPS-25 (0.025 mg Se/L) with L-cysteine (0.1%), there was a significant decrease in peroxidase activity to 42% and 79% in comparison with the variant where only DAPS-25 was added. A decrease in peroxidase activity indicates a decrease in the blocking effect of DAPS-25 on ion channels in maize plant cells to reduce electrolyte outflow and lower protein concentration, including the peroxidase enzyme.

A similar, but much weaker effect on the increase in peroxidase activity is exerted by an inorganic salt of selenium, sodium selenite, in the roots (Fig. 8a) and aboveground parts of corn plants (Fig. 8b), which also interacts with sulfhydryl groups like DAPS-25 to form selenodisulfides [34].

In general, starting from the highest (0.025 mg Se/L) and low concentrations (0.00025 mg Se/L), all concentrations of sodium selenite slightly stimulated peroxidase activity in the roots; this effect was closer towards the end of the experiment and somewhat stronger in the aerial part of corn seedlings. It is likely that the relatively weak stimulation of peroxidase activity is associated with the difficulty of transporting the negatively charged selenite ion into the cell interior. For example, thimerosal, which is poorly permeable to membranes, inhibits channel activity only when applied to the intracellular surface of the plasma membrane. On the contrary, DTBNP, which is a lipophilic substance, causes potassium channel blocking and, as a result, membrane potential depolarization even when applied extracellularly [35].

In the experiment with the amino acid L-selenocystin, which also interacts with sulfhydryl groups, peroxidase-like activity was increased by 8.8–30.3% both in the roots and in the aerial part of the plant throughout the entire experiment (Fig. 9.).

The lowest concentration of L-selenocystin (0.00025 mg Se/L) weakly stimulates peroxidase activity in the roots and aerial parts of corn seedlings.

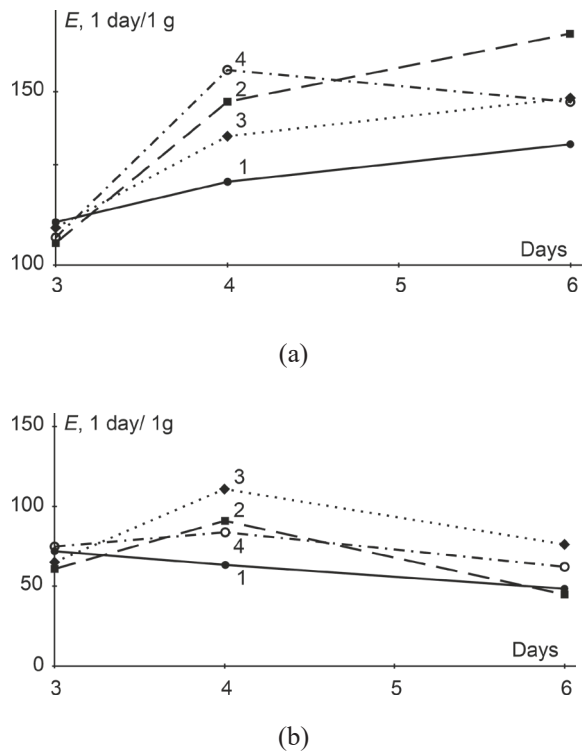

Fig. 9. Effect of L-selenocystine (Sec) on peroxidase activity in roots (a) and sprouts (b) of maize seedlings. The ordinate is the change in optical density (E_{610}); the abscissa axis is the processing time, starting from 3 days from the moment of the beginning of the corn germination. 1 – Control; 2 – 0.025 mg Se/L; 3 – 0.0025 mg Se/L; 4 – 0.00025 mg Se/L.

A more significant increase in peroxidase activity is observed under the action of an average concentration (0.0025 mg Se/L) and to a lesser extent under the action of a high concentration (0.025 mg Se/L) in the aerial part of corn seedlings.

The data obtained demonstrate a similar relationship between the increase in peroxidase activity in selenite- and L-selenocystin-treated corn seedlings. Evidently, the amino acid L-selenocystin enters the cell more easily due to being a less polar compound than selenite; by interacting with the sulfhydryl groups of the cell, it causes a stronger induction of peroxidase activity compared to the inorganic selenium salt.

The total selenium content in the roots of corn seedlings also depends on the presence of thiols in the solution. It is maximum in the variant with DAPS-25 and significantly lower in the variant of combined use of DAPS-25 and L-cysteine (Table 5).

A decrease in the total selenium content indicates a decrease in the intake of DAPS-25 into the plant due to the presence of exogenous sulfhydryl groups of L-cysteine in solution, but not in the tissues of the roots of corn seedlings, which also confirms the effect of the sulfur-containing amino acid as an antidote for thiol poisons.

CONCLUSIONS

The conducted studies showed that the thiol-dependent redox mechanisms of action of DAPS-25 and the organic thiol poison tolylfluanid increase the water permeability of corn root cell membranes, which leads to electrolyte leakage. The action of thiol poisons leads to plasmolysis of maize plant cells and an increase in the concentration of proteins, primarily albumins. An increase in the content of proteins in plant biomass leads to an increase in the concentration of the enzyme and consequent increase in peroxidase activity. The addition of a thiol, L-cystine, to a solution containing DAPS-25 leads to a decrease in the concentration of proteins in plant biomass and a decrease in peroxidase activity. While sodium selenite and L-selenocystin interact with sulfhydryl groups of peroxidase cells to increase peroxidase activity in a similar manner to lipophilic DAPS-25 and tolylfluanid, the effect is much weaker.

Authors' contributions

P.A. Poluboyarinov, N.V. Shchetinina, N.A. Golubkina – conducting the experiments;

P.A. Poluboyarinov, I.Ya. Moiseeva, N.I. Mikulyak – writing the text of the article and the analysis of the obtained results;

N.A. Golubkina, A.P. Kaplun, I.Ya. Moiseeva – scientific editing;

P.A. Poluboyarinov, A.P. Kaplun – idea of the study and general management.

The authors declare no obvious and potential conflicts of interest related to the publication of this article.

Table 5. Selenium content in roots and sprouts of maize seedlings (μg/kg of dry weight)

Plant part	Control	DAPS-25 0.025 mg Se/L	DAPS-25 0.025 mg Se/L + cysteine, 0.1%
Roots	40 ± 3 a	19300 ± 428 c	4853 ± 167 e
Sprouts	53 ± 4 b	5099 ± 278 d	4812 ± 135 e

REFERENCES

1. Behn D., Weiss-Nowak C., Kalcklösch M., Westphal C., Gessner H., Kyriakopoulos A. Studies on the distribution and characteristics of new mammalian selenium-containing proteins. *Analyst*. 1995;120(3):823–825. https://doi.org/10.1039/an9952000823

2. Sies H. Ebselen, a selenoorganic compound as glutathione peroxidase mimic. *Free Radic. Biol. Med.* 1993;14(3):313–323. https://doi.org/10.1016/0891-5849(93)90028-s

3. Drevko B.I., Antipov V.A., Zhukov O.I., *et al*. *Means for the treatment and prevention of diseases caused by selenium deficiency in the body of farm animals and birds*: RF Pat. 2051681. Publ. 10.01.1996. (in Russ.).

4. Usubova E.Z., Zhizhaev A.M., Mironov P.V. Effect of selenium on physiological parameters and efficiency of bean (*Phaseolus vulgaris* L.). *Fundamental'nye issledovaniya = Fundamental Research*. 2012;(3):257–260 (in Russ.).

5. Poluboyarinov P.A., Golubkina N.A. Investigation of the biochemical function of selenium and its influence on the content of protein fractions and peroxidase activity in maize seedlings. *Russ. J. Plant Physiol*. 2015;62(3):367–374. https://doi.org/10.1134/S1021443715030164

6. Castillo-Godina R.G., Foroughbakhch-Pournavab R., Benavides-Mendoza A. Effect of selenium on elemental concentration and antioxidant enzymatic activity of tomato plants. *J. Agr. Sci. Tech*. 2016;18(1):233–244.

7. Huang C., Qin N., Sun L., Yu M., Hu W., Qi Z. Selenium improves physiological parameters and alleviates oxidative stress in strawberry seedlings under low-temperature stress. *Int. J. Mol. Sci*. 2018;19(7):1900–1913. https://doi.org/10.3390/ijms19071913

8. Bebien M., Lagniel G., Garin J., Touati D., Vermeglio A., Labarre J. Involvement of superoxide dismutases in the response of *Escherichia coli* to selenium oxides. *J. Bacteriol.* 2002;184(6):1556–1564. https://doi.org/10.1128/jb.184.6.1556-1564.2002

9. Strogov V.V., Rodionova T.N. Influence of selenium on the functional state and economic parameters of honeybee colonies. *Vestnik veterinarii*. 2011;59(4):150–152 (in Russ.).

10. Wang H.W., Cai D.B., Xiao G.H., Zhao C.L., Wang Z.H., Xu H.M., Guan Y.Q. Effects of selenium on the activity of antioxidant enzymes in the shrimp, *Neocaridina heteropoda*. *The Israeli Journal of Aquaculture – Bamidgeh*. 2009;61(4):322–332.

11. Boryaev G.I., Gavryushina I.V., Fedorov Yu.N. Biochemical and physiological status of lambs in early postnatal ontogenesis against the background of selenium compounds injections to ewe in yean. *Sel'skokhozyaistvennaya biologiya = Agricultural Biology*. 2010;45 (2):65–70 (in Russ.).

12. Dzobo K., Naik Y.S. Effect of selenium on cadmium-induced oxidative stress and esterase activity in rat organs. *South Afr. J. Sci.* 2013;109(5–6):1–8. https://doi.org/10.1590/sajs.2013/965

13. Xiao H., Parkin K.L. Induction of phase II enzyme activity by various selenium compounds. *Nutr. Cancer*. 2006;55(2):210–223. https://doi.org/10.1207/s15327914nc5502_13

14. Filov V.A. Bandman A.L. Volkova N.V. Grekhova T.D. *Vrednye khimicheskie veshchestva. Neorganicheskie soedineniya elementov V–VIII grupp* (*Harmful Chemical Substances. Inorganic Compounds of Elements of V–VIII groups*). Leningrad: Khimiya; 1989. P. 263–282 (in Russ.).

СПИСОК ЛИТЕРАТУРЫ

1. Behn D., Weiss-Nowak C., Kalcklösch M., Westphal C., Gessner H., Kyriakopoulos A. Studies on the distribution and characteristics of new mammalian selenium-containing proteins. *Analyst.* 1995;120(3):823–825. https://doi.org/10.1039/an9952000823

2. Sies H. Ebselen, a selenoorganic compound as glutathione peroxidase mimic. *Free Radic. Biol. Med.* 1993;14(3):313–323. https://doi.org/10.1016/0891-5849(93)90028-s

3. Древко Б.И., Антипов В.А., Жуков О.И. и др. *Средство для лечения и профилактики болезней, вызываемых недостаточностью селена в организме сельскохозяйственных животных и птиц*: пат. 2051681 РФ. Заявка № 93045743/15, заявл. 24.09.1993; опубл. 10.01.1996.

4. Усубова Е.З., Жижаев А.М., Миронов П.В. Влияние селена на физиологические показатели и продуктивность фасоли сорта «сакса» (*Phaseolus vulgaris* L.). *Фундаментальные исследования*. 2012;(3):257–260.

5. Полубояринов П.А., Голубкина Н.А. Изучение биохимической функции селена и его влияние на содержание белковых фракций и активность пероксидазы в проростках кукурузы. *Физиология растений.* 2015;62(3):396–403. https://doi.org/10.7868/S0015330315030161

6. Castillo-Godina R.G., Foroughbakhch-Pournavab R., Benavides-Mendoza A. Effect of selenium on elemental concentration and antioxidant enzymatic activity of tomato plants. *J. Agr. Sci. Tech.* 2016;18(1):233–244.

7. Huang C., Qin N., Sun L., Yu M., Hu W., Qi Z. Selenium improves physiological parameters and alleviates oxidative stress in strawberry seedlings under low-temperature stress. *Int. J. Mol. Sci*. 2018;19(7):1900–1913. https://doi.org/10.3390/ijms19071913

8. Bebien M., Lagniel G., Garin J., Touati D., Vermeglio A., Labarre J. Involvement of superoxide dismutases in the response of *Escherichia coli* to selenium oxides. *J. Bacteriol.* 2002;184(6):1556–1564. https://doi.org/10.1128/jb.184.6.1556-1564.2002

9. Строгов В.В., Родионова Т.Н. Влияние селена на функциональное состояние и хозяйственно-полезные качества пчелиных семей. *Вестник ветеринарии.* 2011;59(4):150–152.

10. Wang H.W., Cai D.B., Xiao G.H., Zhao C.L., Wang Z.H., Xu H.M., Guan Y.Q. Effects of selenium on the activity of antioxidant enzymes in the shrimp, *Neocaridina heteropoda*. *The Israeli Journal of Aquaculture – Bamidgeh.* 2009;61(4):322–332.

11. Боряев Г.И., Гаврюшина И.В., Федоров Ю.Н. Биохимический и физиологический статус ягнят в раннем постнатальном онтогенезе на фоне инъекций соединений селена суягным овцематкам. *Сельскохозяйственная биология.* 2010;45(2):65–70.

12. Dzobo K., Naik Y.S. Effect of selenium on cadmium-induced oxidative stress and esterase activity in rat organs. *South Afr. J. Sci.* 2013;109(5–6):1–8. https://doi.org/10.1590/sajs.2013/965

13. Xiao H., Parkin K.L. Induction of phase II enzyme activity by various selenium compounds. *Nutr. Cancer*. 2006;55(2):210–223. https://doi.org/10.1207/s15327914nc5502_13

14. Филов В.А. Бандман А.Л. Волкова Н.В. Грехова Т.Д. *Вредные химические вещества. Неорганические соединения элементов V–VIII групп*. Химия: Ленинград; 1989. С. 263–282.

15. Avtsin A.P., Zhavoronkov A.A., Rish M.A., Strochkova L.S. *Mikroelementozy cheloveka* (*Human Microelementoses*). Moscow: Meditsina; 1991. P. 196–231 (in Russ.).

16. Sahu G.K., Upadhyay S., Sahoo B.B. Mercury induced phytotoxicity and oxidative stress in wheat (*Triticum aestivum* L.) plants. *Physiol. Mol. Biol. Plants*. 2012;18(1):21–31. https://doi.org/10.1007/s12298-011-0090-6

17. Sofo A., Scopa A., Nuzzaci M., Vitti A. Ascorbate peroxidase and catalase activities and their genetic regulation in plants subjected to drought and salinity stresses. *Int. J. Mol. Sci*. 2015;16(6):13561–13578. https://doi.org/10.3390/ijms160613561

18. Golyshin N.M. *Fungitsidy* (*Fungicides*). Moscow: Kolos; 1993. 318 p. (in Russ.).

19. Yoshida M., Yokimoto M. Effects of fungicides on channels in the fungal membrane. *Pesticide Biochemistry and Physiology*. 1993;47(3):171–177. https://doi.org/10.1006/pest.1993.1076

20. Dudka I.A., Vasser S.P. *Metody eksperimental'noi mikologii* (*Experimental mycology methods*). Kiev: Naukova Dumka; 1982. 550 p. (in Russ.).

21. Mineev V.G., Sychev V.G., Amel'yanchik O.A., Bolysheva T.N., Gomonova N.F., Durynina E.P., Egorov B.C., Egorova E.V., Edemskaya N.L., Karpova E.A., Prizhukova V.G. *Praktikum po agrokhimii* (*Practical work on agrochemistry*). Moscow: MGU; 2001. 689 p. (in Russ.).

22. Bradford M.M. A rapid and sensitive method for the quantitation of microgram quantities of protein utilizing the principle of protein-dye binding. *Anal. Biochem*. 1976;72(1–2):248–254. https://doi.org/10.1006/abio.1976.9999

23. Gavrilenko V.F., Ladygina M.E., Khandobina L.M. *Bol'shoi praktikum po fiziologii rastenii. Fotosintez. Dykhanie* (*A Large Workshop on Plant Physiology. Photosynthesis. Breath*). Moscow: Vysshaya shkola; 1975. 392 p. (in Russ.).

24. Nazarenko I.I., Ermakov A.N. *Analiticheskaya khimiya selena i tellura* (*Analytical Chemistry of Selenium and Tellurium*). Moscow: Nauka; 1971. 248 p. (in Russ.).

25. Ugai Ya.A. *Neorganicheskaya khimiya* (*Inorganic Chemistry*). Moscow: Vysshaya shkola; 1989. 463 p. (in Russ.).

26. Bienert G.P., Cavez D., Besserer A., Berny M.C., Gilis D., Rooman M., Chaumont F. A conserved cysteine residue is involved in disulfide bond formation between plant plasma membrane aquaporin monomers. *Biochem. J.* 2012;445(1):101–111. https://doi.org/10.1042/bj20111704

27. Frick A., Järvå M., Ekvall M., Uzdavinys P., Nyblom M., Törnroth-Horsefield S. Mercury increases water permeability of a plant aquaporin through a non-cysteine-related mechanism. *Biochem. J.* 2013;454(3):491–499. https://doi.org/10.1042/bj20130377

28. Sadok W., Sinclair T.R. Transpiration response of 'slow-wilting' and commercial soybean (*Glycine max* (L.) Merr.) genotypes to three aquaporin inhibitors. *J. Exp. Bot.* 2010;61(3):821–829. https://doi.org/10.1093/jxb/erp350

29. Poluboyarinov P.A., Vikhreva V.A., Leshchenko P.P., Aripovsky A.N., Likhachev A.N. Formation of elementary selenium decay of molecules of selenium-organic preparation DAFS-25 under influence of growing micella of mushrooms. *Vestnik Moskovskogo Universiteta. Seriya 16. Biologiya.* 2009;16(4):33–37 (in Russ.).

30. Poluboyarinov P.A., Leshchenko P.P. A qualitative reaction for cysteine, reduced glutathione and diacetophenonyl selenide. *J. Anal. Chem*. 2013;68(11):949–952. https://doi.org/10.1134/S1061934813110105

15. Авцин А.П., Жаворонков А.А., Риш М.А., Строчкова Л.С. *Микроэлементозы человека*. М.: Медицина; 1991. С. 196–231.

16. Sahu G.K., Upadhyay S., Sahoo B.B. Mercury induced phytotoxicity and oxidative stress in wheat (*Triticum aestivum* L.) plants. *Physiol. Mol. Biol. Plants*. 2012;18(1):21–31. https://doi.org/10.1007/s12298-011-0090-6

17. Sofo A., Scopa A., Nuzzaci M., Vitti A. Ascorbate peroxidase and catalase activities and their genetic regulation in plants subjected to drought and salinity stresses. *Int. J. Mol. Sci.* 2015;16(6):13561–13578. https://doi.org/10.3390/ijms160613561

18. Голышин Н.М. *Фунгициды*. М.: Колос; 1993. 318 с.

19. Yoshida M., Yokimoto M. Effects of fungicides on channels in the fungal membrane. *Pesticide Biochemistry and Physiology*. 1993;47(3):171–177. https://doi.org/10.1006/pest.1993.1076

20. Дудка И.А., Вассер С.П. *Методы экспериментальной микологии*. Киев: Наукова Думка; 1982. 550 с.

21. Минеев В.Г., Сычев В.Г., Амельянчик О.А., Болышева Т.Н., Гомонова Н.Ф., Дурынина Е.П., Егоров В.С., Егорова Е.В., Едемская Н.Л., Карпова Е.А., Прижукова В.Г. *Практикум по агрохимии*. М.: МГУ; 2001. 689 с.

22. Bradford M.M. A rapid and sensitive method for the quantitation of microgram quantities of protein utilizing the principle of protein-dye binding. *Anal. Biochem*. 1976;72(1–2):248–254. https://doi.org/10.1006/abio.1976.9999

23. Гавриленко В.Ф., Ладыгина М.Е., Хандобина Л.М. *Большой практикум по физиологии растений. Фотосинтез. Дыхание*. М.: Высшая школа; 1975. 392 с.

24. Назаренко И.И., Ермаков А.Н. *Аналитическая химия селена и теллура*. М.: Наука; 1971. 248 с.

25. Угай Я.А. *Неорганическая химия*. М.: Высшая школа; 1989. 463 с.

26. Bienert G.P., Cavez D., Besserer A., Berny M.C., Gilis D., Rooman M., Chaumont F. A conserved cysteine residue is involved in disulfide bond formation between plant plasma membrane aquaporin monomers. *Biochem. J.* 2012;445(1):101–111. https://doi.org/10.1042/bj20111704

27. Frick A., Järvå M., Ekvall M., Uzdavinys P., Nyblom M., Törnroth-Horsefield S. Mercury increases water permeability of a plant aquaporin through a non-cysteine-related mechanism. *Biochem. J*. 2013;454(3):491–499. https://doi.org/10.1042/bj20130377

28. Sadok W., Sinclair T.R. Transpiration response of 'slow-wilting' and commercial soybean (*Glycine max* (L.) Merr.) genotypes to three aquaporin inhibitors. *J. Exp. Bot.* 2010;61(3):821–829. https://doi.org/10.1093/jxb/erp350

29. Полубояринов П.А., Вихрева В.А., Лещенко П.П., Ариповский А.Н., Лихачев А.Н. Образование элементарного селена при распаде молекулы селенорганического препарата ДАФС-25 под влиянием растущего мицелия грибов. *Вестник Московского университета. Серия 16. Биология*. 2009;16(4):33–37.

30. Полубояринов П.А., Лещенко П.П. Качественная реакция на цистеин, восстановленный глутатион и диацетофенонилселенид. *Журн. аналит. химии*. 2013;68(11):1063. https://doi.org/10.7868/S0044450213110108

31. Полубояринов П.А., Лещенко П.П., Моисеева И.Я., Колесникова С.Г., Эпштейн Н.Б. Механизм реакции элиминирования селена в диацетофенонилселениде под действием восстановленного глутатиона. *Журн. аналит. химии*. 2017;72(7):633–638. https://doi.org/10.7868/S0044450217070118

[Original Russian Text: Poluboyarinov P.A., Leshchenko P.P. A qualitative reaction for cysteine, reduced glutathione and diacetophenonyl selenide. *Zhurnal Analiticheskoi Khimii.* 2013;68(11):1063–1066 (in Russ.). https://doi.org/10.7868/S0044450213110108]

31. Poluboyarinov P.A., Leshchenko P.P., Moiseeva I.Ya., Kolesnikova S.G., Epshtein N.B. Mechanism of the reaction of selenium elimination in diacetophenonyl selenide under the action of reduced glutathione. *J. Anal. Chem.* 2017;72(7):739–744. https://doi.org/10.1134/S1061934817070103

[Original Russian Text: Poluboyarinov P.A., Leshchenko P.P., Moiseeva I.Ya., Kolesnikova S.G., Epshtein N.B. Mechanism of the reaction of selenium elimination in diacetophenonyl selenide under the action of reduced glutathione. *Zhurnal Analiticheskoi Khimii.* 2017;72(7):633–638 (in Russ.). https://doi.org/10.7868/S0044450217070118]

32. Busher J.T. Serum Albumin and Globulin. In: Walker H.K., Hall W.D., Hurst J.W. (Eds.). *Clinical Methods: The History, Physical, and Laboratory Examinations*: 3rd ed. Boston: Butterworths; 1990. Chapter 101. ISBN 978-0409900774.

33. Islam M.S., Berggren P.O., Larsson O. Sulfhydryl oxidation induces rapid and reversible closure of the ATP-regulated K^+ channel in the pancreatic β-cell. *FEBS Lett*. 1993;319(1–2):128–132. https://doi.org/10.1016/0014-5793(93)80051-u

34. Poluboyarinov P.A., Elistratov D.G., Shvets V.I. Metabolism and mechanism of toxicity of selenium-containing drugs supplements used for optimizing human selenium status. *Tonk. Khim. Tekhnol. = Fine Chem. Technol.* 2019;14(1):5–24 (in Russ.). https://doi.org/10.32362/2410-6593-2019-14-1-5-24

32. Busher J.T. Serum Albumin and Globulin. In: Walker H.K., Hall W.D., Hurst J.W. (Eds.). *Clinical Methods: The History, Physical, and Laboratory Examinations*: 3rd ed. Boston: Butterworths; 1990. Chapter 101. ISBN 978-0409900774.

33. Islam M.S., Berggren P.O., Larsson O. Sulfhydryl oxidation induces rapid and reversible closure of the ATP-regulated K^+ channel in the pancreatic β-cell. *FEBS Lett*. 1993;319(1–2):128–132. https://doi.org/10.1016/0014-5793(93)80051-u

34. Полубояринов П.А., Елистратов Д.Г., Швец В.И. Метаболизм и механизм токсичности селенсодержащих препаратов, используемых для коррекции дефицита микроэлемента селена. *Тонкие химические технологии*. 2019;14(1):5–24. https://doi.org/10.32362/2410-6593-2019-14-1-5-24

About the authors:

Pavel A. Poluboyarinov, Cand. Sci. (Agricul.), Associate Professor, Department of General and Clinical Pharmacology, Penza State University (40, Krasnaya ul., Penza, 440026, Russia). E-mail: poluboyarinovpavel@yandex.ru. Scopus Author ID 55913331500, RSCI SPIN-code 1855-6069, https://orcid.org/0000-0001-9870-0272

Natalia V. Shchetinina, Cand. Sci. (Biol.), Associate Professor, Department of Human Physiology, Penza State University (40, Krasnaya ul., Penza, 440026, Russia). E-mail: singl71@list.ru. Scopus Author ID 6603851588, RSCI SPIN-code 1027-6691, https://orcid.org/0000-0002-0076-2553

Inessa Ya. Moiseeva, Dr. Sci. (Med.), Dean of the Faculty of Medicine, Penza State University (40, Krasnaya ul., Penza, 440026, Russia). E-mail: moiseeva_pharm@mail.ru. Scopus Author ID 7004249589, RSCI SPIN-code 9607-0306, https://orcid.org/0000-0003-1168-2871

Nadezhda I. Mikulyak, Dr. Sci. (Med.), Head of the Department of Human Physiology, Penza State University (40, Krasnaya ul., Penza, 440026, Russia). E-mail: normphys@mail.ru. Scopus Author ID 55904922500, ResearcherID S-7843-2016, RSCI SPIN-code 5278-7302, https://orcid.org/0000-0001-8473-5781

Nadezhda A. Golubkina, Dr. Sci. (Agricul.), Chief Researcher, Laboratory and Analytical Center, Federal Scientific Center of Vegetable Production (14, Selektsionnaya ul., VNIISSOK, Odintsovo urban district, Moscow oblast, 143080, Russia). E-mail: segolubkina45@gmail.com. Scopus Author ID 7004449622, ResearcherID AAV-1695-2020, RSCI SPIN-code 9284-3454, https://orcid.org/0000-0003-1803-9168

Alexander P. Kaplun, Dr. Sci. (Chem.), Professor, N.A. Preobrazhensky Department of Chemistry and Technology of Biologically Active Compounds, Medicinal and Organic Chemistry, M.V. Lomonosov Institute of Fine Chemical Technologies, MIREA – Russian Technological University (86, Vernadskogo pr., Moscow, 119571, Russia). E-mail: alexander.p.kaplun@gmail.com. Scopus Author ID 7006433250, RSCI SPIN-code 5856-0218, https://orcid.org/0000-0002-5600-8648

Об авторах:

Полубояринов Павел Аркадьевич, к.с.-х.н., доцент кафедры «Общая и клиническая фармакология» ФГБОУ ВО «Пензенский государственный университет» (440026, Россия, г. Пенза, ул. Красная, д. 40). E-mail: poluboyarinovpavel@yandex.ru. Scopus Author ID 55913331500, SPIN-код РИНЦ 1855-6069, https://orcid.org/0000-0001-9870-0272

Щетинина Наталья Викторовна, к.б.н., доцент кафедры «Физиология человека» ФГБОУ ВО «Пензенский государственный университет» (440026, Россия, г. Пенза, ул. Красная, д. 40). E-mail: singl71@list.ru. Scopus Author ID 6603851588, SPIN-код РИНЦ 1027-6691, https://orcid.org/0000-0002-0076-2553

Моисеева Инесса Яковлевна, д.м.н., декан лечебного факультета ФГБОУ ВО «Пензенский государственный университет» (440026, Россия, г. Пенза, ул. Красная, д. 40). E-mail: moiseeva_pharm@mail.ru. Scopus Author ID 7004249589, SPIN-код РИНЦ 9607-0306, https://orcid.org/0000-0003-1168-2871

Микуляк Надежда Ивановна, д.м.н., заведующий кафедрой «Физиология человека» ФГБОУ ВО «Пензенский государственный университет» (440026, Россия, г. Пенза, ул. Красная, д. 40). E-mail: normphys@mail.ru. Scopus Author ID 55904922500, ResearcherID S-7843-2016, SPIN-код РИНЦ 5278-7302, https://orcid.org/0000-0001-8473-5781

Голубкина Надежда Александровна, д.с.-х.н., главный научный сотрудник лабораторно-аналитического центра ФГБНУ «Федеральный научный центр овощеводства» (143080, Россия, Московская обл., Одинцовский городской округ, поселок ВНИИССОК, ул. Селекционная, д. 14). E-mail: segolubkina45@gmail.com. Scopus Author ID 7004449622, ResearcherID AAV-1695-2020, SPIN-код РИНЦ 9284-3454, https://orcid.org/0000-0003-1803-9168

Каплун Александр Петрович, д.х.н., профессор кафедры химии и технологии биологически активных соединений, медицинской и органической химии им. Н.А. Преображенского Института тонких химических технологий им. М.В. Ломоносова ФГБОУ ВО «МИРЭА – Российский технологический университет» (119571, Россия, Москва, пр-т Вернадского, д. 86). E-mail: alexander.p.kaplun@gmail.com. Scopus Author ID 7006433250, SPIN-код РИНЦ 5856-0218, https://orcid.org/0000-0002-5600-8648

The article was submitted: February 04, 2022; approved after reviewing: March 30, 2022; accepted for publication: September 26, 2022.

Translated from Russian into English by H. Moshkov
Edited for English language and spelling by Thomas Beavitt

SYNTHESIS AND PROCESSING OF POLYMERS AND POLYMERIC COMPOSITES

СИНТЕЗ И ПЕРЕРАБОТКА ПОЛИМЕРОВ И КОМПОЗИТОВ НА ИХ ОСНОВЕ

ISSN 2686-7575 (Online)
https://doi.org/10.32362/2410-6593-2022-17-5-410-426
UDC 678.7; 678.764.43; 678.01

RESEARCH ARTICLE

Synthesis of new photo-cured phosphorus-containing oligoestermethacrylates with a spacer in the structure [1]

Boris A. Buravov✉, Ali Al-Khamzawi, Eugene S. Bochkarev, Nazmiya Kh. Grichishkina, Sergey V. Borisov, Nina V. Sidorenko, Oleg I. Tuzhikov, Oleg O. Tuzhikov

Volgograd State Technical University, Volgograd, 400005 Russia
✉Corresponding author, e-mail: byravov@ya.ru

Abstract

Objectives. *To synthesize phosphorus-containing oligoestermethacrylates spatially separated by spacers of aliphatic or aromatic structure and evaluate their effect on photocuring kinetics.*
Methods. *For determining the qualitative and quantitative composition of the synthesized compounds, the following methods were used: thin layer chromatography; chromatographic and mass spectrometry; infrared spectroscopy; ^{1}H, ^{13}C, ^{31}P nuclear magnetic resonance spectroscopy; differential scanning calorimetry. The dielectric loss tangent was determined on a specially designed optical cell with an ultraviolet (UV) light source to an immittance meter. Elemental analysis was performed on an energy dispersive X-ray fluorescence spectrometer.*
Results. *Spatially separated oligoestermethacrylates based on phosphorus trichloride containing aliphatic or aromatic spacers in the structure were synthesized. During the interaction of glycidyl methacrylate with phosphorus trichloride in the mass of the latter, reaction products were shown to be formed both according to the Krasusky rule from the side of the α-carbon atom, as well as against this rule with the formation of isomeric products. Obtaining these compounds in bulk is possible only in the presence of a homopolymerization inhibitor. The influence of the spacer*

[1] This paper is an updated and translated from Russian version of the original article in Russian published in *Izvestiya VolgGTU*, 2020. Original Russian Text © Buravov B.A., Bochkarev E.S., Al-Khamzawi A., Sidorenko N.V., Tuzhikov O.O., Tuzhikov O.I. Study of the influence of spacer on features of UV curing of photosphorose-containing metacrylates of various functionality. *Izvestiya VolgGTU*. 2020;12(247):136–143. https://doi.org/10.35211/1990-5297-2020-12-247-136-143

structure on the curing rate of oligoestermethacrylates under the action of UV radiation has been established. It has been shown that the introduction of a spacer into the oligomer structure is accompanied by an increase in the induction period by a factor of 39 compared to a sample without a spacer.

Conclusions. *The results obtained indicate the possibility of obtaining new oligoestermethacrylates with aliphatic and aromatic spacers in the structure. The influence of the structure of the spacer on the kinetics of photocuring is determined.*

Keywords: *synthesis, oligoestermethacrylates, polymerization, phosphorus-containing flame retardants, kinetics, photocuring, DSC*

For citation: Buravov B.A., Al-Khamzawi A., Bochkarev E.S., Grichishkina N.Kh., Borisov S.V., Sidorenko N.V., Tuzhikov O.I., Tuzhikov O.O. Synthesis of new photo-cured phosphorus-containing oligoestermethacrylates with a spacer in the structure. *Tonk. Khim. Tekhnol. = Fine Chem. Technol*. 2022;17(5):410–426. https://doi.org/10.32362/2410-6593-2022-17-5-410-426

НАУЧНАЯ СТАТЬЯ

Синтез новых фотоотверждаемых фосфорсодержащих олигоэфирметакрилатов со спейсером в структуре

Б.А. Буравов✉, А. Аль-Хамзави, Е.С. Бочкарев, Н.Х. Гричишкина, С.В. Борисов, Н.В. Сидоренко, О.И. Тужиков, О.О. Тужиков

Волгоградский государственный технический университет, Волгоград, 400005 Россия
✉Автор для переписки, e-mail: byravov@ya.ru

Аннотация

Цели. *Синтез фосфорсодержащих олигоэфирметакрилатов, пространственно-разделенных спейсерами алифатического или ароматического строения, и оценка их влияния на кинетику фотоотверждения.*

Методы. *Для определения качественного и количественного состава синтезированных соединений использованы: тонкослойная хроматография; хромато-масс-спектрометрия; инфракрасная спектроскопия; ^{1}H, ^{13}C, ^{31}P спектроскопия ядерного магнитного резонанса; дифференциальная сканирующая калориметрия. Тангенс диэлектрических потерь определяли на специально разработанной оптической ячейке с УФ-источником света к измерителю иммитанса. Элементный анализ проводили на энергодисперсионном рентгенофлуоресцентном спектрометре.*

Результаты. *Синтезированы пространственно разделенные олигоэфирметакрилаты на основе трихлорида фосфора, содержащие в структуре алифатический или ароматический спейсеры. Установлено, что при взаимодействии глицидилметакрилата с трихлоридом фосфора в массе последнего, образуются продукты реакции как по правилу Красуского со стороны α-углеродного атома, так и против правила с образованием изомерных продуктов. Получение данных соединений в массе возможно только в присутствии ингибитора гомополимеризации. Установлено влияние структуры спейсера на скорость отверждения олигоэфирметакрилатов под действием УФ-излучения. Показано, что введение спейсера в структуру олигомера сопровождается увеличением индукционного периода в 39 раз по сравнению с образцом, не содержащим спейсера.*

Выводы. *Достигнутые результаты свидетельствуют о возможности получения новых олигоэфирметакрилатов со спейсерами алифатического и ароматического строения в структуре. Установлено влияние строения спейсера на кинетику фотоотверждения.*

Ключевые слова: *синтез, олигоэфирметакрилаты, полимеризация, фосфорсодержащие антипирены, кинетика, фотоотверждение, ДСК*

Для цитирования: Buravov B.A., Al-Khamzawi A., Bochkarev E.S., Grichishkina N.Kh., Borisov S.V., Sidorenko N.V., Tuzhikov O.I., Tuzhikov O.O. Synthesis of new photo-cured phosphorus-containing oligoestermethacrylates with a spacer in the structure. *Tonk. Khim. Tekhnol. = Fine Chem. Technol*. 2022;17(5):410–426. https://doi.org/10.32362/2410-6593-2022-17-5-410-426

INTRODUCTION

To solve the problem of combustibility of composite materials based on oligomeric binders, fire retardants of various nature are added to them. Some of these do not react with the main polymer during processing and operation, while others act as a reactive additive, for example, integrating into the structure of the cured binder [1, 2]. However, it should be noted that it is not always possible to balance the set of required performance characteristics necessary to obtain desired final products. For example, some flame retardants are able to transfer materials to the class of low combustibility, while worsening the physical-mechanical, dielectric, technological and operational properties [3]. The production of polymeric binders that reduce flammability while simultaneously improving physical and mechanical properties solves a number of the above problems, which are related, among other things, to the thermodynamic incompatibility of the binder and flame retardant.

In order to ensure the required level of properties in terms of resistance to combustion, phosphorus-containing polymeric materials and fillers based on organophosphorus, organophosphorus-element compounds are widely used. A promising method involves the synthesis and use of reactive compounds containing fragments of different sizes and structures (spacers) between reactive centers in a single molecule. However, the works describing such methods either present spacers that are located in the side chain of the resulting polymer, or compounds having different spacer structures as co-reagents in the preparation of the cured material [4–6].

From our point of view, a more promising approach sets out to obtain bi, tri-, and tetra-functional compounds of the (meth)acrylate series in which the spacer is located between the functional polymerizable centers. For obtaining compounds with spacers, three reagents of different functionalities can be used. As a result of their sequential interaction, it is possible to obtain an oligomeric structure (Scheme 1).

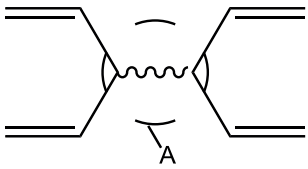

Scheme 1. Structure of oligoestermethacrylate with spacers of various structures; A is a spacer of different structure and molecular weight.

Subsequently, in the process of polymerization at double bonds, the structures of a rigid-chain polymer are formed, in the mass of which there is a movable or limitedly movable spacer.

It is known that chemically bound phosphorus in the structure of (meth)acrylate compounds makes it possible to obtain polymers with reduced flammability. For example, the use of phosphorus-containing monomers and oligomers of the (meth)

acrylate series [7, 8] or phosphorus-containing epoxy resins [9] makes it possible to obtain materials with a satisfactory balance of physico-mechanical and heat-resistant properties with reduced flammability.

EXPERIMENTAL

For the synthesis of phosphorus-containing compounds capable of polymerization under the action of ultraviolet (UV) radiation, we used freshly distilled phosphorus trichloride (98%, analytical grade, TU 2152-380-0763441-2002), glycidyl methacrylate (GMA) (no less than 97%, purity, analytical grade, *Sigma-Aldrich*, USA), active diluent for epoxy resins grade E-181 (mass fraction of epoxy groups ≥25%, *Chimex Limited*, Russia, TU 2225-606-11131395-2003) and epoxy resin grade ED-20 (mass fraction of epoxy groups, 20.0–22.5%, *Chimex Limited*, GOST 10587-84[2]). Prior to synthesis, the exact content of epoxy groups in epoxy resins was analytically determined. To obtain the polymers, a photoinitiator comprising bis(2,4,6-trimethylbenzoyl)-phenylphosphine oxide (BAPhO) (no more than 100%, chemically pure, *Sigma-Aldrich*, USA) was used. For thin layer chromatography (TLC), benzene (99.8%, chemically pure, *Ekos-1*, Russia) and freshly distilled ethanol (96.3%, *Ferein*, Russia) were used as the eluent.

Chromatographic and mass spectrometry were carried out on a GC/MS Saturn 2100T instrument (*Varian*, USA) with a VF-1ms quartz capillary column (100% methylpolysiloxane, 30 M × 0.25 mm, ID = 0.25 mm, DF = 0.25 μm, helium was used as a carrier gas) using a prepared 0.2% solution of the substance in acetone (99.8%, chemically pure, *Ekos-1*, Russia). Nuclear magnetic resonance (NMR) ^{1}H, ^{13}C, and ^{31}P spectroscopy was performed on a Mercury 300 plus instrument (*Varian*, USA) with operating frequencies of 300, 75, and 121 MHz, respectively; here, $CDCl_3$ was used as a solvent. Chemical shifts are given on a scale of δ (ppm) relative to tetramethylsilane (TMS) as an internal standard. Spin-spin coupling constants (*J*) are given in Hz. Differential scanning calorimetry (DSC) was performed on a NETZSCH DSC 204 F1 instrument with a compressor cooling system and an OmniCure S2000 UV irradiation unit in an inert gas flow (argon, 90 mL/min) (*Netzsch*, Germany). The sample was placed in a standard open aluminum crucible. Controlled irradiation was carried out according to a temperature program (20°C, 4 min) comprising two identical isothermal segments using the full spectrum of the radiation source (power 1 W/cm^2). The resulting curve was obtained by subtracting the second segment from the first in the NETZSCH Proteus software environment[3]. To determine the dielectric loss tangent, we used a specially designed optical cell with a UV light source connected to an E7-25 immittance meter (*MNIPI*, Belarus). Infrared (IR) spectra were recorded on an FT-801 spectrometer (*SIMEX*, Russia). Elemental analysis was performed on an EDX-8000 energy dispersive X-ray fluorescence spectrometer (*Shimadzu*, Japan).

For the study, several phosphorus-containing polymerizable compounds (PPC) were synthesized:

– (PPC-1) is the reactive monomer without spacer;

– (PPC-2) is the spacer is introduced with E-181 epoxy resin;

– (PPC-3) is the spacer is inserted with epoxy resin ED-20.

The synthesis of phosphorus-containing polymerizable compounds was carried out in two stages. At the first stage, the reaction was carried out in a molar ratio of 1:2 according to the scheme:

$$PCl_3 + 2A \rightarrow (A')_2\text{-}PCl,$$

where A is one of unsaturated alpha oxides; A′ is the structure of addition of unsaturated alpha oxides. At the second stage, the interaction of the bifunctional epoxide with residual chlorine in a ratio of 2:1 was carried out, leading to the preparation of a compound with a spacer, according to the scheme:

$$2(A')_2\text{-}PCl + B \rightarrow (A')_2\text{-}P\text{-}B'\text{-}P\text{-}(A')_2,$$

where B is one of diepoxy oligomers, B′ is the structure formed as a result of addition of diepoxy oligomers.

As an object of comparison, a PPC-1 product was synthesized that did not contain a spacer. The reaction was carried out in excess of PCl_3 in one stage in a ratio of 1:3 with GMA (Scheme 2).

The synthesis of substances with spacers was carried out in two stages. At the first stage, a disubstituted intermediate was obtained (Scheme 3).

At the second stage, the disubstituted intermediate was added to epoxy resins (epoxy resin E-181 was used for PPC-2, ED-20 was used for PPC-3), the reactions were carried out in bulk (Schemes 4 and 5).

[2] GOST 10587-84. USSR State Standard. Uncured epoxy resins. Specifications. Moscow: Izd. Standartov; 1989.

[3] https://analyzing-testing.netzsch.com/ru/pribory-resheniya/differenczialnaya-skaniruyushhaya-kalorimetriya-dsk-differenczialnyj-termicheskij-analiz-dta/dsc-204-f1-phoenix, accessed April 15, 2022.

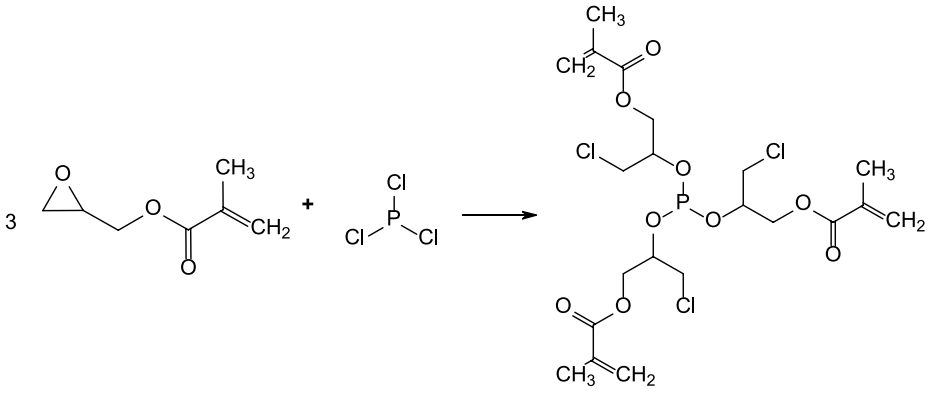

Scheme 2. Reaction of glycidyl methacrylate with phosphorus trichloride to produce the PPC-1 product.

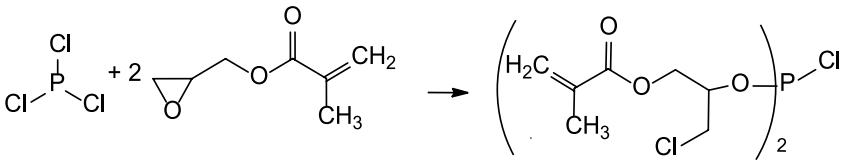

Scheme 3. Reaction of phosphorus trichloride with glycidyl methacrylate to produce an intermediate.

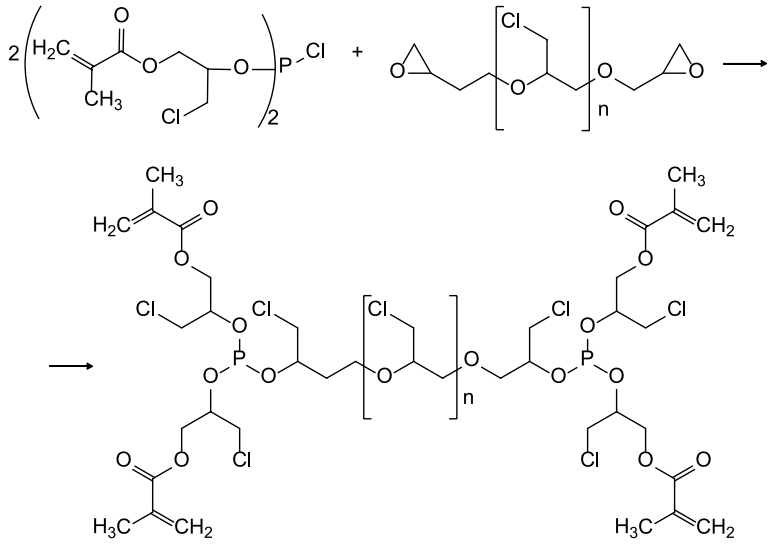

Scheme 4. Reaction of the intermediate with epoxy resin E-181 to obtain the product PPC-2.

The composition and structure of the synthesized products were confirmed by IR and NMR spectral studies.

PPC-1, PPC-2, and PPC-3 products were used to prepare photocurable compositions in order to evaluate the effect of the spacer on the properties of the cured material.

PPC-1. Tris-[(1-chloromethyl-2-methacryloxy)-ethoxy]phosphine (RF Pat. No. 2697721 [10])

A four-necked reactor equipped with a stirrer, a dropping funnel, a reflux condenser, and a thermometer, which had been preliminarily purged with dry argon for 30 min (purging with argon was subsequently carried out throughout the entire process), was loaded with 5 g (0.036 mol) of phosphorus trichloride. A mixture of 15.49 g (0.11 mol) of glycidyl methacrylate (GMA) and 0.155 g (1 wt % of the mass of GMA) *N*-nitrosodiphenylamine was fed to it with constant stirring through a dropping funnel at such a rate that the temperature of the reaction mass did not exceed 15°C, the reactor cooled with a mixture of salt and ice. After the addition of the mixture, the resulting reaction mass was kept for 2 h at 45°C. Then, following evacuation for 60 min at a residual pressure

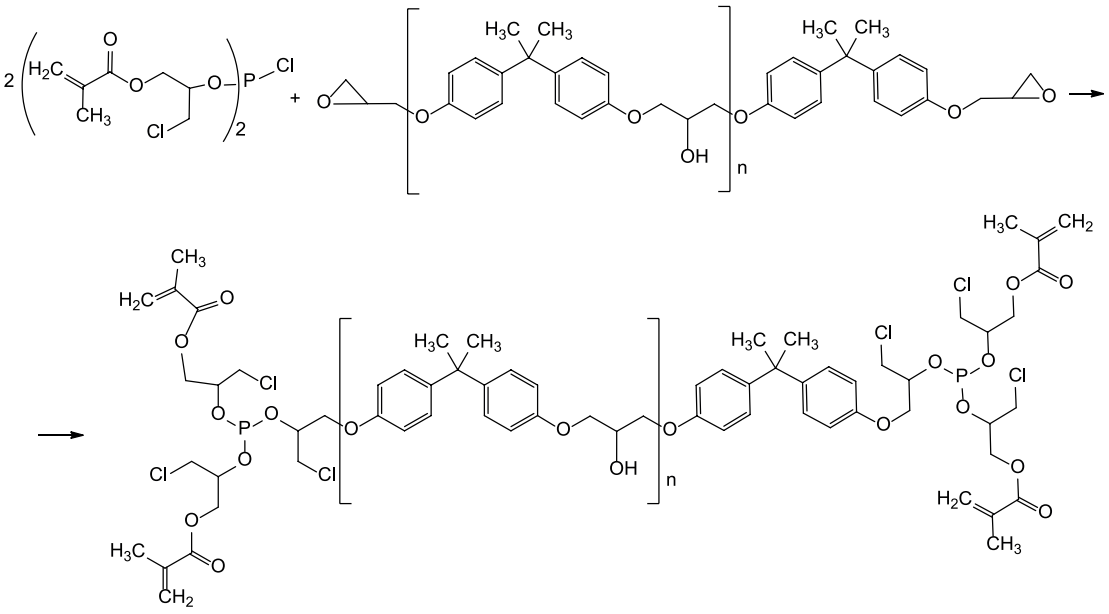

Scheme 5. Reaction of the intermediate with the epoxy resin ED-20 to obtain the product PPC-3.

of 5 mm Hg, the reaction mass was filtered on a Schott filter from the precipitated crystalline *N*-nitrosodiphenylamine. The yield of PPC-1 was 20.49 g (99.0%).

The product is a mobile liquid of light-yellow color, readily soluble in acetone and chloroform. Analysis for the content of epoxy groups showed their almost complete absence. Epoxy value (E.V.) = 0.066%, n_D^{20} = 1.4935; acid number (A.N.) = 11.58 mg KOH/g; bromine number (B.N.) = 85.3 g/100 g of organic substance.

The identification of the obtained product was carried out using NMR spectroscopy:

^{1}H NMR spectrum (300 MHz, $CDCl_3$) δ, ppm: 1.85 (s, 9H), 3.51 (m, 6H), 3.72 (m, 6 H), 4.20 (m, 6 H), 4.42 (m, 6 H), 5.55 (s, 6 H), 6.6 (s, 6 H), 4.62 (m, 3 H) (d, J = 1.7 Hz, 1 H).

^{13}C NMR spectrum (75 MHz, $CDCl_3$, TMC) δ, ppm: 17.9 (3C); 41.5; 62.4; 69.9; 124.3; 134.5; 164.5.

^{31}P NMR spectrum (121 MHz, $CDCl_3$) δ, ppm: 140.54 $P(OR)_3$.

In order to determine the elemental composition, a sample of the test material was placed in a cuvette for measuring liquid samples equipped with a thin film window. The material of the cuvette bottom was polypropylene; the medium was vacuum. The study was conducted according to the standard procedure for the energy dispersive X-ray fluorescence spectrometer EDX-8000. Detection limits of P and Cl ~10 ppm. Found (%): P 6.14; Cl 18.44. Calculated (%): P 5.49; Cl 18.86.

PPC-2. ((((4-((1-(2-((bis((1-chloro-3-(methacryloyloxy)propan-2-yl)oxy)phosphine)oxy)-3-chlorophenoxy)-3-chloropropan-2-yl)oxy)-1-chlorobutan-2-yl)oxy)phosphindiyl)bis(oxy))-bis(3-chloropropan-2,1-diyl)bis(2-methacrylate) (RF Pat. No. 2712107 [11])

A four-necked reactor equipped with a stirrer, a dropping funnel, a reflux condenser, and a thermometer, preliminarily purged with dry argon for 30 min (purging with argon was subsequently carried out throughout the entire process), was loaded with 5 g (0.036 mol) of phosphorus trichloride. A mixture of 10.33 g (0.073 mol) of HMA and 0.1 g (1 wt % of the mass of HMA) *N*-nitrosodiphenylamine was added to it, with constant stirring, from a dropping funnel at such a rate that the temperature of the reaction mass did not exceed 15°C, the reactor was cooled a mixture of salt and ice. After the mixture was added, the resulting reaction mass was kept for 2 h at 45°C. Then, the resulting intermediate was loaded into a dropping funnel and dosed into another four-necked reactor equipped with a stirrer, a thermometer, and a reflux condenser with E-181 diepoxide in the amount of 5.73 g (0.033 mol, based on the actual amount of epoxy groups). Upon completion of the addition of the mixture, the resulting reaction mass was kept for 2 h at 45°C.

The reaction mass was additionally evacuated for 60 min at a residual pressure of 5 mm Hg and filtered on a Schott filter from the precipitated

crystalline *N*-nitrosodiphenylamine. The yield of PPC-2 was 21.06 g (99.0%).

The product is a mobile liquid of light-yellow color, readily soluble in acetone and chloroform. Analysis for the content of epoxy groups showed their almost complete absence. E.V. = 0.04%; n_D^{20} = 1.4951; A.N. = 12.19 mg KOH/g; B.N. = 72.6 g/100 g of organic substance.

The product obtained was identified by NMR spectroscopy:

^{1}H NMR spectrum (300 MHz, $CDCl_3$) δ, ppm: 1.66, 3.63, 3.65, 4.42 (17 CH_2), 3.48, 3.53, 3.86, 4.13 (7 CH), 2.01 (4 CH_3), 6.40, 6.48 (8 H).

^{13}C NMR spectrum (75 MHz, $CDCl_3$, TMC) δ, ppm: 43.7, 46.9, 47, 50.7 (7 CH_2), 167.2 (4 C); 70.6, 71.6, 67.2, 86.2 (7 CH); 62.7, 67.9, 74.8, 73.4 (7 CH_2), 136 (4 C), 34.3, 125.2 (6 CH_2), 17.9 (4 CH_3).

^{31}P NMR spectrum (121 MHz, $CDCl_3$) δ, ppm: 141 $P(OR)_3$.

Found (%): P 5.02; Cl 22.41. Calculated (%): P 5.74; Cl 22.98.

PPC-3. ((((((((((2-hydroxypropane-1,3-diyl)-bis(oxy))bis(4,1-phenylene))bis(propan-2,2-diyl))-bis(4.1-phenylene))bis(hydroxy))-bis(1-chloropropane-3,2-diyl))bis(oxy))-bis(phosphintriyl))tetrakis(oxy))tetrakis-(3-chloropropane-2,1-diyl)tetrakis(2-methyl acrylate) (RF Pat. No. 2712116 [12])

A four-necked reactor equipped with a stirrer, a dropping funnel, a reflux condenser, and a thermometer, which had been preliminarily purged with dry argon for 30 min (purging with argon was subsequently carried out throughout the entire process), was loaded with 5 g (0.036 mol) of phosphorus trichloride. With constant stirring, a mixture of 10.33 g (0.073 mol) of HMA and 0.1 g (1 wt % of the mass of HMA) *N*-nitrosodiphenylamine was added from a dropping funnel at a rate such that the temperature of the reaction mixture did not exceed 15°C; the reactor was cooled with a mixture of salt and ice. After the mixture was added, the resulting reaction mass was kept for 2 h at 45°C. Then, the resulting intermediate product was loaded into a dropping funnel and dosed into another four-necked reactor equipped with a stirrer, a thermometer, and a reflux condenser with ED-20 epoxy resin in the amount of 7.66 g (0.035 mol, based on the actual amount of epoxy groups). Upon completion of the addition of the mixture, the reaction mixture was kept for 2 h at 45°C.

Before unloading the product, the reaction mass was evacuated for 60 min at a residual pressure of 5 mm Hg, filtered on a Schott filter from the precipitated crystalline *N*-nitrosodiphenylamine. The yield of PPC-3 was 22.99 g (99.0%).

The product is a mobile liquid of light-yellow color, readily soluble in acetone and chloroform. Analysis carried out to identify the content of epoxy groups revealed their almost complete absence. E.V. = 0.09%; n_D^{20} = 1.5210; A.N. = 13.46 mg KOH/g; B.N. = 74.62 g/100 g of organic substance.

The IR spectra of the synthesized compounds PPC-1, PPC-2, PPC-3 contain characteristic absorption bands of stretching vibrations of the C=O (1720 cm^{-1}), C=C (1640 cm^{-1}), C-Hal (760–770 cm^{-1}). There are no absorption bands corresponding to vibrations of the epoxy cycle (860 and 910 cm^{-1}) and P=O (1280–1300 cm^{-1}). Chemical analysis for the content of epoxy groups also showed their absence.

The product obtained was identified by NMR spectroscopy:

^{1}H NMR spectrum (300 MHz, $CDCl_3$) δ, ppm: 1.66, 3.63, 3.65, 4.09, 4.21, 4.42 (14 CH_2); 4.04, 4.23, 4.13, 6.91, 7,19 (22 CH); 1.72, 2.01 (8 CH_3), 6.40, 6.48 (8 H); 3.58 (OH).

^{13}C NMR spectrum (75 MHz, $CDCl_3$, TMC) δ, ppm: 46.9, 47, 67.9, 70.1, 125.2 (7 CH_2); 69, 70.6, 71.2, 86.2, 114.9, 127.7 (23 CH); 42.4, 136, 146.3, 156.9, 167.2 (18 C); 17.9, 30.9 (8 CH_3).

^{31}P NMR spectrum (121 MHz, $CDCl_3$) δ, ppm: 141 $P(OR)_3$.

Found (%): P 4.98; Cl 14.71. Calculated (%): P 5.23; Cl 17.97.

The obtained samples were studied by TLC (GOST 28366-89[4]) with subsequent determination of retention factor R_f values according to formula (1), sorbent: Sorbfil TLCP-AF-A plates (*SORBFIL*, Russia), eluents—benzene and ethanol in a ratio of 95:5, respectively. A chamber filled with iodine vapor was used to detect substances.

$$R_f = \frac{a}{b}, \quad (1)$$

where *a* is the distance from the center of the spot to the starting line, mm; *b* is the distance from the solvent front to the starting line, mm.

RESULTS AND DISCUSSION

While it was not possible to obtain any monomeric products of the addition of GMA to PCl_3 in the absence of an inhibitor of GMA polymerization, whether in excess or in deficiency

[4] GOST 28366-89. Interstate Standard. Reagents. Method of thin-layer chromatography. Moscow: Standartinform; 2008.

of phosphorus trichloride, the stabilizer (hydroquinone monomethyl ether) contained in the original monomer in the amount of 150 ppm did not prevent the polymerization process, which led to crosslinking of the product in the reactor.

Taking into account the data of [13–15], we used *N*-nitrosodiphenylamine dissolved in the monomer to prevent the polymerization of GMA in the reaction with phosphorus trichloride. The resulting product, according to the data of the authors of [16], can be a mixture of isomers **a**, **b**, and **c** (Fig. 1).

Characteristic peaks in the ^{1}H NMR spectra of PPC-1 were present in the following regions, ppm: 1.85 (s, 9H, ($\underline{H}_3C$–C=); 3.51 and 3.72 (m, 6H, –CH_2–Cl); 4.20 and 4.42 (m, 6 H, =CH–C$\underline{H}_2$–O–C(O)–); 5.55 and 6.6 (s, 6 H, –CH=C$\underline{H}_2$); 4,62 (m, 3H, >P–O–C$\underline{H}$).

The ^{13}C NMR spectra of PPC-1 contain the following peaks: at 17.9 ppm—assigned to the CH_3 groups at the carbon atom at the double bond; at 41.5 ppm—assigned to the groups (–CH_2–Cl) formed during the opening of the epoxy ring; at 62.4 ppm—referred to ester acrylate groups (–CH_2–O–); line at 69.9 ppm—assigned to groups (>CH–O–P<); at 124.3 ppm—referred to the disubstituted carbon atom groups at the double bond (–CH=CH_2); at 134.5 ppm—referred to the trisubstituted carbon atom of the double bond (–CH=CH_2); at 164.5 ppm—referred to the carbon of the ether group (–O–C(O)–).

The ^{31}P NMR spectra of PPC-1 contain characteristic peaks at 140.54 ppm assigned to the $P(OR)_3$ group; the absence of peaks at 3.3 ppm characteristic of P=O groups also indicates the absence of pentavalent phosphorus in the products.

The IR spectrum of PPC-1 contains characteristic absorption bands in the range of C=O (1720 cm^{-1}), C=C (1640 cm^{-1}), and C–Hal (760–770 cm^{-1}) stretching vibrations. The bands at 1340 cm^{-1} and 1500 cm^{-1} are attributed to the vibrations of NO groups and the aromatic ring of the stabilizer *N*-nitrosodiphenylamine, respectively. The absorption band in the region of 1160 cm^{-1} is assigned to bending vibrations of the C=O group. The absence of characteristic bands at 860 and 910 cm^{-1} corresponding to vibrations of the epoxy cycle indicates their complete opening upon interaction with phosphorus trichloride. The absence of epoxy groups in the reaction product was also confirmed by chemical analysis. The absence of bands in the region of 1100–1200 cm^{-1} characteristic of P=O groups indicates that pentavalent phosphorus is not formed during the synthesis of PPC-1.

The route of interaction is also confirmed by a decrease in the acid number of the synthesized products from 335.7 to 9.75 mg KOH/g and the absence of epoxy groups in them (see above), which is in agreement with the results of earlier studies [17].

Thus, the performed spectral studies confirm the formation of products of addition of GMA to phosphorus trichloride in the presence of nitrosodiphenylamine at three chlorine atoms.

The R_f value for PPC-1 was determined as the ratio of the distance from the spot center to the start to the distance from the mobile phase front to the start. The following results were obtained: R_f (A) = 0.124; R_f (B) = 0.299; R_f (C) = 0.39.

According to the results of TLC studies, the PPC-1 product is characterized by three separating spots, which were assigned to isomeric products **a**, **b**, and **c** (Fig. 1) formed during the synthesis of PPC-1. This is confirmed by studies [16, 18], which describe the possibility of forming compounds both according to the Krasusky rule and against this rule.

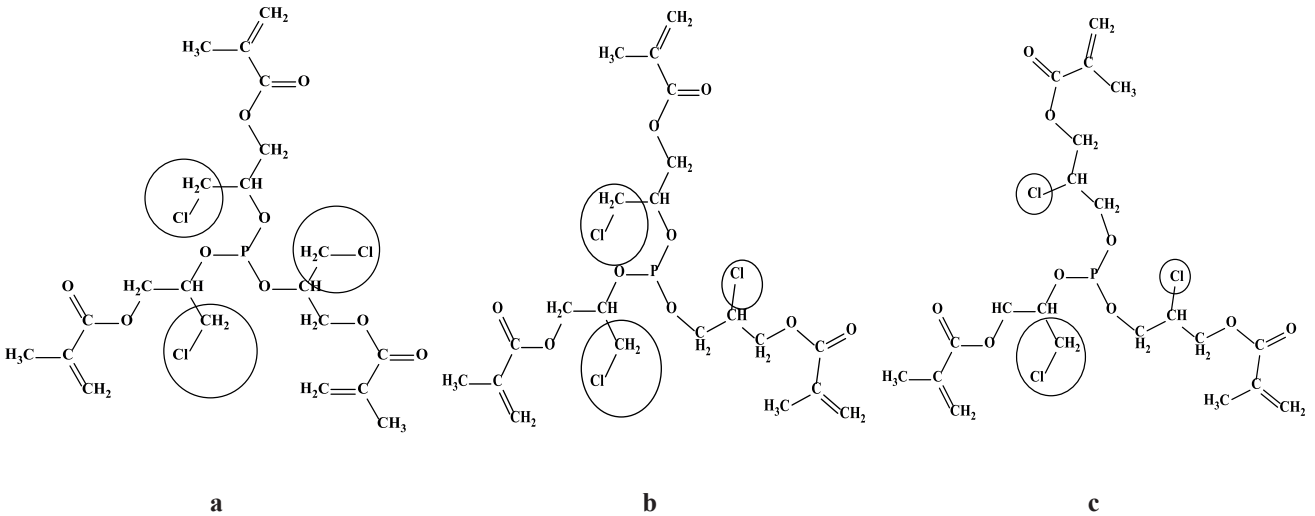

a **b** **c**

Fig. 1. Structures of PPC-1 isomers.

Any violation of the Krasusky rule as a result of an excess of PCl_3 can subsequently lead to the formation of a mixture of products. The rule can be violated under the influence of functional groups at the oxirane ring [19]. In view of the above, the formation of three spots during TLC studies is determined by the presence of three compounds in the mixture: a product in which the addition of the GMA oxirane ring occurs only according to the Krasusky rule; only against Krasusky rule; the simultaneous presence of the attached GMA, both under the rule and against the Krasusky rule. This can occur during the interaction of phosphorus trichloride at different depths of its transformation.

Chromatographic and mass spectral studies have shown that PPC-1 isomers are capable of producing several fragment ions (Figs. 2 and 3).

Along with the results of IR and NMR analyses of the primary TLC data, chromatographic and mass spectral studies confirmed that a mixture of isomers was formed during the synthesis. Thus, the obtained results confirm the formation of putative PPC-1 isomeric compounds **a**, **b**, and **c** (Fig. 1).

The synthesis of spatially separated bis-[phosphorus-di-etheracrylates] with spacers of various structures was carried out using intermediate products by partial replacement of chlorine atoms in phosphorus trichloride with glycidyl methacrylate. The resulting reaction mass was added to a bifunctional epoxide, for example, E-181 or ED-20 taken in a ratio of 2:1, respectively. Under such conditions, the diepoxide is inserted between two phosphorus atoms along the chlorine atoms. The basis for the conditions for the synthesis of substances with spacers (PPC-2 and PPC-3) was the experimental data obtained during the synthesis of PPC-1.

The ultimate goal of the research was to evaluate the effect of the spacer structure on the properties of crosslinked polymeric materials, which were determined by the structure of the bifunctional epoxide. Products of total chlorine substitution obtained by the interaction of phosphorus trichloride with GMA in a ratio of 1:3 were used as the basic object of comparison.

Figure 4 shows the IR spectra of GMA and end products that do not contain (PPC-1) and contain spacers (PPC-2, PPC-3). The insignificant difference seen in the spectra of the presented data is associated with the similar structure in the structure of the compounds.

The oxirane ring in glycidyl methacrylate has two transmission bands. The first band in the middle range of deformation of the C–O bond of the terminal oxirane group is centered at 906 cm^{-1}, while the second band observed at 3052 cm^{-1} is related to the C–H vibration of the methylene group of the epoxy ring. As well as being quite low, the intensity of this band is also very close to the transmission of the hydroxyl group; however, in epoxy monomers possessing a low degree of polymerization, it can be used to assess the qualitative presence of epoxy groups [20]. Here, it can be seen that a similar band is present in glycidyl methacrylate and absent in samples PPC-1, PPC-2, and PPC-3. The absence of vibrations of the C–O–C bonds

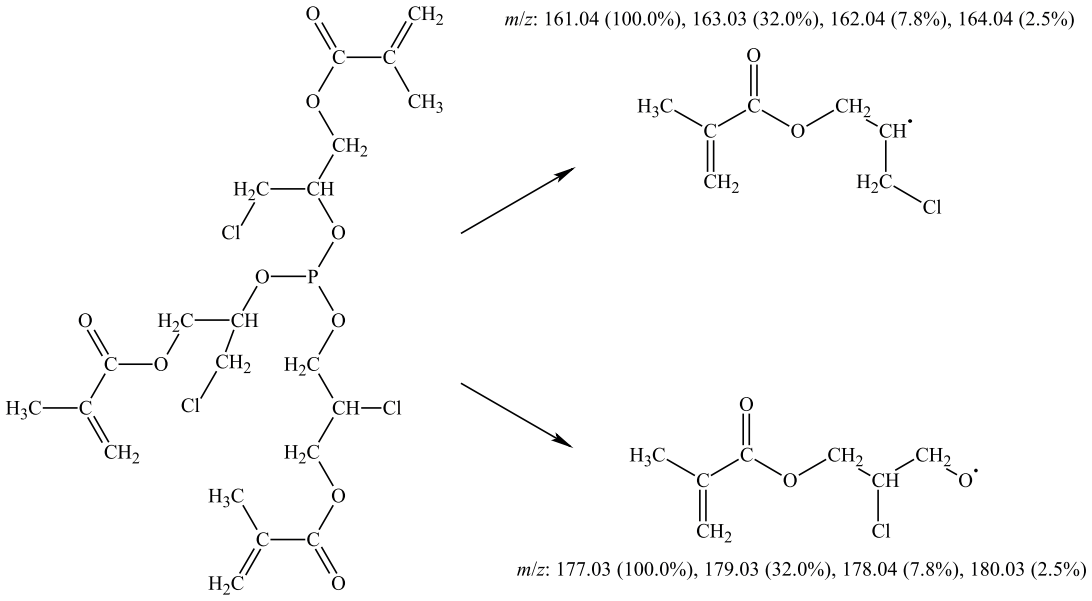

Fig. 2. PPC-1b fragment ion formation scheme (3-chloropropyl methacrylate fragment and 2-chloro-3-oxypropyl methacrylate fragment).

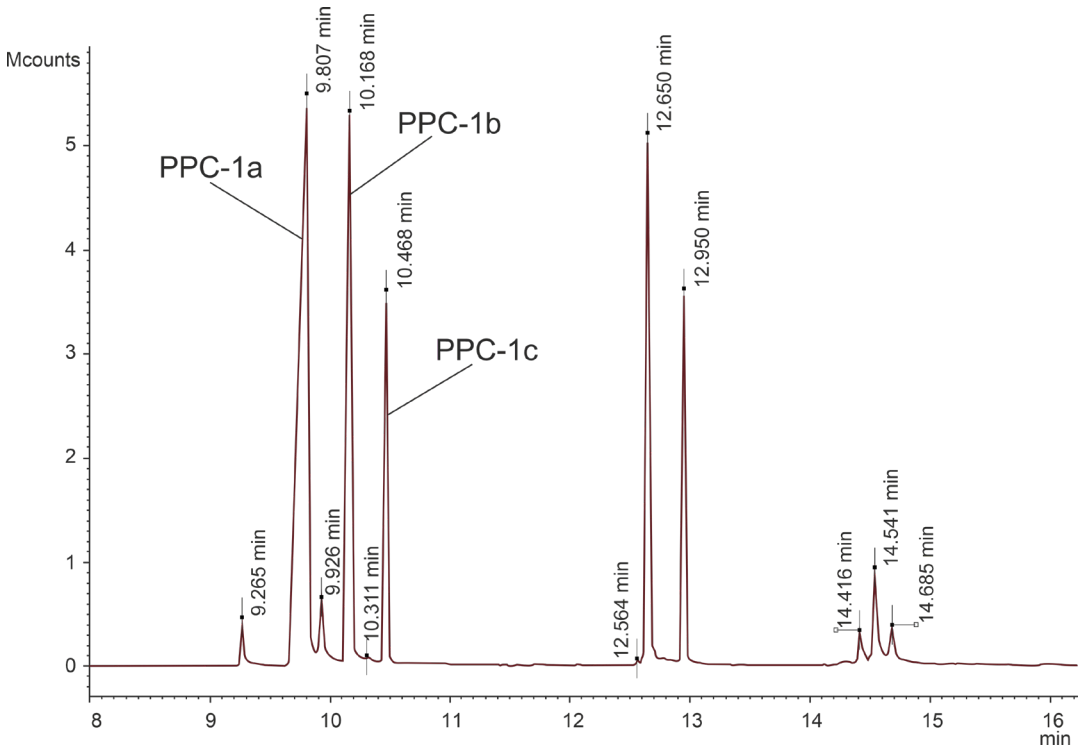

Fig. 3. Fragment of the chromatogram of a 0.2% solution of PPC-1 in acetone.

of the oxirane group in the region of 810–840 cm^{-1} and $–CH_2$ in the region of 760–770 cm^{-1} in the samples indicates the complete opening of oxirane rings.

Phosphorus containing samples contain bands corresponding to the carbonyl group >C=O in the region of 1719 cm^{-1}, $>C=CH_2$ in the region of 880–900 cm^{-1}, ether bond in the region of 1100–1200 cm^{-1}, C=C vibrations in the region of 1635 cm^{-1}, P–OR in the region of 940–945 cm^{-1}, R–CI in the region of 760–770 cm^{-1}. The addition of a spacer between two reaction centers binding the phosphorus atoms is not accompanied by a significant difference in the spectra of PPC-2 and PPC-1. The band in the region of about 1500 cm^{-1} in the IR spectrum of PPC-3 is assigned to vibrations of the aromatic ring; the band in the region of about 3000 cm^{-1} can be attributed to the hydroxyl group contained in the structure of ED-20.

Synthesized products PPC-1, PPC-2, and PPC-3 were used to obtain photocurable compositions.

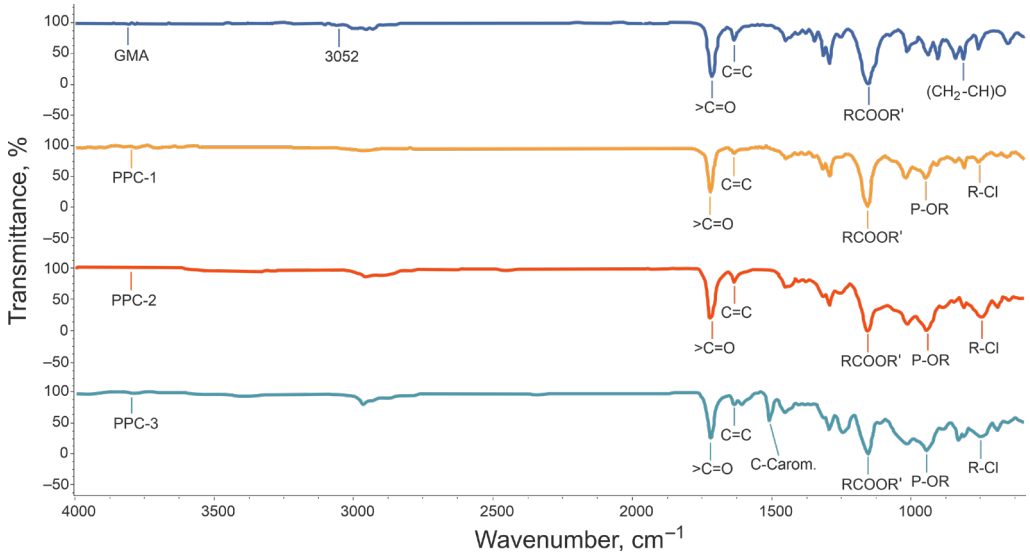

Fig. 4. IR spectra of PPC-1, PPC-2, PPC-3, and GMA products.

Investigation of the processes of curing synthesized compounds

The curing of the compositions with peroxide initiators (benzoyl peroxide, dicumyl peroxide) did not lead to a positive result, which is probably due to the presence of trivalent phosphorus in the structure of the oligoether methacrylate, which deactivates peroxides. In this regard, curing was carried out under the action of UV radiation in the presence of a photoinitiator.

Phenyl bis(2,4,6-trimethylbenzoyl)phosphine oxide (BAPhO), which is effective in a wide range of the UV spectrum with acceptable initiation parameters, was chosen as the initiator of the UV curing process, as recommended by a number of authors [21–23].

Determination of the degree of completion of the processes of photocuring of the synthesized products was carried out using DSC.

The presented data (Fig. 5 and Table) demonstrates the influence of the spacer on the thermal effects of the photocuring process. Although the introduction of an aliphatic spacer (PPC-2) has little effect on both the maximum heat release and the time taken to achieve it, an aromatic moiety (PPC-3) has a greater effect on photocuring processes, increasing the time taken to reach maximum heat release to 0.6 min, probably as a result of steric hindrances.

The introduction of a spacer with an increase in the overall functionality of the resulting compound reduces the number of polymerizable groups due to the steric factor, which is also accompanied by a decrease in the thermal effect of photocuring. According to DSC data, the contribution of one methacrylic group to the total thermal effect of the gross curing process of the synthesized products was estimated, which was 0.09376, 0.03113, 0.01822 J/(mol·eq) for PPC-1, PPC-2, PPC-3, respectively. In the case of the PPC-3 sample, which has a more massive rigid spacer as compared to PPC-2, a lower density of the spatial structure is formed. This is probably due to the steric factor, which limits polymerization to a greater extent to groups in the side chain.

This fact was substantiated in [24] when calculating the quadratic critical conversion, whose physical meaning is the necessity to carried out at least two reactions of functional groups sequentially in order to ensure the formation of a crosslink. As a result of the first reaction, the polyfunctional oligomer must be integrated into the polymer chain and, therefore, suspended functional groups *X* must appear. Due to the second reaction of the interaction of the *X* group, the crosslink itself is formed. The authors conclude that the main reason for the deviation of the experimental gel point from the calculated one is the cyclization reaction, which limits the mobility of the polymerizing units, ultimately leading to a decrease in the thermal effect, which is also observed in our case.

Of additional interest was the determination of the degree of completion of the mass photocuring processes. For this purpose, an E7-25 immittance meter was used as part of a device with a photocell equipped with LEDs with a total luminous flux of 0.0172 mW/cm^2 and a wavelength of 397 nm, which made it possible to evaluate the change in the dielectric properties of the material with time. The use of the developed measuring system was based on the well-known fact [24] that cured polymers have increased dielectric

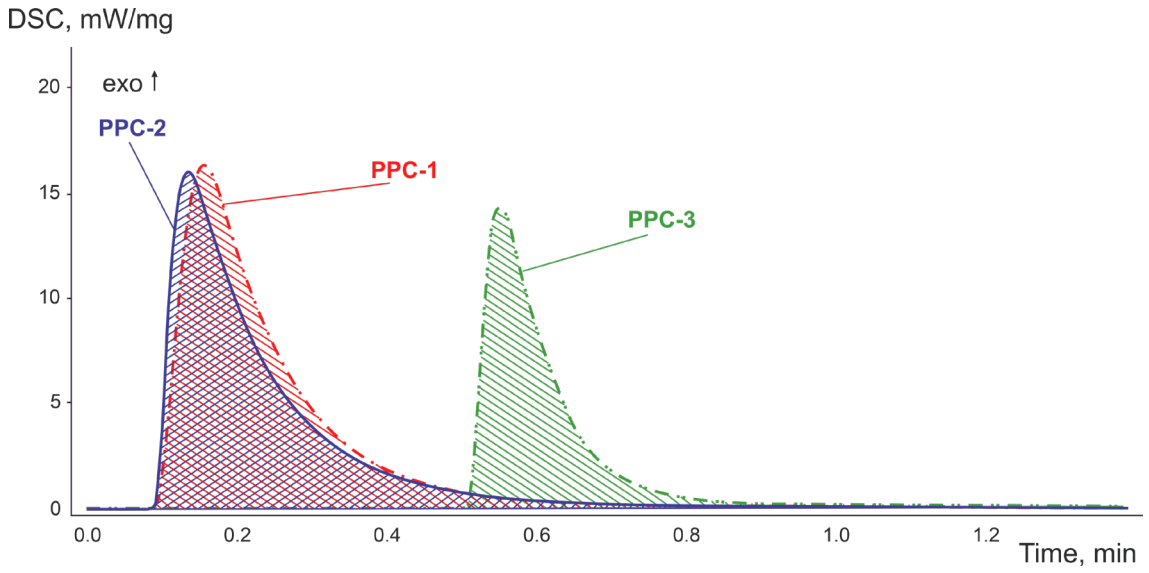

Fig. 5. Time dependences of thermal effects of photo-curing PPC-1, PPC-2, and PPC-3.

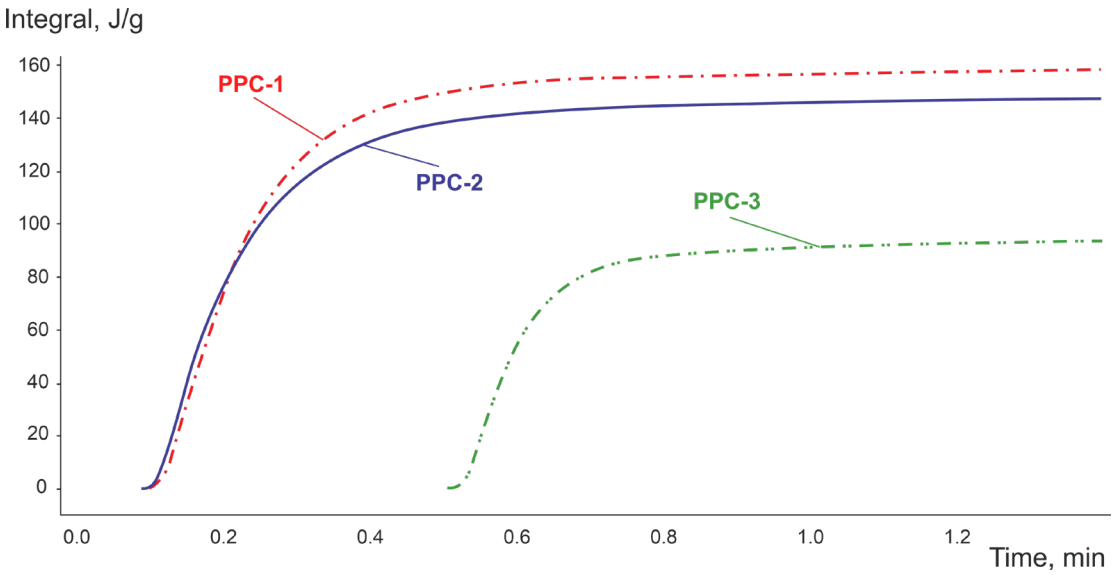

Fig. 6. Integral dependences of thermal effects of photo-curing PPC-1, PPC-2, and PPC-3.

Table. Experimental data of the photo-curing process

Method	Parameters	PPC-1	PPC-2	PPC-3
DSC	Q_{max}, mW/mg	16.36	15.99	14.43
	Q_{sum}, J/g	158.5	147.8	93.4
	Q_{sum}, J/mol	0.2813	0.1245	0.0729
	Q_{sum}, J/(mol·eq)	0.09376	0.03113	0.01822
	Time at Q_{max}, min	0.2	0.1	0.6
DEA	τ_{ind}	50	1650	150
	$\tau_{0.9}$	1100	2050	1430
	$a = \tau_{0.9} - \tau_{ind}$	1050	400	1280
	$1/a$, s^{-1}	$9.52 \cdot 10^{-4}$	$2.5 \cdot 10^{-3}$	$7.81 \cdot 10^{-4}$

Note: DEA is dielectric analysis. Q_{max} is the maximum heat flow; Q_{sum} is the sum heat effect; τ_{ind} is the induction period; $\tau_{0.9}$ is 90% process completion time; a is the time of the initiated photo-curing process; $1/a$ is the photo-curing process rate.

properties due to the limitation of molecular mobility as a result of the formation of intermolecular chemical bonds.

For oligomers, the inductive effect turned out to be significant, the influence of which quickly leveled off as the chain length increased, and the reactivity of the group depended on the number of atoms located next to it [25]. In molecules with spacers, steric hindrances become of great importance, which determine the decrease in the reactivity of side functional groups.

The obtained measurement results were processed mathematically using the calculation method given below according to formula (2) [26].

$$\beta = \frac{C_{a\,max} - C_a}{C_{a\,max} - C_{a\,min}}, \qquad (2)$$

where C_a is the current value of the cell dielectric property index; $C_{a\,max}$ and $C_{a\,min}$ are the maximum and minimum value of the dielectric property index of the cell. The results are presented in Fig. 7.

The presented results indicate the effect of the spacer in the synthesized compounds on the curing process.

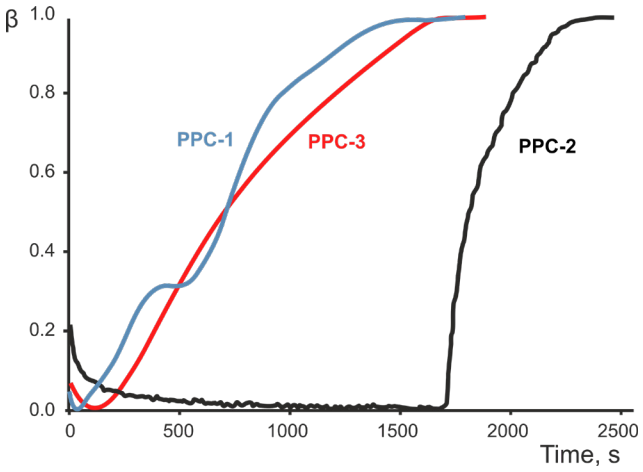

Fig. 7. Conversion degree of the photo-curing process PPC-1, PPC-2, and PPC-3 in the presence of the photoinitiator BAPhO 0.5 wt %.

Phosphorus-containing oligoether methacrylates cure relatively quickly without a spacer (PPC-1, Fig. 7). The pronounced inflection of the change curve of the dielectric properties of the studied oligomer can be used to characterize the time interval for the end of the gelation process, following which the rate of change in the dielectric properties increases and the polymerization process passes into the final phase of formation of the crosslinked polymer structure. The dynamics of photocuring of oligoether methacrylates with a spacer of different structure differs significantly from the one under consideration, including due to the absence of a pronounced gel formation area. The formation of a cross-linked PPC-2 polymer matrix proceeds with a significant induction period, which can be explained by the relatively higher mobility of ions not only of the oligomer, but also of the forming linear polymer, due to the presence of a flexible aliphatic space in its hinged part.

CONCLUSIONS

The possibility of obtaining new oligoether methacrylates with spacers in the chemical structure based on phosphorus trichloride, glycidyl methacrylate, and E-181 and ED-20 epoxy resins is confirmed. It is shown that the process of addition of the oxirane ring to phosphorus trichloride occurs both according to the Krasusky rule from the side of the α-carbon atom, and against this rule, with the formation of isomeric products.

The influence of the structure of the spacer on the rate of curing of oligomers under the action of UV radiation is determined.

According to dielectric analysis, photocuring in the bulk of oligoether methacrylates containing an aliphatic spacer is accompanied by an increase in the induction period of curing by a factor of 39, and an aromatic spacer by a factor of 4 compared to a sample without a spacer.

DSC studies established that the maximum thermal effect of UV curing (158.5 J/g) has an oligomer that does not contain a spacer. Meanwhile, the introduction of aliphatic and aromatic spacers leads to a decrease in the total thermal effect of the curing process to 147.8 and 93.4 J/g, respectively.

Acknowledgments

The work was supported by the Ministry of Science and Higher Education of the Russian Federation as a part of the state assignment (project code FZUS-2021-0013).

Authors' contributions

B.A. Buravov – carrying out syntheses, processing experimental data, and writing the text of the article;

A. Al-Hamzawi – conducting the experiment, data processing, and analysis of the results;

E.S. Bochkarev – analysis of research results, data processing;

N.Kh. Grichishkina – literature analysis, formalization of the list of references and interpretation of IR spectra;

S.V. Borisov – conducting IR research;

N.V. Sidorenko – conducting DSC research;

O.I. Tuzhikov – consultation on the chemistry of phosphorus-containing compounds, as well as planning, methodology, and implementation of the study;

O.O. Tuzhikov – the idea of the study, consultation on conducting experiments, writing the text of the article.

The authors declare no conflicts of interest.

REFERENCES

1. Levchik S.V. Introduction to Flame Retardancy and Polymer Flammability. In: Morgan A.B., Wilkie C.A. (Eds.). *Flame Retardant Polymer Nanocomposites*. John Wiley & Sons, Inc.; 2006. P. 1–29. https://doi.org/10.1002/9780470109038.ch1

2. Tuzhikov O.I., Khokhlova T.V., Bondarenko S.N., *et al*. *Elastomery i plastiki s ponizhennoi goryuchest'yu: monografiya* (*Elastomers and plastics with reduced flammability: monograph*). Volgograd: Politekhnik; 2005. 214 p. (in Russ.). ISBN 5-230-04464-0

3. Berlin Al.Al. Combustion of polymers and polymer materials of reduced flammability. *Sorosovskii obrazovatel'nyi zhurnal = Soros Educational Journal*. 1996;2(9):57–63 (in Russ.).

4. Wang Z, Liang B. Synthesis and properties of phosphorus and nitrogen containing intumescent flame-retardant curing agent for epoxy resin. *Plast. Rubber Compos*. 2018;47(7):306–314. https://doi.org/10.1080/14658011.2018.1491702

5. Bier F., Six J.-L., Durand A. DOPO-Based Phosphorus-Containing Methacrylic (Co)Polymers: Glass Transition Temperature Investigation. *Macromol. Mater. Eng*. 2019;304(4). https://doi.org/10.1002/mame.201800645

6. Harada M., Hirotani M., Ochi M. Synthesis and improved mechanical properties of twin-mesogenic epoxy thermosets using siloxane spacers with different lengths. *J. Appl. Polym. Sci*. 2019;136(34):47891. https://doi.org/10.1002/app.47891

7. Luo C., Zuo J., Wang F., Lin F., Zhao J., Xu Z. Click chemistry-assisted preparation and properties of phosphorus and nitrogen synergistic flame retardant optical resin with a high refractive index. *J. Appl. Polym. Sci*. 2018;135(38):46648. https://doi.org/10.1002/app.46648

8. Yang X., Chen S., Chen S., Xu H. Influencing factors on liquid crystalline properties of cholesterol side-chain liquid crystalline polymers without spacer: molecular weight and copolymerisation. *Liq. Cryst*. 2019;46(12):1827–1842. https://doi.org/10.1080/02678292.2019.1606352

9. Brigadnov K.A., Bilichenko Y.V., Polyakov V.A., Borisov R.S., Gusev K.I., Rudakova T.A., *et al*. Epoxy oligomers modified with epoxyphosphazenes. *Polym. Sci. Ser. B.* 2016;58(5):549–555. https://doi.org/10.1134/S1560090416050018

[Original Russian Text: Brigadnov K.A., Bilichenko Y.V., Polyakov V.A., Borisov R.S., Gusev K.I., Rudakova T.A., Filatov S.N., Kireev V.V. Epoxy oligomers modified with epoxyphosphazenes. *Vysokomolekulyarnye Soedineniya. Seriya B.* 2016;58(5):387–393 (in Russ.). https://doi.org/10.7868/S2308113916050016]

10. Tuzhikov O.I., Tuzhikov O.O., Buravov B.A., *et al.* Method for obtaining thermo- and heat-resistant polymers based on tris-[(1-chloromethyl-2-methacryloxy)ethoxy]-phosphines. RF Pat. 2697721, MPK C07F9/141, C08G 79/04. Volgograd: VolgGTU; 18.08.2019.

11. Tuzhikov O.I., Tuzhikov O.O., Buravov B.A., *et al.* Application of oligoesteracrylate ((((4-((1-(2-((bis((1-chloro-3-(methacryloyloxy)propan-2-yl)oxy)phosphine)-oxy)-3-chlorophenoxy)-3-chloropropan-2-yl)oxy)-1-chlorobutan-2-yl)oxy)phosphindiyl)bis(oxy))bis(3-chloropropan-2,1-diyl)-bis(2-methacrylate) as a monomer for the production of thermo- and heat-resistant polymers with reduced flammability. RF Pat. 2712107. MPK C08G 79/04, C08F 279/06, C07F 9/00. Volgograd: VolgGTU; 24.01.2020.

СПИСОК ЛИТЕРАТУРЫ

1. Levchik S.V. Introduction to Flame Retardancy and Polymer Flammability. In: Morgan, A.B., Wilkie C.A. (Eds.). *Flame Retardant Polymer Nanocomposites*. John Wiley & Sons, Inc.; 2006. P. 1–29. https://doi.org/10.1002/9780470109038.ch1

2. Тужиков О.И., Хохлова Т.В., Бондаренко С.Н. и др. *Эластомеры и пластики с пониженной горючестью: монография*. Волгоград: Политехник; 2005. 214 с. ISBN 5-230-04464-0

3. Берлин Ал. Ал. Горение полимеров и полимерные материалы пониженной горючести. *Соросовский образовательный журнал*. 1996;2(9):57–63.

4. Wang Z., Liang B. Synthesis and properties of phosphorus and nitrogen containing intumescent flame-retardant curing agent for epoxy resin. *Plast. Rubber Compos*. 2018;47(7):306–314. https://doi.org/10.1080/14658011.2018.1491702

5. Bier F., Six J.-L., Durand A. DOPO-Based Phosphorus-Containing Methacrylic (Co)Polymers: Glass Transition Temperature Investigation. *Macromol. Mater. Eng*. 2019;304(4). https://doi.org/10.1002/mame.201800645

6. Harada M., Hirotani M., Ochi M. Synthesis and improved mechanical properties of twin-mesogenic epoxy thermosets using siloxane spacers with different lengths. *J. Appl. Polym. Sci.* 2019;136(34):47891. https://doi.org/10.1002/app.47891

7. Luo C., Zuo J., Wang F., Lin F., Zhao J., Xu Z. Click chemistry-assisted preparation and properties of phosphorus and nitrogen synergistic flame retardant optical resin with a high refractive index. *J. Appl. Polym. Sci*. 2018;135(38):46648. https://doi.org/10.1002/app.46648

8. Yang X., Chen S., Chen S., Xu H. Influencing factors on liquid crystalline properties of cholesterol side-chain liquid crystalline polymers without spacer: molecular weight and copolymerisation. *Liq. Cryst*. 2019;46(12):1827–1842. https://doi.org/10.1080/02678292.2019.1606352

9. Бригаднов К.А., Биличенко Ю.В., Поляков В.А., Борисов Р.С., Гусев К.И., Рудакова Т.А., Филатов С.Н., Киреев В.В. Эпоксидные олигомеры, модифицированные эпоксифосфазенами. *Высокомолекулярные соединения. Серия Б.* 2016;58(5):387–393. https://doi.org/10.7868/S2308113916050016

10. Тужиков О.И., Тужиков О.О., Буравов Б.А. и др. Способ получения термо- и теплостойких полимеров на основе трис-[(1-галогенметил-2-метакрилокси)-этоксифосфинов. Пат. 2697721 РФ. МПК C07F9/141, C08G 79/04. Заявитель патентообладатель ВолгГТУ (RU). № 2019117090, заявл. 03.06.2019. опубл. 18.08.2019.

11. Тужиков О.И., Тужиков О.О., Буравов Б.А., Бочкарев Е.С., Солодовникова К.В., Хохлова Т.В., Сидоренко Н.В., Аль-Хамзави А.Х.Д. Применение олигоэфиракрилата ((((4-((1-(2-((бис((1-галоген-3-(метакрилоилокси)-пропан-2-ил)окси)фосфин)окси)-3-галогенпропокси)3-хлорпропан-2-ил)окси)-1-галоген-бутан-2-ил)окси)фосфиндиил)бис(окси))бис(3-галоген-пропан-2,1-диил)бис(2-метакрилата) в качестве мономера для получения термо- и теплостойких полимеров с пониженной горючестью. Пат. 2712107 РФ. МПК C08G79/04, C08F279/06, C07F9/00. Волгоград: ВолгГТУ; 2020.

12. Tuzhikov O.I., Tuzhikov O.O., Buravov B.A., *et al.* Application of oligoesteracrylate ((((((((((2-hydroxypropane-1,3-diyl)bis(oxy))bis(4,1-phenylene))bis(propan-2,2-diyl))-bis(4.1-phenylene))bis(hydroxy))-bis(1-chloropropane-3,2-diyl))bis(oxy))-bis(phosphintriyl))tetrakis(oxy))-tetrakis(3-chloropropane-2,1-diyl)tetrakis(2-methyl acrylate) as a monomer for the production of thermo- and heat-resistant polymers with reduced flammability. RF Pat. 2712116. MPK C08G 79/04, C07F 9/141. Volgograd: VolgGTU; 24.01.2020.

13. Dogadkin B.A, Dontsov A.A., Shershnev V.A. *Khimiya elastomerov* (*Chemistry of elastomers*). Moscow: Khimiya; 1981. 376 p. (in Russ.).

14. Efros L.S., Gorelik M.V. *Khimiya i tekhnologiya promezhutochnykh produktov* (*Chemistry and technology of intermediate products*). Leningrad: Khimiya; 1979. 544 p. (in Russ.).

15. Gorbunov B.N., Gurvich Ya.A., Maslova I.P. *Khimiya i tekhnologiya stabilizatorov polimernykh materialov* (*Chemistry and technology of stabilizers of polymer materials*). Moscow: Khimiya; 1981. 368 p. (in Russ.).

16. Khardin A.P., Tuzhikov O.I., V'yunov K.A., Khokhlova T.V. Kinetics of the reaction of phenoxymethylphosphonic acid chloride with glycidyl methacrylate. *Zhurnal Obshchei Khimii.* 1979;49(5):1031–1035 (in Russ.). URL: https://www.elibrary.ru/item.asp?id=22974331

17. Tuzhikov O.I., Khokhlova T.V., Bondarenko S.N., Dkhaibe M., Orlova S.A. Modification of epoxy-4,4′-isopropylidenediphenol resins with phosphorylated methacrylates for preparing compounds of the interpenetrating polymer network type. *Russ. J. Appl. Chem*. 2009;82(11):2034–2040. https://doi.org/10.1134/S107042720911024X

[Original Russian Text: Tuzhikov O.I., Khokhlova T.V., Bondarenko S.N., Dkhaibe M., Orlova S.A. Modification of epoxy-4,4′-isopropylidenediphenol resins with phosphorylated methacrylates for preparing compounds of the interpenetrating polymer network type. *Zhurnal Prikladnoi Khimii*. 2009;82(11):1887–1893 (in Russ.). URL: https://www.elibrary.ru/item.asp?id=44517526]

18. Khardin A.P., Tuzhikov O.I., V'yunov K.A., Khokhlova T.V., Rygalov L.N. Kinetics of reactions of phenoxymethylphosphonic acid chloride with unsymmetrical alpha-oxides. *Zhurnal Obshchei Khimii*. 1980;50(8):1733–1738 (in Russ.). URL: https://elibrary.ru/item.asp?id=21264731

19. Malinovskii M.S. *Okisi olefinov i ikh proizvodnye* (*Oxides of olefins and their derivatives*). Moscow: Goskhimtekhizdat; 1961. 553p. (in Russ.).

20. Chike K.E., Myrick M.L., Lyon R.E., Angel S.M. Raman and near-infrared studies of an epoxy resin. *Appl. Spectrosc.* 1993;47(10):1631–1635. https://doi.org/10.1366/0003702934334714

21. Guerra A.J., Lammel-Lindemann J., Katko A., Kleinfehn A., Rodriguez C.A., Catalani L.H., *et al*. Optimization of photocrosslinkable resin components and 3D printing process parameters. Acta Biomater. 2019;97:154–161. https://doi.org/10.1016/j.actbio.2019.07.045

22. Lima A.F., Salvador M.V.O., Dressano D., Saraceni C.H.C., Gonçalves L.S., Hadis M., *et al*. Increased rates of photopolymerisation by ternary type II photoinitiator systems in dental resins. *J. Mech. Behav. Biomed. Mater.* 2019;98:71–78. https://doi.org/10.1016/j.jmbbm.2019.06.005

23. Salgado V.E., Albuquerque P.P.A.C., Cavalcante L.M., Pfeifer C.S., Moraes R.R., Schneider L.F.J. Influence of photoinitiator system and nanofiller size on the optical properties and cure efficiency of model composites. *Dent. Mater*. 2014;30(10):e264–e271. https://doi.org/10.1016/j.dental.2014.05.019

12. Тужиков О.И., Тужиков О.О., Буравов Б.А. и др. Применение олигоэфиракрилата ((((((((((2-гидроксипропан-1,3-диил) бис (окси)) бис (4,1-фенилен)) бис (пропан-2,2-диил)) бис (4,1-фенилен)) бис(окси)) бис (1-галогенпропан-3,2-диил)) бис (окси)) бис(фосфинтриил)) тетракис (окси)) тетракис (3-галогенпропан-2,1-диил) тетракис (2-метилакрилата) в качестве мономера для получения термо- и теплостойких полимеров с пониженной горючестью. Пат. 2712116 РФ. МПК C08G79/04, C07F 9/141. Заявитель патентообладатель ВолгГТУ (RU). № 2019126186, заявл. 20.08.2019. опубл. 24.01.2020. Бюл. № 3.

13. Догадкин Б.А, Донцов А.А., Шершнев В.А. *Химия эластомеров*. 2-е изд., перераб. и доп. М.: Химия; 1981. 376 с.

14. Эфрос Л.С., Горелик М.В. *Химия и технология промежуточных продуктов*. Л.: Химия; 1979. 544 с.

15. Горбунов Б.Н., Гурвич Я.А., Маслова И.П. *Химия и технология стабилизаторов полимерных материалов*. М.: Химия; 1981. 368 с.

16. Хардин А.П., Тужиков О.И., Вьюнов К.А., Хохлова Т.В. Кинетика реакции хлорангидрида феноксиметилфосфоновой кислоты с глицидилметакрилатом. *Журн. общей химии*. 1979;49(5):1031–1035. URL: https://www.elibrary.ru/item.asp?id=22974331

17. Тужиков О.И., Хохлова Т.В., Бондаренко С.Н., Дхайбе М., Орлова С.А. Модификация эпоксидиановых смол фосфорсодержащими метакрилатами для получения компаундов типа взаимопроникающих полимерных сеток. *Журн. прикладной химии*. 2009;82(11):1887–1893. URL: https://www.elibrary.ru/item.asp?id=44517526

18. Хардин А.П., Тужиков О.И., Вьюнов К.А., Хохлова Т.В., Рыгалов Л.Н. Кинетика реакций хлорангидрида феноксиметилфосфоновой кислоты с нессиметричными альфа-окисями. Журн. общей химии.1980;50(8):1733–1738. URL: https://elibrary.ru/item.asp?id=21264731

19. Малиновский М.С. *Окиси олефинов и их производные*. М.: Госхимтехиздат; 1961. 553 с.

20. Chike K.E., Myrick M.L., Lyon R.E., Angel S.M. Raman and near-infrared studies of an epoxy resin. *Appl. Spectrosc*. 1993;47(10):1631–1635. https://doi.org/10.1366/0003702934334714

21. Guerra A.J., Lammel-Lindemann J., Katko A., Kleinfehn A., Rodriguez C.A., Catalani L.H., *et al.* Optimization of photocrosslinkable resin components and 3D printing process parameters. Acta Biomater. 2019;97:154–161. https://doi.org/10.1016/j.actbio.2019.07.045

22. Lima A.F., Salvador M.V.O., Dressano D., Saraceni C.H.C., Gonçalves L.S., Hadis M., *et al*. Increased rates of photopolymerisation by ternary type II photoinitiator systems in dental resins. *J. Mech. Behav. Biomed. Mater.* 2019;98:71–78. https://doi.org/10.1016/j.jmbbm.2019.06.005

23. Salgado V.E., Albuquerque P.P.A.C., Cavalcante L.M., Pfeifer C.S., Moraes R.R., Schneider L.F.J. Influence of photoinitiator system and nanofiller size on the optical properties and cure efficiency of model composites. *Dent. Mater*. 2014;30(10):e264–e271. https://doi.org/10.1016/j.dental.2014.05.019

24. Иржак В.И., Межиковский С.М. Кинетика отверждения олигомеров. *Успехи химии*. 2008;77(1):78–104. URL: https://elibrary.ru/item.asp?id=9933186

25. Иржак В.И., Межиковский С.М. *Химическая физика отверждения олигомеров*: монография. М.: Издательство Юрайт; 2020. 276 с.

24. Irzhak V.I., Mezhikovskii S.M. Kinetics of Oligomer Curing. *Russ. Chem. Rev*. 2008;77(1):77–103. https://doi.org/10.1070/RC2008v077n01ABEH003752

[Original Russian Text: Irzhak V.I., Mezhikovskii S.M. Kinetics of Oligomer Curing. *Uspekhi Khimii*. 2008;77(1):78–104 (in Russ.). URL: https://elibrary.ru/item.asp?id=9933186]

25. Irzhak V.I., Mezhikovskii S.M. *Khimicheskaya fizika otverzhdeniya oligomerov: monografiya* (*Chemical physics of curing oligomers: monograph*). Moscow: Yurait; 2020. 276 p. (in Russ.).

26. Tuzhikov O.O., Buravov B.A., Bochkarev E.S., Avvakumov V.E., Sidorenko N.V., *et al*. Effect of soluble PVC and copolimer A-15-O in epoxy resin on physical-mechanical properties of hydroxo- silicated polymerated systems and their fire retardant effect. *Izvestiya VolgGTU = Izvestia VSTU*. 2018;12(222):106–113 (in Russ.).

26. Тужиков О.О., Буравов Б.А., Бочкарев Е.С., Аввакумов В.Е., Сидоренко Н.В. и др. Влияние растворенных ПВХ и сополимера А-15-О в эпоксидном связующем на физико-механические свойства и огнестойкость наполненных гидроксосиликатами отвержденных полимерных систем. *Известия ВолгГТУ*. 2018;12(222):106–113.

About the authors:

Boris A. Buravov, Cand. Sci. (Chem.), Associate Professor, Department of General and Inorganic Chemistry; Senior Researcher, Laboratory of Polymer, Composite and Hybrid Functional Materials, Volgograd State Technical University (28, pr. im. V.I. Lenina, Volgograd, 400005, Russia). E-mail: byravov@ya.ru. ResearcherID AAH-5810-2021, RSCI SPIN-code 6730-5763, https://orcid.org/0000-0001-9039-571X

Ali Al-Khamzawi, Postgraduate Student, Department of General and Inorganic Chemistry, Volgograd State Technical University (28, pr. im. V.I. Lenina, Volgograd, 400005, Russia). E-mail: ali.alhamzawi80@gmail.com. ResearcherID M-2885-2017, RSCI SPIN-code 2551-0018, https://orcid.org/0000-0003-4491-494X

Eugene S. Bochkarev, Junior Researcher, Laboratory of Polymer, Composite and Hybrid Functional Materials, Volgograd State Technical University (28, pr. im. V.I. Lenina, Volgograd, 400005, Russia). E-mail: w_tovn@mail.ru. Scopus Author ID 57222574440, RSCI SPIN-code 6024-6675, https://orcid.org/0000-0002-2343-1562

Nazmiya Kh. Grichishkina, Senior Lecturer, Department of General and Inorganic Chemistry, Volgograd State Technical University (28, pr. im. V.I. Lenina, Volgograd, 400005, Russia). E-mail: nazmija3545@mail.ru. RSCI SPIN-code 5661-4527, https://orcid.org/0000-0002-2208-4992

Sergey V. Borisov, Cand. Sci. (Eng.), Associate Professor, Department of Chemistry and Processing Technology of Elastomers; Senior Researcher, Laboratory of Polymer, Composite and Hybrid Functional Materials, Volgograd State Technical University (28, pr. im. V.I. Lenina, Volgograd, 400005, Russia). E-mail: borisov.volgograd@yandex.ru. Researcher ID AAF-1221-2021, Scopus Author ID 57193435253, RSCI SPIN-code 4774-4238, https://orcid.org/0000-0003-4400-0822

Nina V. Sidorenko, Cand. Sci. (Eng.), Associate Professor, Department of Chemistry and Processing Technology of Elastomers, Volgograd State Technical University (28, pr. im. V.I. Lenina, Volgograd, 400005, Russia). E-mail: nvsidorenko@vstu.ru. ResearcherID A-9544-2014, Scopus Author ID 16308435400, RSCI SPIN-code 5155-3692, https://orcid.org/0000-0002-6113-290X

Oleg I. Tuzhikov, Dr. Sci. (Chem.), Professor, Department of Technology of Macromolecular and Fibrous Materials, Volgograd State Technical University (28, pr. im. V.I. Lenina, Volgograd, 400005, Russia). E-mail: tuzhikov_oi@vstu.ru. Scopus Author ID 6507272270, RSCI SPIN-code 7255-0330, https://orcid.org/0000-0003-1893-2861

Oleg O. Tuzhikov, Dr. Sci. (Eng.), Associate Professor, Head of the Department of General and Inorganic Chemistry, Volgograd State Technical University (28, pr. im. V.I. Lenina, Volgograd, 400005, Russia). E-mail: cand@vstu.ru. Scopus Author ID 12645529200, RSCI SPIN-code 8142-5915, https://orcid.org/0000-0001-6316-8896

Об авторах:

Буравов Борис Андреевич, к.х.н., доцент кафедры общей и неорганической химии; старший научный сотрудник лаборатории полимерных, композитных и гибридных функциональных материалов ФГБОУ ВО «Волгоградский государственный технический университет» (400005, Россия, Волгоград, пр-т им. В.И. Ленина, д. 28). E-mail: byravov@ya.ru. ResearcherID AAH-5810-2021, SPIN-код РИНЦ 6730-5763, https://orcid.org/0000-0001-9039-571X

Аль-Хамзави Али, аспирант кафедры общей и неорганической химии ФГБОУ ВО «Волгоградский государственный технический университет» (400005, Россия, Волгоград, пр-т им. В.И. Ленина, д. 28). E-mail: ali.alhamzawi80@gmail.com. ResearcherID M-2885-2017, SPIN-код РИНЦ 2551-0018, https://orcid.org/0000-0003-4491-494X

Бочкарев Евгений Сергеевич, младший научный сотрудник лаборатории полимерных, композитных и гибридных функциональных материалов ФГБОУ ВО «Волгоградский государственный технический университет» (400005, Россия, Волгоград, пр-т им. В.И. Ленина, д. 28). E-mail: w_tovn@mail.ru. Scopus Author ID 57222574440, SPIN-код РИНЦ 6024-6675, https://orcid.org/0000-0002-2343-1562

Гричишкина Назмия Хуршид-кызы, старший преподаватель кафедры общей и неорганической химии ФГБОУ ВО «Волгоградский государственный технический университет» (400005, Россия, Волгоград, пр-т им. В.И. Ленина, д. 28). E-mail: nazmija3545@mail.ru. SPIN-код РИНЦ 5661-4527, https://orcid.org/0000-0002-2208-4992

Борисов Сергей Владимирович, к.т.н., доцент кафедры химии и технологии переработки эластомеров; старший научный сотрудник лаборатории полимерных, композитных и гибридных функциональных материалов ФГБОУ ВО «Волгоградский государственный технический университет» (400005, Россия, Волгоград, пр-т им. В.И. Ленина, д. 28). E-mail: borisov.volgograd@yandex.ru. Researcher ID AAF-1221-2021, Scopus Author ID 57193435253, SPIN-код РИНЦ 4774-4238, https://orcid.org/0000-0003-4400-0822

Сидоренко Нина Владимировна, к.т.н., доцент кафедры химии и технологии переработки эластомеров ФГБОУ ВО «Волгоградский государственный технический университет» (400005, Россия, Волгоград, пр-т им. В.И. Ленина, д. 28). E-mail: nvsidorenko@vstu.ru. ResearcherID A-9544-2014, Scopus Author ID 16308435400, SPIN-код РИНЦ 5155-3692, https://orcid.org/0000-0002-6113-290X

Тужиков Олег Иванович, д.х.н., профессор кафедры технологии высокомолекулярных и волокнистых материалов ФГБОУ ВО «Волгоградский государственный технический университет» (400005, Россия, Волгоград, пр-т им. В.И. Ленина, д. 28). E-mail: tuzhikov_oi@vstu.ru. Scopus Author ID 6507272270, SPIN-код РИНЦ 7255-0330, https://orcid.org/0000-0003-1893-2861

Тужиков Олег Олегович, д.т.н., доцент, заведующий кафедрой общей и неорганической химии ФГБОУ ВО «Волгоградский государственный технический университет» (400005, Россия, Волгоград, пр-т им. В.И. Ленина, д. 28). E-mail: cand@vstu.ru. Scopus Author ID 12645529200, SPIN-код РИНЦ 8142-5915, https://orcid.org/0000-0001-6316-8896

The article was submitted: July 04, 2022; approved after reviewing: July 14, 2022; accepted for publication: October 04, 2022.

Translated from Russian into English by H. Moshkov
Edited for English language and spelling by Thomas Beavitt

CHEMISTRY AND TECHNOLOGY OF INORGANIC MATERIALS

ХИМИЯ И ТЕХНОЛОГИЯ НЕОРГАНИЧЕСКИХ МАТЕРИАЛОВ

ISSN 2686-7575 (Online)

https://doi.org/10.32362/2410-6593-2022-17-5-427-438

UDC 546.05

RESEARCH ARTICLE

Interaction of the anion $[2\text{-}B_{10}H_9O(CH_2)_4O]^-$ with secondary amines

Evgeniy Yu. Matveev[1,2,✉], Sergey S. Novikov[1], Valeriya Ya. Levitskaya[1], Artemiy I. Nichugovskiy[1], Ilya E. Sokolov[1,3], Konstantin Yu. Zhizhin[1,2], Nikolay T. Kuznetsov[2]

[1]MIREA – Russian Technological University (M.V. Lomonosov Institute of Fine Chemical Technologies), Moscow, 119571 Russia
[2]Kurnakov Institute of General and Inorganic Chemistry, Russian Academy of Sciences, Moscow, 119991 Russia
[3]Federal Research Center of Nutrition, Biotechnology and Food Safety, Moscow, 109240 Russia
✉Corresponding author, e-mail: cat1983@yandex.ru

Abstract

Objectives. *One of the most promising methods of treating malignant tumors is ^{10}B-neutron capture therapy. While compounds based on cluster boron anions $[B_nH_n]^{2-}$ (n = 10, 12) are often used as boron-containing agents due to the very high specific concentration of boron atoms per particle, the use of such compounds is associated with the need to develop new methods for the functionalization of boron clusters associated with the production of boron-containing derivatives containing biologically active functional groups. One of the most convenient methods of modification of $[B_nH_n]^{2-}$ (n = 10, 12) anions is the interaction of their derivatives containing cyclic oxonium-type substituents with negatively charged or neutral nucleophilic reagents. The disclosure of substituents of this type leads to the formation of closo-borates with functional groups separated from the cluster by an alkoxyl spacer chain. The purpose of this study is to develop methods for the synthesis of derivatives of the closo-decaborate anion $[B_{10}H_{10}]^{2-}$ with pendant nitrogen-containing groups.*

Methods. *The general control of the reactions of the disclosure of cyclic substituents was carried out on the basis of ^{11}B nuclear magnetic resonance (NMR) spectroscopy data. The structure of the obtained derivatives, including the nature of the attached functional groups, was determined using ^{1}H, ^{13}C attached proton test (APT) NMR and infrared (IR) spectroscopy data. The molecular weight of the synthesized compounds was confirmed by electrospray ionization mass-spectrometry (ESI–MS).*

Results. *The interaction of the anion $[2\text{-}B_{10}H_9O(CH_2)_4O]^-$ with secondary amines (dimethylamine, dipropylamine, diallylamine, dibutylamine, diisobutylamine, morpholine, di-sec-butylamine) in an ethanol environment is investigated. As a result of the reactions, a cyclic substituent is shown to expand with the addition of a nucleophilic reagent. Seven new derivatives of the closo-decaborate anion with pendant nitrogen-containing groups have been synthesized.*

Conclusions. *A developed method for obtaining closo-decaborates with ammonium groups separated from the boron cluster by an alkoxyl spacer group is presented. It is shown that the use of amines of various structures does not fundamentally affect the course of the reactions, allowing the composition and structure of the target derivatives to be effectively regulated. The resulting compounds can be involved in further modification reactions due to a reactive pendant group, as well as being suitable for use as effective polydentate ligands. Closo-decaborates with pendant nitrogen-containing groups and their derivatives are of considerable interest in the synthesis of compounds for use in ^{10}B-neutron capture therapy of malignant tumors.*

Keywords: *cluster boron anions, closo-decaborate anion, oxonium derivatives of closo-decaborate anion, disclosure of cyclic substituent, secondary amines, ^{10}B-neutron capture therapy of malignant tumors*

For citation: Matveev E.Yu., Novikov S.S., Levitskaya V.Ya., Nichugovskiy A.I., Sokolov I.E., Zhizhin K.Yu., Kuznetsov N.T. Interaction of the anion $[2\text{-}B_{10}H_9O(CH_2)_4O]^-$ with secondary amines. *Tonk. Khim. Tekhnol. = Fine Chem. Technol.* 2022;17(5):427–438 (Russ., Eng.). https://doi.org/10.32362/2410-6593-2022-17-5-427-438

НАУЧНАЯ СТАТЬЯ

Взаимодействие аниона $[2\text{-}B_{10}H_9O(CH_2)_4O]^-$ с вторичными аминами

Е.Ю. Матвеев[1,2,✉], С.С. Новиков[1], В.Я. Левицкая[1], А.И. Ничуговский[1], И.Е. Соколов[1,3], К.Ю. Жижин[1,2], Н.Т. Кузнецов[2]

[1]МИРЭА – Российский технологический университет (Институт тонких химических технологий им. М.В. Ломоносова), Москва, 119571 Россия

[2]Институт общей и неорганической химии им. Н.С. Курнакова Российской академии наук, Москва, 119991 Россия

[3]Федеральный исследовательский центр питания, биотехнологии и безопасности пищи, Москва, 109240 Россия

[✉]Автор для переписки, e-mail: cat1983@yandex.ru

Аннотация

Цели. *^{10}B-нейтронозахватная терапия является одним из наиболее перспективных методов лечения злокачественных опухолей. В качестве борсодержащих агентов нередко применяются соединения на основе кластерных анионов бора $[B_nH_n]^{2-}$ (n = 10, 12), как имеющие очень высокую удельную концентрацию атомов бора в расчете на одну частицу. Однако использование таких соединений связано с необходимостью разработки новых методов функционализации борных кластеров, связанных*

с получением борсодержащих производных с биологически активными функциональными группами. Одним из наиболее удобных методов модификации анионов $[B_nH_n]^{2-}$ (n = 10, 12) является взаимодействие их производных, содержащих циклические заместители оксониевого типа, с отрицательно заряженными или нейтральными нуклеофильными реагентами. Раскрытие заместителей данного типа приводит к образованию клозо-боратов с функциональными группами, отделенными от кластера алкоксильной спейсерной цепочкой. Целью настоящего исследования является разработка методов синтеза производных клозо-декаборатного аниона $[B_{10}H_{10}]^{2-}$ с пендантными азотсодержащими группами.

Методы. *Общий контроль протекания реакций раскрытия циклических заместителей осуществлялся на основании данных ^{11}B спектроскопии ядерного магнитного резонанса (ЯМР). Строение полученных производных, в том числе природу присоединенных функциональных групп определяли на основании данных ^{1}H, ^{13}C ЯМР с тестом на присоединенные протоны (АРТ) и инфракрасной спектроскопии (ИК). Молекулярную массу синтезированных соединений подтверждали методом масс-спектрометрии с ионизацией электрораспылением (ИЭР-МС).*

Результаты. *Исследовано взаимодействие аниона $[2\text{-}B_{10}H_9O(CH_2)_4O]^-$ с вторичными аминами (диметиламин, дипропиламин, диаллиламин, дибутиламин, диизобутиламин, морфолин, ди-втор-бутиламин) в среде этанола. Показано, что в результате реакций происходит раскрытие циклического заместителя с присоединением нуклеофильного реагента. Синтезированы семь новых производных клозо-декаборатного аниона с пендантными азотсодержащими группами.*

Выводы. *Разработан новый метод получения клозо-декаборатов с аммониевыми группами, отделенными от борного кластера алкоксильной спейсерной группой. Показано, что применение аминов различного строения принципиально не влияет на ход протекающих реакций и позволяет эффективно регулировать состав и строение целевых производных. Полученные соединения могут быть вовлечены в дальнейшие реакции модификации за счет реакционноспособной пендантной группы, а также могут быть использованы в роли эффективных полидентатных лигандов. Клозо-декабораты с пендантными азотсодержащими группами и их производные представляют значительный интерес в синтезе соединений, перспективных для применения в ^{10}B-нейтронозахватной терапии злокачественных опухолей.*

Ключевые слова: *кластерные анионы бора, клозо-декаборатный анион, оксониевые производные клозо-декаборатного аниона, раскрытие циклического заместителя, вторичные амины, ^{10}B-нейтронозахватная терапия злокачественных опухолей*

Для цитирования: Матвеев Е.Ю., Новиков С.С., Левицкая В.Я., Ничуговский А.И., Соколов И.Е., Жижин К.Ю., Кузнецов Н.Т. Взаимодействие аниона $[2\text{-}B_{10}H_9O(CH_2)_4O]^-$ с вторичными аминами. *Тонкие химические технологии*. 2022;17(5):427–438. https://doi.org/10.32362/2410-6593-2022-17-5-427-438

INTRODUCTION

Cluster boron anions $[B_nH_n]^{2-}$ (n = 10, 12) are one of the unique examples of completely inorganic clusters that are highly resistant to oxidizing agents and tend to replace *exo*-polyhedral hydrogen atoms with various functional groups [1–3]. Derivatives based on boron polyhedra of this class are increasingly being used in science and technology, with the medical field, namely, ^{10}B neutron capture therapy of malignant tumors, remaining one of the most significant areas [4–14]. In this regard, it is very important to develop new methods for the synthesis of *closo*-borates containing biologically active groups that can also be modified.

As well as being associated directly with the boron cluster, the functionalization of boron

cluster anions can involve already introduced functional groups. One of the main methods for the direct functionalization of $[B_nH_n]^{2-}$ (n = 10, 12) anions is electrophilic-induced nucleophilic substitution (EINS) of *exo*-polyhedral hydrogen atoms for various functional groups [15–19]. While this method can be used to obtain a wide range of *closo*-borates, its disadvantages are associated with the possible interaction of nucleophilic reagents with Lewis acids used to initiate such processes. By modifying the already introduced *exo*-polyhedral groups, it becomes possible to significantly expand the range of obtained boron-containing compounds. For example, in recent years, the method of modifying thiol and nitrile derivatives of $[B_nH_n]^{2-}$ anions has gained popularity [20–23]. However, it is often necessary to obtain compounds containing so-called pendant functional groups separated by a relatively inert fragment from the boron cluster in order to avoid the influence of the latter. Therefore, one of the most convenient methods for the functionalization of boron clusters involves the substitution of *exo*-polyhedral hydrogen atoms for molecules of cyclic ethers, followed by the opening of the resulting oxonium-type cyclic substituents with the help of nucleophiles. As a result of such reactions, *closo*-borates are formed with pendant functional groups attached to the boron cluster through an alkoxy spacer chain. Derivatives of $[B_nH_n]^{2-}$ anions with a given structure can be obtained by using a wide range of nucleophilic reagents [24–30].

The purpose of this work is to reveal the conditions and features of the interaction of the 1,4-dioxane derivative of the *closo*-decaborate anion, $[2\text{-}B_{10}H_9O(CH_2)_4O]^-$, with secondary amines (dimethylamine, dipropylamine, diallylamine, dibutylamine, diisobutylamine, di-*sec*-butylamine, morpholine), during which *closo*-decaborates with pendant ammonium groups are formed.

EXPERIMENTAL SECTION

Physical and chemical analysis methods

The infrared (IR) spectra of the compounds were recorded on an Infralum FT-02 IR Fourier spectrometer (*Lumex*, Russia) in the range 400–4000 cm^{-1}. Samples were prepared in the form of tablets from a mixture of the test compound and KBr. ^1H, ^{11}B, ^{13}C nuclear magnetic resonance (NMR) spectra of test substance solutions in fully deuterated dimethyl sulfoxide (DMSO-d_6) with attached proton test (APT) were recorded on a DPX-300 NMR spectrometer (*Bruker*, Germany) at frequencies of 300.3, 96.32, and 75.49 MHz, respectively, with internal deuterium stabilization. Mass spectra were recorded using a TSQ Quantum Access MAX triple quadrupole mass spectrometer (*Thermo Fisher Scientific*, USA) equipped with an API source (HESI-II), an Agilent 1200 G1311A four-channel pump (*Agilent*, USA), and a 6-port injector with an external volume loop of 0.002 cm^3. Samples were introduced into the ion source by manual loop injection into the solvent stream. Acetonitrile (ACN) for the high-performance liquid chromatography (HPLC) and deionized water obtained on a Milli-Q unit (*Millipore*, USA) were used as solvents. The pump flow was set at 0.4 mL/min in ACN/H_2O isocratic mode (50:50). Electrospray ionization (ESI) was carried out in the negative ion detection mode under the following conditions: sputtering voltage –2.5 kV, ion transfer tube temperature 350 °C, evaporator temperature 300 °C, gas pressure (N_2) 35 a.u., auxiliary gas flow rate 10 a.u. Mass spectra (MS) in the full scan mode were recorded in the range m/z 100–600. Data collection and processing was carried out using Xcalibur software (version 2.0).

Elemental analysis of the sample was performed on an ELAN DRC-e inductively coupled plasma mass spectrometer (*PerkinElmer*, USA). The content of carbon, hydrogen, and nitrogen in the samples was determined on a EuroEA 3000 elemental CHNS analyzer (*Eurovector Instrument*, Italy).

Materials

Tetrabutylammonium [2-(1-(1,4-dioxanium))]-nonahydro-*closo*-decaborate, (n-Bu_4N)$[B_{10}H_9O(CH_2)_4O]$ was synthesized according to a previously developed procedure [31]. 1,4-dioxane was purified according to [32]. Dimethylamine (33% aqueous solution, *Sigma-Aldrich*, USA), dibutylamine (>99.5%, *Sigma-Aldrich*, USA), dipropylamine (99%, *Sigma-Aldrich*, USA), diallylamine (99%, *Sigma-Aldrich*, USA), di(*sec*-butyl)amine (99%, *Sigma-Aldrich*, USA), diisobutylamine (99%, *Sigma-Aldrich*, USA), morpholine (99%, *Sigma-Aldrich*, USA), ethanol (95%, *Sigma-Aldrich*, USA), 1-pentanol (99%, *Sigma-Aldrich*, USA), methanol (99.9%, *Merck*, Germany), cesium iodide (chemically pure, *Himmed*, Russia), tetraphenylphosphonium chloride (99.9%, *Sigma-Aldrich*, USA), dimethylformamide (99.8%, *Sigma-Aldrich*, USA).

Experiments

To a suspension of 45 mg (0.1 mmol) (Bu_4N)$[B_{10}H_9O(CH_2)_4O]$ in 10 mL of ethanol (95%)

was added 0.6 mmol of a secondary amine (40 μL of a 33% aqueous solution of dimethylamine or 85 μL of dipropylamine or 105 μL of dibutylamine or 105 μL of diisobutylamine or 52 μL of morpholine or 75 μL of diallylamine) and heated with stirring for 2 h at reflux temperature. 200 μL of a 2 *M* solution of cesium fluoride in methanol was then added the resulting colorless or light-yellow solution. The resultant white or light-yellow precipitate was filtered off, recrystallized from a mixture of water-methanol (1:1) and dried under high vacuum.

Cesium 2-[2-(2-dimethylammonioethoxy)ethoxy)]-nonahydro-*closo*-decaborate, $Cs[B_{10}H_9O(CH_2)_2O(CH_2)_2NH(CH_3)_2]$

Yield: 0.030 g (79%). ^{1}H NMR (DMSO-d_6, δ, ppm): 10.16 (s, 1H, NH), 3.65 (t, 2H, CH$_2$ (α)), 3.40 (t, 2H, CH$_2$ (γ)), 3.16 (m, 4H, CH$_2$ (β, δ)), 2.77 (s, 6H, CH$_3$ (ε)), from 1.00 to −0.50 (m, 9H, $B_{10}H_9$). ^{11}B {^{1}H} NMR (DMSO-d_6, δ, ppm): 0.8 (s, BO (2)), −0.3, −3.5 (both s, by 1B, BH (10, 1)), −21.5 (s, BH (3, 5, 6, 9)), −27.2 (s, 2B, BH (7, 8)), −31.5 (s, 1B, BH (4)). ^{13}C APT NMR, (DMSO-d_6, δ, ppm): 71.2 (CH$_2$ (β)), 70.1 (CH$_2$ (γ)), 63.2 (CH$_2$ (α)), 55.2 (CH$_2$ (δ)), 42.8 (CH$_3$ (ε)). IR (KBr, cm^{-1}): 3075, 2720 (ν(N$^+$–H)), 2467 (ν(B–H)), 1471 (δ(H–N$^+$–H)). Found (%): C, 18.59; H, 3.58; N, 3.61; B, 28.12; $C_6H_{24}B_{10}CsNO_2$. Calculated (%): C, 18.80; H, 3.61; N, 3.65; B, 28.20. ESI-MS. Found, *m*/*z*: 250.3 $[B_{10}H_9O(CH_2)_2O(CH_2)_2NH(CH_3)_2]^-$. ($C_6H_{24}B_{10}NO_2$). Calculated: *M* = 250.3.

Cesium 2-[2-(2-dipropylammonioethoxy)ethoxy)]-nonahydro-*closo*-decaborate, $Cs[B_{10}H_9O(CH_2)_2O(CH_2)_2NH(CH_2CH_2CH_3)_2]$

Yield: 0.036 g (81%). ^{1}H NMR (DMSO-d_6, δ, ppm): 9.81 (s, 1H, NH), 3.68 (t, 2H, CH$_2$ (α)), 3.38 (t, 2H, CH$_2$ (γ)), 3.20 (t, 2H, CH$_2$ (β)), 3.13 (t, 2H, CH$_2$ (δ)), 2.51 (t, 4H, CH$_2$ (ε)), 1.72 (m, 4H, CH$_2$ (ζ)), 0.93 (t, 6H, CH$_2$ (η)), from 1.00 to −0.50 (m, 9H, $B_{10}H_9$). ^{11}B {^{1}H} NMR (DMSO-d_6, δ, ppm): 1.4 (s, BO (2)), −0.1, −3.7 (both s, by 1B, BH (10, 1)), −21.3 (s, BH (3, 5, 6, 9)), −27.3 (s, 2B, BH (7,8)), −31.2 (s, 1B, BH (4)). ^{13}C APT NMR (DMSO-d_6, δ, ppm): 70.5 (CH$_2$ (β)), 70.1 (CH$_2$ (γ)), 54.9 (CH$_2$ (α)), 50.8 (CH$_2$ (δ)), 23.1 (CH$_3$ (ε)), 16.3 (CH$_3$ (ζ)), 10.9 (CH$_3$ (η)). IR (KBr, cm^{-1}): 3079, 2715 (ν(N$^+$–H)), 2449 (ν(B–H)), 1481 (δ(H–N$^+$–H)). Found (%): C, 27.14; H, 7.26; N, 3.15; B, 24.49; $C_{10}H_{32}B_{10}CsNO_2$. Calculated (%): C, 27.33; H, 7.34; N, 3.18; B, 24.60. ESI-MS. Found, *m*/*z*: 306.4 $[B_{10}H_9O(CH_2)_2O(CH_2)_2NH(C_3H_7)_2]^-$. ($C_{10}H_{32}B_{10}NO_2$). Calculated: *M* = 306.3.

Cesium 2-[2-(2-dibutylammonioethoxy)ethoxy)]-nonahydro-*closo*-decaborate, $Cs[B_{10}H_9O(CH_2)_2O(CH_2)_2NH(CH_2CH_2CH_2CH_3)_2]$

Yield: 0.38 g (82%). ^{1}H NMR (DMSO-d_6, δ, ppm): 9.80 (s, 1H, NH), 3.63 (t, 2H, CH$_2$ (α)), 3.35 (t, 2H, CH$_2$ (γ)), 3.17 (t, 2H, CH$_2$ (β)), 3.12 (t, 2H, CH$_2$ (δ)), 2.51 (t, 4H, CH$_2$ (ε)), 1.62 (m, 4H, CH$_2$ (ζ)), 1.33 (m, 4H, CH$_2$ (η)), 0.93 (t, 6H, CH$_3$ (θ)), from 1.00 to −0.50 (m, 9H, $B_{10}H_9$). ^{11}B {^{1}H} NMR (DMSO-d_6, δ, ppm): 1.9 (c, BO (2)), 0.1, −3.6 (both s, by 1B, BH (10, 1)), −21.4 (s, BH (3, 5, 6, 9)), −27.3 (s, 2B, BH (7,8)), −31.4 (s, 1B, BH (4)). ^{13}C APT NMR (DMSO-d_6, δ, ppm): 70.5 (CH$_2$ (β)), 57.6 (CH$_2$ (γ)), 53.2 (CH$_2$ (α)), 50.8 (CH$_2$ (δ)), 23.1 (CH$_2$ (ε)), 19.6 (CH$_2$ (ζ)), 19.2 (CH$_3$ (η)), 13.7 (CH$_3$ (θ)). IR (KBr, cm^{-1}): 3079, 2715 (ν(N$^+$–H)), 2449 (ν(B–H)), 1483 (δ(H–N$^+$–H)). Found (%): C, 30.65; H, 7.72; N, 2.93; B, 22.98; $C_{12}H_{36}B_{10}CsNO_2$. Calculated (%): C, 30.83; H, 7.76; N, 2.99; B, 23.12. ESI-MS. Found, *m*/*z*: 334.2 $[B_{10}H_9O(CH_2)_2O(CH_2)_2NH(CH_2CH_2CH_2CH_3)_2]^-$. ($C_{12}H_{36}B_{10}NO_2$). Calculated: *M* = 334.4.

Cesium 2-[2-(2-di(2-methylpropyl)ammonioethoxy)-ethoxy)]nonahydro-*closo*-decaborate, $Cs[B_{10}H_9O(CH_2)_2O(CH_2)_2NH(CH_2CH(CH_3)_2)_2]$

Yield: 0.36 g (77%). ^{1}H NMR (DMSO-d_6, δ, ppm): 9.82 (s, 1H, NH), 3.32 (t, 2H, CH$_2$ (α)), 3.17 (t, 2H, CH$_2$ (γ)), 3.07 (t, 2H, CH$_2$ (β)), 2.43 (t 2H, CH$_2$ (δ)), 2.08 (d, 4H, CH$_2$ (ε)), 1.61 (m, 2H, CH (ζ)), 0.82 (d, 6H, CH$_3$ (η)), from 1.00 to −0.50 (m, 9H, $B_{10}H_9$). ^{11}B {^{1}H} NMR (DMSO-d_6, δ, ppm): 0.6 (s, BO (2)), −0.4, −3.1 (both s, by 1B, BH (10, 1)), −21.3 (s, BH (3, 5, 6, 9)), −27.0 (s, 2B, BH (7, 8)), −31.6 (s, 1B, BH (4)). ^{13}C APT NMR (DMSO-d_6, δ, ppm): 72.2 (CH$_2$ (β)), 69.4 (CH$_2$ (γ)), 68.6 (CH$_2$ (α)), 64.0 (CH$_2$ (δ)), 54.0 (CH (ε)), 26.3 (CH$_3$ (ζ)), 20.7 (CH$_3$ (η)). IR (KBr, cm^{-1}): 3082, 2694 (ν(N$^+$–H)), 2448 (ν(B–H)), 1468 (δ(H–N$^+$–H)). Found (%): C, 30.62; H, 7.70; N, 2.94; B, 23.02; $C_{12}H_{36}B_{10}CsNO_2$. Calculated (%): C, 30.83; H, 7.76; N, 2.99; B, 23.12. ESI-MS. Found, *m*/*z*: 334.3 $[B_{10}H_9O(CH_2)_2O(CH_2)_2NH(CH_2CH(CH_3)_2)_2]^-$. ($C_{12}H_{36}B_{10}NO_2$). Calculated: *M* = 334.4.

Cesium 2-[2-(2-*N*-morpholylammonioethoxy)ethoxy)]-nonahydro-*closo*-decaborate, $Cs[B_{10}H_9O(CH_2)_2O(CH_2)_2NH(CH_2CH_2)_2O)]$

Yield: 0.36 g (85%). ^{1}H NMR (DMSO-d_6, δ, ppm): 4.55 (s, 1H, NH), 3.56 (t, 2H, CH$_2$ (ζ)), 3.35 (t, 2H, CH$_2$ (α)), 3.19 (t, 2H, CH$_2$ (γ)), 3.05 (t, 2H, CH$_2$ (β)), 2.36 (t, 2H, CH$_2$ (δ)), 2.32 (m, 2H, CH$_2$ (ε)), from 1.00 to −0.50 (m, 9H, $B_{10}H_9$). ^{11}B {^{1}H} NMR (DMSO-d_6, δ, ppm): 1.5 (s, BO (2)), −0.2, −3.2 (both s, by 1B, BH (10, 1)), −21.3 (s, BH (3, 5, 6, 9)), −27.0 (s, 2B, BH (7,8)), −31.4 (s, 1B, BH (4)). ^{13}C APT NMR

(DMSO-d_6, δ, ppm): 72.2 ($\underline{C}H_2$ (β)), 69.3 ($\underline{C}H_3$ (ζ)), 66.7 ($\underline{C}H_2$ (γ)), 65.9 ($\underline{C}H_2$ (α)), 58.0 ($\underline{C}H_2$ (δ)), 53.4 ($\underline{C}H_2$ (ε)). IR (KBr, cm^{-1}): 3071, 2726 (ν(N^+–H)), 2454 (ν(B–H)), 1456 (δ(H–N^+–H)). Found (%): C, 22.41; H, 6.10; N, 3.23; B, 25.24; $C_8H_{26}B_{10}CsNO_3$. Calculated (%): C, 22.59; H, 6.16; N, 3.29; B, 25.41. ESI-MS. Found, *m/z*: 292.2 $[B_{10}H_9O(CH_2)_2O(CH_2)_2NH(CH_2CH_2)_2O)]^-$. ($C_8H_{26}B_{10}NO_3$). Calculated: *M* = 292.3.

Cesium 2-[2-(2-diallylammonioethoxy)ethoxy)]-nonahydro-*closo*-decaborate, $Cs[B_{10}H_9O(CH_2)_2O(CH_2)_2NH(CH_2CH{=}CH_2)_2)]$

Yield: 0.34 g (79%). ^{1}H NMR (DMSO-d_6, δ, ppm): 9.85 (s, 1H, N$\underline{H}$), 5.83 (m, 2H, C$\underline{H}$ (ζ)), 5.12 (d, 4H, C$\underline{H}_2$ (η)), 3.38 (t, 2H, C$\underline{H}_2$ (α)), 3.20 (t, 2H, C$\underline{H}_2$ (γ)), 3.11 (t, 2H, C$\underline{H}_2$ (β)), 3.04 (d, 4H, C$\underline{H}_2$ (ε)), 2.52 (t, 2H, C$\underline{H}_2$ (δ)), from 1.00 to −0.50 (m, 9H, $B_{10}\underline{H}_9$). ^{11}B {^{1}H} NMR (DMSO-d_6, δ, ppm): 1.1 (s, $\underline{B}$O (2)), −0.3, −3.2 (both s, by 1B, $\underline{B}$H (10, 1)), −21.4 (s, $\underline{B}$H (3, 5, 6, 9)), −27.2 (s, 2B, BH (7, 8)), −31.7 (s, 1B, BH (4)). ^{13}C APT NMR (DMSO-d_6, δ, ppm): 135.7 ($\underline{C}$H (ζ)), 117.4 ($\underline{C}H_2$ (η)), 72.2 ($\underline{C}H_2$ (β)), 69.4 ($\underline{C}H_2$ (γ)), 67.9 ($\underline{C}H_2$ (α)), 56.4 ($\underline{C}H_2$ (δ)), 52.2 ($\underline{C}H_2$ (ε)). IR (KBr, cm^{-1}): 3079, 2716 (ν(N^+–H)), 3025 (ν(=C–H)), 2455 (ν(B–H)), 1446 (δ(H–N^+–H)). Found (%): C, 27.40; H, 6.42; N, 3.17; B, 24.68; $C_{10}H_{28}B_{10}CsNO_2$. Calculated (%): C, 27.58; H, 6.48; N, 3.21; B, 24.83. ESI-MS. Found, *m/z*: 302.4 $[B_{10}H_9O(CH_2)_2O(CH_2)_2NH(CH_2CH{=}CH_2)_2)]^-$. ($C_{10}H_{28}B_{10}NO_2$). Calculated: *M* = 302.3.

Cesium 2-[2-(2-di(2-butyl)ammonioethoxy)-ethoxy)]nonahydro-*closo*-decaborate, $Cs[B_{10}H_9O(CH_2)_2O(CH_2)_2NH(CH(CH_3)(CH_2CH_3))_2]$

To a suspension of 45 mg (0.1 mmol) of (Bu_4N)[$B_{10}H_9O(CH_2)_4O$] in 10 mL of 1-pentanol (95%) was added 0.6 mmol (105 μL) of di-*sec*-butylamine and heated with stirring for 6 h at 110–120°C. To the resulting colorless solution was added 200 μL of a 2 *M* solution of cesium fluoride in methanol. The resulting white or light-yellow precipitate was filtered off, recrystallized from a mixture of water-methanol (1:1) and dried in a high vacuum.

Yield: 0.33 g (72%). ^{1}H NMR (DMSO-d_6, δ, ppm): 6.57 (s, 1H, N$\underline{H}$), 3.38 (t, 2H, C$\underline{H}_2$ (α)), 3.16 (t, 2H, C$\underline{H}_2$ (γ)), 3.06 (t, 2H, C$\underline{H}_2$ (β)), 2.55 (t, 2H, C$\underline{H}_2$ (δ)), 1.23 (t, 2H, C$\underline{H}$ (ε)), 1.09 (m, 4H, C$\underline{H}_2$ (ζ)), 0.89 (t, 6H, CHC$\underline{H}_3$ (η)), 0.80 (t, 6H, $CH_2C\underline{H}_3$ (θ)), from 1.00 to −0.50 (m, 9H, $B_{10}\underline{H}_9$). ^{11}B {^{1}H} NMR (DMSO-d_6, δ, ppm): 1.3 (s, $\underline{B}$O (2)), −0.4, −3.2 (both s, by 1B, $\underline{B}$H (10, 1)), −21.4 (s, $\underline{B}$H (3, 5, 6, 9)), −27.1 (s, 2B, $\underline{B}$H (7, 8)), −31.9 (s, 1B, $\underline{B}$H (4)). ^{13}C APT NMR (DMSO-d_6, δ, ppm): 72.2 ($\underline{C}H_2$ (β)), 69.4 ($\underline{C}H_2$ (γ)), 65.5 ($\underline{C}H_2$ (α)), 62.7 ($\underline{C}H_2$ (δ)), 28.6 ($\underline{C}$H (ε)), 18.1 ($\underline{C}H_2$ (ζ)), 17.3 (CH$\underline{C}H_3$ (η)), 11.7 ($CH_2\underline{C}H_3$ (θ)). IR (KBr, cm^{-1}): 3079, 2732 (ν(N^+–H)), 2456 (ν(B–H)), 1457 (δ(H–N^+–H)). Found (%): C, 30.63; H, 7.70; N, 2.91; B, 23.00; $C_{12}H_{36}B_{10}CsNO_2$. Calculated (%): C, 30.83; H, 7.76; N, 2.99; B, 23.12. ESI-MS. Found, *m/z*: 334.3 $[B_{10}H_9O(CH_2)_2O(CH_2)_2NH(CH(CH_3)(CH_2CH_3))_2]^-$. ($C_{12}H_{36}B_{10}NO_2$). Calculated: *M* = 334.4.

RESULTS AND DISCUSSION

We have studied the interaction of the 1,4-dioxane derivative of the *closo*-decaborate anion $[B_{10}H_9O(CH_2)_4O]^-$ with secondary amines in ethanol. In the course of research, it was shown that as a result of the reactions, the cyclic substituent of the oxonium type is opened, followed by the addition of pendant ammonium functional groups (see Scheme).

^{11}B {^{1}H} NMR spectroscopy is a very convenient method for the primary monitoring of 1,4-dioxane substituent opening reactions in the $[B_{10}H_9O(CH_2)_4O]^-$

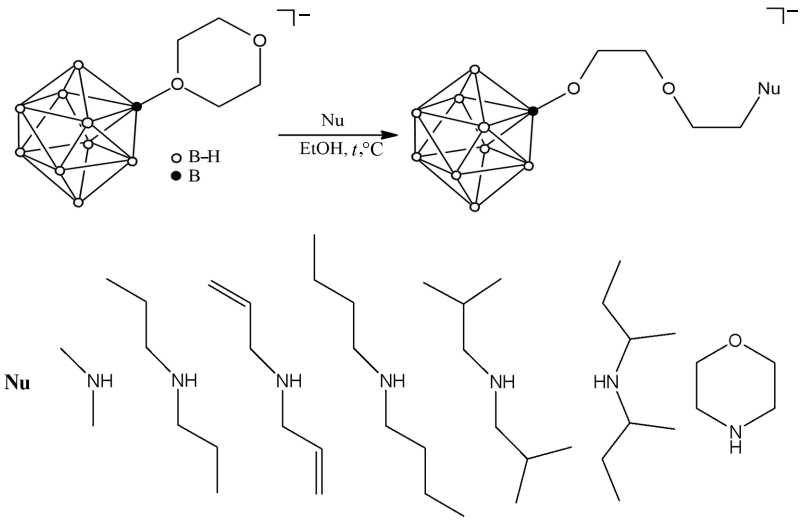

Scheme. Interaction of the $[B_{10}H_9O(CH_2)_4O]^-$ anion with secondary amines.

anion. Here, it is important to note that, while the general form of the spectrum characteristic of monosubstituted *closo*-decaborates $[B_{10}H_9R]^{x-}$ (x = 1, 2) is preserved, a significant change in the chemical shifts of the signals is observed (Fig. 1).

Thus, the signals from apical boron atoms appear in the ^{11}B NMR spectrum of the starting compound $Bu_4N[B_{10}H_9O(CH_2)_4O]$ at 0.8 ppm and −6.4 ppm; and −3.1 ppm, respectively. The singlet from the ipso boron atom bonded to the oxygen atom is shifted from 7.9 ppm. up to 0.6 ppm. This is the only signal that does not split into a doublet in the absence of broadband suppression of the B–H spin-spin interaction. Signals from other equatorial atoms in a strong field are redistributed with respect to the spectrum of the initial $[B_{10}H_9O(CH_2)_4O]^-$ anion: three signals are observed in the spectrum of the reaction product at –21.3, –27.0, and –31.56 ppm., having a ratio of integral intensities of 4:2:1. Such changes in the spectral pattern can be explained by the redistribution of the electron density on boron atoms due to the change in the B–O bond type from oxonium to alkoxy.

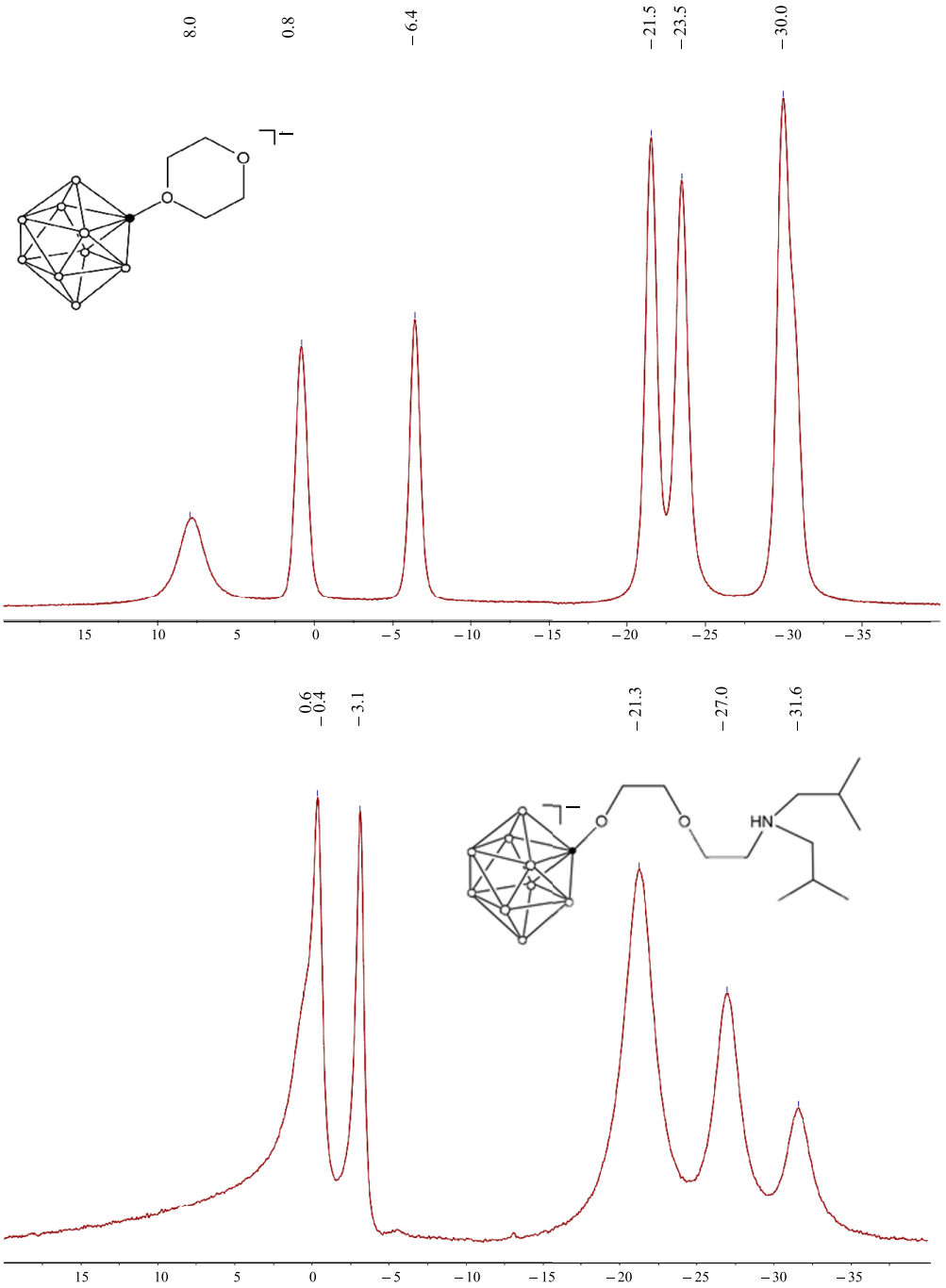

Fig. 1. ^{11}B {^1H} NMR spectra of $Bu_4N[B_{10}H_9O(CH_2)_4O]$ (top) and $Cs[B_{10}H_9O(CH_2)_2O(CH_2)_2NH(CH_2CH(CH_3)_2)_2]$ (bottom).

While the course of the opening of the cyclic substituent in the 1,4-dioxane derivative of the *closo*-decaborate anion can be unambiguously determined according to the described changes, practically no information about the structure of the alkoxy spacer and the introduced pendant group is provided, due to their similarity for all obtained connections. Accordingly, this data was obtained by analyzing the IR, ^{13}C APT and ^1H NMR spectra of the obtained derivatives.

Thus, the absorption bands in the regions of 2690–3100 cm^{-1} and 1440–1490 cm^{-1} in the IR spectra of the synthesized compounds with pendant ammonium groups can be related to stretching vibrations of the N^+–H bonds and bending vibrations of the H–N^+–H bonds, respectively. The boron cluster is represented in the IR spectra of the products by a high-intensity absorption band from B–H stretching vibrations in the range 2449–2467 cm^{-1}. This type of spectra indicates the opening of the cyclic substituent and the addition of pendant nitrogen-containing groups.

The ^1H NMR spectra of the obtained derivatives of the *closo*-decaborate anion undergo significant changes compared to the spectrum of the starting $[B_{10}H_9O(CH_2)_4O]^-$ anion. In particular, its ^1H NMR spectrum contains only two triplets at 3.85 ppm. and 4.31 ppm from nonequivalent methylene groups of the cyclic substituent, while in the spectrum of $Cs[B_{10}H_9O(CH_2)_2O(CH_2)_2NH(CH_2CH(CH_3)_2)_2]$ four triplets appear with equal integrated intensity from the protons of the alkoxy chain at 3.32 ppm (α), 3.17 ppm (γ), 3.07 ppm (β), and 2.43 ppm (δ), along with signals from the pendant group at 2.08 (d, CH_2 (ε)), 1.61 (m, 2H, CH (ζ)), and 0.82 (d, 6H, CH_3 (η)) ppm (Fig. 2). Similar changes are observed in the spectra of other obtained compounds. Since the signals from the hydrogen atoms of the boron cluster typically represent an extremely broad multiplet in the range from 1.00 to −0.50 ppm., they are not of significant interest.

The ^{13}C APT spectra of the synthesized compounds also depict interesting changes associated with the opening of the 1,4-dioxane substituent and the introduction of a terminal ammonium group. Thus, the spectrum of the cesium salt of the anion $[B_{10}H_9O(CH_2)_2O(CH_2)_2NH(CH_2CH(CH_3)_2)_2]^-$ contains four signals at 54.0, 26.3, and 20.7 ppm. from ε-, ζ-, and η-carbon atoms of the $–NH(CH_2CH(CH_3)_2)_2$ group. Signals from carbon atoms of the spacer chain are observed at 72.2 (β), 69.4 (γ), 68.6 (α), and 64.0 (δ) ppm (Fig. 3).

The composition of the synthesized derivatives of the *closo*-decaborate anion was confirmed using the ESI-MS method. For example, the mass spectrum of the compound $Cs[B_{10}H_9O(CH_2)_2O(CH_2)_2NH(CH_2CH_2CH_2CH_3)_2]$ in the negative ionization mode of ESI-MS shows an ion with a maximum intensity at *m*/*z* 334.22 from a singly charged anion of the composition $[B_{10}H_9O(CH_2)_2O(CH_2)_2NH(CH_2CH_2CH_2CH_3)_2]^-$ (Fig. 4).

It is interesting to note that the interaction of the anion $[B_{10}H_9O(CH_2)_4O]^-$ with di-*sec*-butylamine

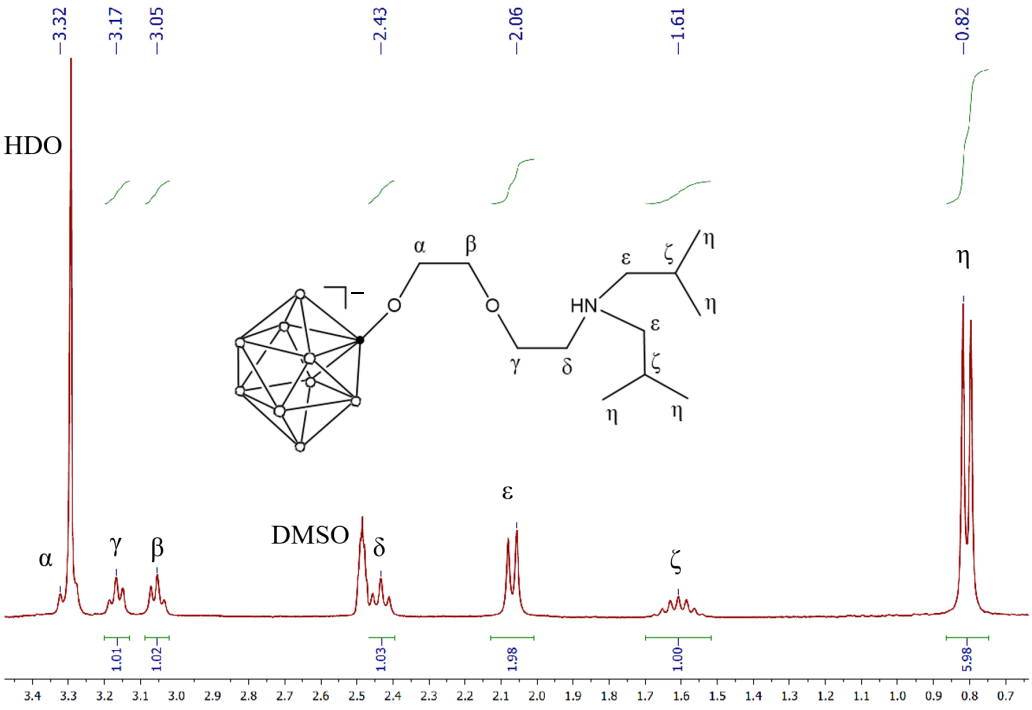

Fig. 2. ^1H NMR spectrum of $Cs[B_{10}H_9O(CH_2)_2O(CH_2)_2NH(CH_2CH(CH_3)_2)_2]$ in DMSO-d_6.

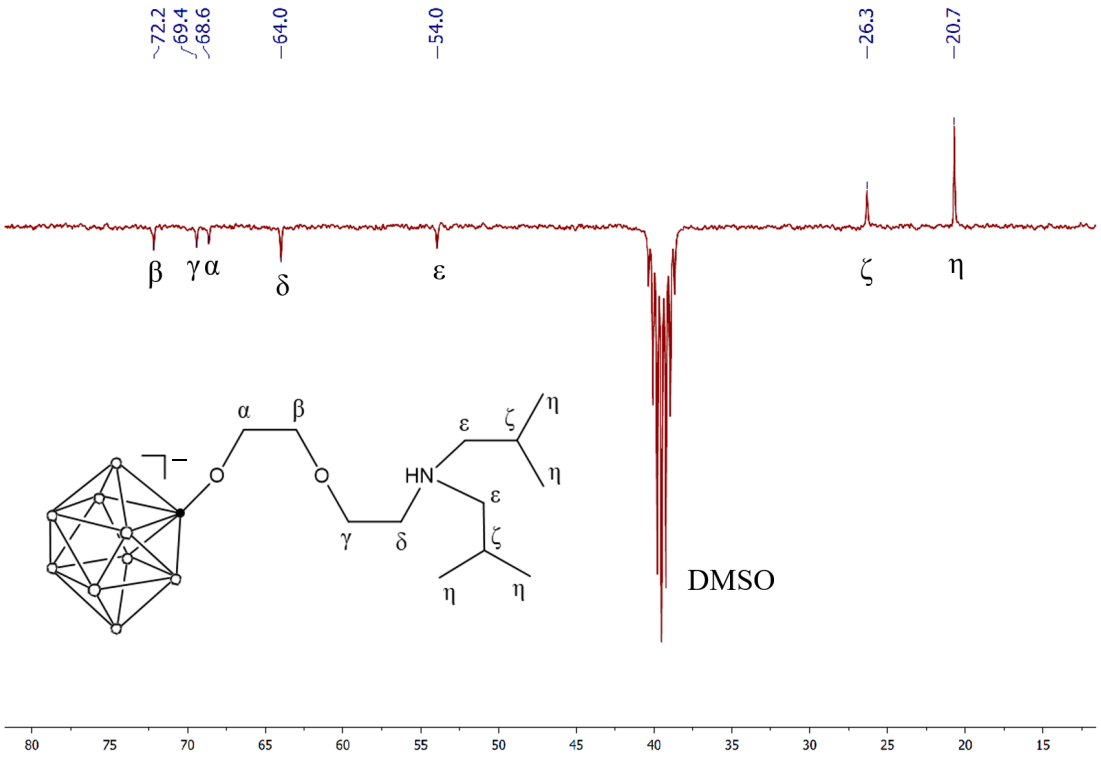

Fig. 3. ^{13}C ART NMR spectrum of $Cs[B_{10}H_9O(CH_2)_2O(CH_2)_2NH(CH_2CH(CH_3)_2)_2]$ in DMSO-d_6.

practically does not occur in ethanol at reflux for 8 h. For this reason, the corresponding reaction was carried out in a medium of a higher-boiling solvent (1-pentanol). This can be attributed to steric hindrance in the formation of the anion $[B_{10}H_9O(CH_2)_2O(CH_2)_2NH(CH(CH_3)(CH_2CH_3))_2]^-$.

CONCLUSIONS

Thus, in the present study, a method was developed for the synthesis of new derivatives of the *closo*-decaborate anion with secondary amine molecules (dimethylamine, dipropylamine, diallylamine,

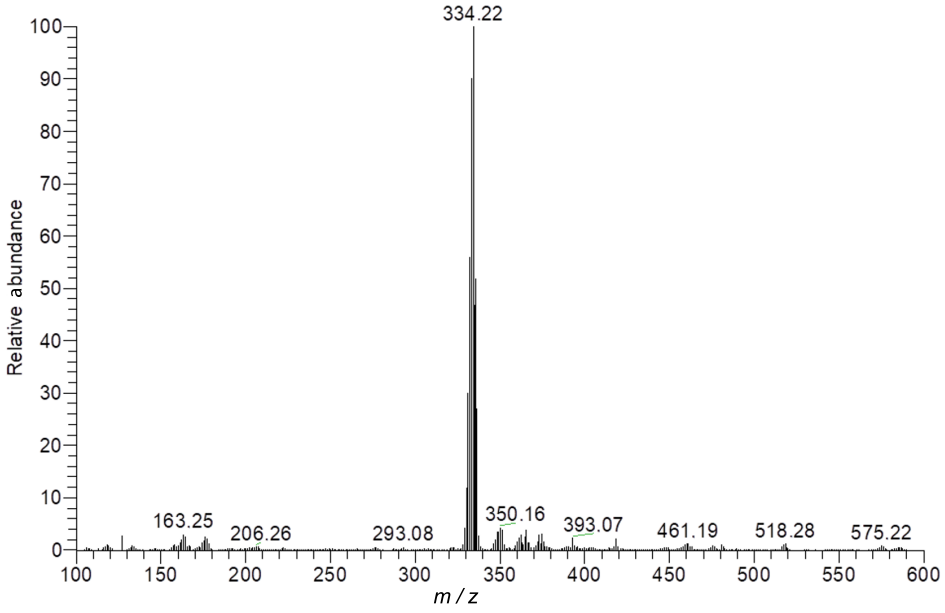

Fig. 4. ESI-MS spectrum of the $Cs[B_{10}H_9O(CH_2)_2O(CH_2)_2NH(CH_2CH_2CH_2CH_3)_2]$ in the negative ionization mode.

dibutylamine, diisobutylamine, morpholine, di-*sec*-butylamine) attached to the cluster anion as pendent groups.

The developed method is shown to achieve high yields of the target compounds (72–88%), simple execution, as well as allowing nitrogen-containing derivatives of the $[B_{10}H_{10}]^{2-}$ anion to be selectively obtained. Such compounds can be used as effective polydentate ligands, as well as being suitable for introduction into further modification reactions due to the attached pendant group.

Acknowledgments

The study was performed using the equipment of the Centers for Collective Use of the MIREA – Russian Technological University, Agreement No. 075-15-2021-689, September 01, 2021.

Authors' contributions

E.Yu. Matveev – formulation of the problem, development of the scientific concept, and writing the text of the article;

S.S. Novikov – performing experimental studies, collecting and analyzing the results;

V.Ya. Levitskaya – performing experimental studies, collecting and analyzing the results;

A.I. Nichugovskiy – obtaining and processing physicochemical characteristics of synthesized compounds;

I.E. Sokolov – obtaining and processing physicochemical characteristics of synthesized compounds;

K.Yu. Zhizhin – development of the scientific concept, consultation on research methodology;

N.T. Kuznetsov – development of the scientific concept, consultation on research methodology.

The authors declare no conflict of interest.

REFERENCES

1. Zhao X., Yang Z., Chen H., Wang Z., Zhou X., Zhang H. Progress in three-dimensional aromatic-like *closo*-dodecaborate. *Coord. Chem. Rev*. 2021;444:214042. https://doi.org/10.1016/j.ccr.2021.214042

2. Sivaev I. B., Prikaznov A.V., Naoufal D. Fifty years of the *closo*-decaborate anion chemistry. *Collect. Czechoslov. Chem. Commun*. 2010;75(11):1149–1199. https://doi.org/10.1135/cccc2010054

3. Sivaev I.B., Bregadze V.I., Sjöberg S. Chemistry of *closo*-dodecaborate anion $[B_{12}H_{12}]^{2-}$: a review. *Collect. Czechoslov. Chem. Commun*. 2002;67(6):679–727. https://doi.org/10.1135/cccc20020679

4. Pakhomov S., Kaszynski P., Young V.G. 10-Vertex *closo*-boranes as potential π linkers for electronic materials. *Inorg. Chem*. 2000;39(10):2243–2245. https://doi.org/10.1021/ic991350t

5. Paskevicius M., Hansen B.R., Jørgensen M., Richter B., Jensen T.R. Multifunctionality of silver *closo*-boranes. *Nat. Commun*. 2017;8(1):15136. https://doi.org/10.1038/ncomms15136

6. Ringstrand B. Boron clusters as structural elements of novel liquid crystalline materials. *Liquid Crystals Today*. 2013;22(2):22–35. https://doi.org/10.1080/1358314X.2013.829932

7. Zharkov D.O., Yudkina A.V., Riesebeck T., Loshchenova P.S., Mostovich E.A., Dianov G.L. Boron-containing nucleosides as tools for boron-neutron capture therapy. *Am. J. Cancer Res*. 2021;11(10):4668–4682.

8. Goszczyński T.M., Fink K., Boratyński J. Icosahedral boron clusters as modifying entities for biomolecules. *Expert Opin. Biol. Ther*. 2018;18(sup1):205–213. https://doi.org/10.1080/14712598.2018.1473369

9. Ali F., Hosmane N.S., Zhu Y. Boron chemistry for medical applications. *Molecules*. 2020;25(4):828. https://doi.org/10.3390/molecules25040828

10. Bregadze V.I., Sivaev I.B., Glazun S.A. Polyhedral boron compounds as potential diagnostic and therapeutic antitumor agents. *Anti-Cancer Agents Med. Chem.* (*Formerly Current Medicinal Chemistry-Anti-Cancer Agents*). 2006;6(2):75–109. http://doi.org/10.2174/187152006776119180

11. Barth R.F., Mi P., Yang W. Boron delivery agents for neutron capture therapy of cancer. *Cancer Commun.* 2018;38(1):1–15. https://doi.org/10.1186/s40880-018-0299-7

12. Jørgensen M., Hansen B.R., Lee Y.S., Cho Y.W., Jensen T.R. Crystal Structures and Energy Storage Properties of Ammine Sodium Decahydro-*closo*-decaboranes ($Na_2B_{10}H_{10}\cdot n NH_3$, n = 1, 2). *J. Phys. Chem. C*. 2019;123(33):20160–20166. https://doi.org/10.1021/acs.jpcc.9b06084

13. Suzuki M. Boron neutron capture therapy (BNCT): a unique role in radiotherapy with a view to entering the accelerator-based BNCT era. *Int. J. Clin. Oncol*. 2020;25(1):43–50. https://doi.org/10.1007/s10147-019-01480-4

14. Moss R.L. Critical review, with an optimistic outlook, on Boron Neutron Capture Therapy (BNCT). *Appl. Radiat. Isot*. 2014;88:2–11. https://doi.org/10.1016/j.apradiso.2013.11.109

15. Matveev E.Y., Kubasov A.S., Razgonyaeva G.A., Polyakova I.N., Zhizhin K.Y., Kuznetsov N.T. Reactions of the $[B_{10}H_{10}]^{2-}$ anion with nucleophiles in the presence of halides of group IIIA and IVB elements. *Russ. J. Inorg. Chem*. 2015;60(7):776–785. https://doi.org/10.1134/S0036023615070104

16. Zhizhin K.Y., Zhdanov A.P., Kuznetsov N.T. Derivatives of *closo*-decaborate anion $[B_{10}H_{10}]^{2-}$ with *exo*-polyhedral substituents. *Russ. J. Inorg. Chem*. 2010;55(14):2089–2127. https://doi.org/10.1134/S0036023610140019

17. Stogniy M.Y., Erokhina S.A., Sivaev I.B., Bregadze V.I. Nitrilium derivatives of polyhedral boron compounds (boranes, carboranes, metallocarboranes): Synthesis and reactivity. *Phosphorus, Sulfur, Silicon Relat. Elem*. 2019;194(10):983–988. https://doi.org/10.1080/10426507.2019.1631312

18. Klyukin I.N., Zhdanov A.P., Matveev E.Y., Razgonyaeva G.A., Grigoriev M.S., Zhizhin K.Y., Kuznetsov N.T. Synthesis and reactivity of *closo*-decaborate anion derivatives with multiple carbon–oxygen bonds. *Inorg. Chem. Commun.* 2014;50:28–30. https://doi.org/10.1016/j.inoche.2014.10.008

19. Klyukin I.N., Kubasov A.S., Limarev I. P., *et al*. The new approach to formation of *exo* boron–oxygen bonds from the decahydro-*closo*-decaborate(2-) anion. *Polyhedron*. 2015;101:215–222. https://doi.org/10.1016/j.poly.2015.09.025

20. Nelyubin A.V., Klyukin I.N., Novikov A.S., *et al*. Nucleophilic addition of amino acid esters to nitrilium derivatives of *closo*-decaborate anion. *Mendeleev Commun*. 2021;31(2):201–203. https://doi.org/10.1016/J.MENCOM.2021.03.018

21. Nelyubin A.V., Selivanov N.A., Bykov A.Y., *et al*. Primary Amine Nucleophilic Addition to Nitrilium *Closo*-Dodecaborate $[B_{12}H_{11}NCCH_3]^-$: A Simple and Effective Route to the New BNCT Drug Design. *Int. J. Mol. Sci*. 2021;22(24):13391. https://doi.org/10.3390/ijms222413391

22. Kubasov A.S., Turishev E.S., Polyakova I.N., Matveev E.Y., Zhizhin K.Y., Kuznetsov N.T. The method for synthesis of 2-sulfanyl *closo*-decaborate anion and its S-alkyl and S-acyl derivatives. *J. Organomet. Chem*. 2017;828:106–115. https://doi.org/10.1016/j.jorganchem.2016.11.035

23. Kubasov A.S., Matveev E.Y., Turyshev E.S., Polyakova I.N., Nichugovskiy A.I., Zhizhin K.Y., Kuznetsov N.T. Synthesis and stability studies of derivatives of the 2-sulfanyl-*closo*-decaborate anion $[2\text{-}B_{10}H_9SH]^{2-}$. *Inorganica Chim. Acta*. 2018;477:277–283. https://doi.org/10.1016/j.ica.2018.03.013

24. Semioshkin A. A., Sivaev I. B., Bregadze V. I. Cyclic oxonium derivatives of polyhedral boron hydrides and their synthetic applications. *Dalton Trans*. 2008;(8):977–992. https://doi.org/10.1039/B715363E

25. Orlova A.V., Kondakov N.N., Kimel B.G., Kononov L.O., Kononova E.G., Sivaev I.B., Bregadze V.I. Synthesis of novel derivatives of *closo*-dodecaborate anion with azido group at the terminal position of the spacer. *Appl. Organomet. Chem*. 2007;21(2):98–100. https://doi.org/10.1002/aoc.1151

26. Matveev E.Yu., Akimov S.S., Kubasov A.S., Nichugovskiy A.I., Nartov A.S., Retivov V.M., Zhizhin K.Yu., Kuznetsov N.T. Reaction of the $[B_{10}H_9O_2C_4H_8]^-$ anion with C-nucleophiles. *Rus. J. Inorg. Chem.* 2017;62(6):808–813 https://doi.org/10.1134/S0036023617060146

27. Matveev E.Y., Limarev I.P., Nichugovskii A.I., Bykov A.Y., Zhizhin K.Y., Kuznetsov N.T. Derivatives of *closo*-decaborate anion with polyamines. *Rus. J. Inorg. Chem.* 2019;64(8):977–983. https://doi.org/10.1134/S0036023619080084

28. Bregadze V.I., Sivaev I.B., Dubey R.D., Semioshkin A., Shmal'ko A.V., Kosenko I.D., Hosmane N.S. Boron-Containing Lipids and Liposomes: New Conjugates of Cholesterol with Polyhedral Boron Hydrides. *Chem. Eur. J.* 2020;26(61),13832–13841. https://doi.org/10.1002/chem.201905083

29. Grin M.A., Semioshkin A.A., Titeev R.A., *et al*. Synthesis of a cycloimide bacteriochlorin *p* conjugate with the *closo*-dodecaborate anion. *Mendeleev Commun.* 2007;17(1):14–15. https://doi.org/10.1016/j.mencom.2007.01.005

30. Matveev E.Y., Akimov S.S., Kubasov A.S., Retivov V.M., Zhizhin K.Y., Kuznetsov N.T. The method for obtaining a derivative *closo*-decaborate anion with pendante DTPA-group. *Fine Chem. Technol*.2019;14(1):59–65. https://doi.org/10.32362/2410-6593-2019-14-1-59-65

31. Zhizhin K.Yu., Mustyatsa V.N., Malinina E.A., *et al*. Interaction of *closo*-decaborate anion $B_{10}H_{10}^{2-}$ with cyclic ethers. *Russ. J. Inorg. Chem.* 2004;49(2):180–189.

32. Becker H., Domshke G., Fanghanel E. *Organikum. Organisch-chemisches Grundpraktikum*. Berlin: VEB Deutscher Verlag der Wissenschaften; 1990. 751 p.

About the authors:

Evgeniy Yu. Matveev, Cand. Sci. (Chem.), Associate Professor, A.N. Reformatskii Department of Inorganic Chemistry, M.V. Lomonosov Institute of Fine Chemical Technologies, MIREA – Russian Technological University (86, Vernadskogo pr., Moscow, 119571, Russia); Researcher, Laboratory of Chemistry of Light Elements and Clusters, N.S. Kurnakov Institute of General and Inorganic Chemistry, Russian Academy of Sciences, (31, Leninskii pr., Moscow, 119991, Russia). E-mail: cat1983@yandex.ru. Scopus Author ID 7005337961, https://orcid.org/0000-0003-0478-0705

Sergey S. Novikov, Student, A.N. Reformatskii Department of Inorganic Chemistry, M.V. Lomonosov Institute of Fine Chemical Technologies, MIREA – Russian Technological University (86, Vernadskogo pr., Moscow, 119571, Russia). E-mail: exsergion@gmail.com. https://orcid.org/0000-0001-8489-1506

Valeriia Ya. Levitskaia, Student, A.N. Reformatskii Department of Inorganic Chemistry, M.V. Lomonosov Institute of Fine Chemical Technologies, MIREA – Russian Technological University (86, Vernadskogo pr., Moscow, 119571, Russia). E-mail: valeriialy9@gmail.com. https://orcid.org/0000-0001-6479-2957

Artemiy I. Nichugovskiy, Junior Researcher, N.A. Preobrazhensky Department of Chemistry and Technology of Biological Active Compounds, Medicinal and Organic Chemistry, M.V. Lomonosov Institute of Fine Chemical Technologies, MIREA – Russian Technological University (86, Vernadskogo pr., Moscow, 119571, Russia). E-mail: ainichugovskiy@gmail.com. Scopus Author ID 57201401857, ResearcherID AAN-9946-2020, RSCI SPIN-code 1153-0929, https://orcid.org/0000-0003-2523-2054

Ilya E. Sokolov, Engineer, Shared Science and Training Center for Collective Use, MIREA – Russian Technological University (86, Vernadskogo pr., Moscow, 119571, Russia); Junior Researcher, Federal Research Center of Nutrition, Biotechnology and Food Safety (2/14, Ustinskii proezd, Moscow, 109240, Russia). E-mail: sokolov_iliya@yahoo.com. Scopus Author ID 57214011688, ResearcherID AAZ-5229-2021, RSCI SPIN-code 6337-4978, https://orcid.org/0000-0003-2819-6001

Konstantin Yu. Zhizhin, Corresponding Member of the Russian Academy of Sciences, Dr. Sci. (Chem.), Professor, A.N. Reformatskii Department of Inorganic Chemistry, M.V. Lomonosov Institute of Fine Chemical Technologies, MIREA – Russian Technological University (86, Vernadskogo pr., Moscow, 119571, Russia); Deputy Director for Research, N.S. Kurnakov Institute of General and Inorganic Chemistry, Russian Academy of Sciences (31, Leninskii pr., Moscow, 119991, Russia). E-mail: kyuzhizhin@igic.ras.ru. Scopus Author ID 6701495620, ResearcherID C-5681-2013, RSCI SPIN-code 4605-4065, https://orcid.org/0000-0002-4475-124X

Nikolay T. Kuznetsov, Full Member at the Russian Academy of Sciences, Dr. Sci. (Chem.), Head of the Laboratory of Chemistry of Light Elements and Clusters, N.S. Kurnakov Institute of General and Inorganic Chemistry, Russian Academy of Sciences, (31, Leninskii pr., Moscow, 119991, Russia). E-mail: ntkuz@igic.ras.ru. Scopus Author ID 56857205300, ResearcherID S-1129-2016, RSCI SPIN-code 3876-6006, https://orcid.org/0000-0002-0131-6387

Об авторах:

Матвеев Евгений Юрьевич, к.х.н., доцент кафедры неорганической химии им. А.Н. Реформатского, Институт тонких химических технологий им. М.В. Ломоносова ФГБОУ ВО «МИРЭА – Российский технологический университет» (119571, Россия, Москва, пр-т Вернадского, 86); научный сотрудник лаборатории химии легких элементов и кластеров, Институт общей и неорганической химии им. Н.С. Курнакова Российской академии наук (119991, Россия, Москва, Ленинский пр-т, 31). E-mail: cat1983@yandex.ru. Scopus Author ID 7005337961, https://orcid.org/0000-0003-0478-0705

Новиков Сергей Сергеевич, студент, кафедра неорганической химии им. А.Н. Реформатского, Институт тонких химических технологий им. М.В. Ломоносова ФГБОУ ВО «МИРЭА – Российский технологический университет» (119571, Россия, Москва, пр-т Вернадского, 86). E-mail: exsergion@gmail.com. https://orcid.org/0000-0001-8489-1506

Левицкая Валерия Ярославовна, студентка, кафедра неорганической химии им. А.Н. Реформатского, Институт тонких химических технологий им. М.В. Ломоносова ФГБОУ ВО «МИРЭА – Российский технологический университет» (119571, Россия, Москва, пр-т Вернадского, 86). E-mail: valeriialy9@gmail.com. https://orcid.org/0000-0001-6479-2957

Ничуговский Артемий Игоревич, младший научный сотрудник, кафедра химии и технологии биологически активных соединений, медицинской и органической химии им. Н.А. Преображенского, Институт тонких химических технологий им. М.В. Ломоносова ФГБОУ ВО «МИРЭА – Российский технологический университет» (119571, Россия, Москва, пр-т Вернадского, 86). E-mail: ainichugovskiy@gmail.com. Scopus Author ID 57201401857, ResearcherID AAN-9946-2020, SPIN-код РИНЦ 1153-0929, https://orcid.org/0000-0003-2523-2054

Соколов Илья Евгеньевич, инженер, Центр коллективного пользования ФГБОУ ВО «МИРЭА – Российский технологический университет» (119571, Россия, Москва, пр-т Вернадского, 86); младший научный сотрудник, ФГБУН Федеральный исследовательский центр питания, биотехнологии и безопасности пищи (109240, Россия, Москва, Устьинский проезд, 2/14). E-mail: sokolov_iliya@yahoo.com. Scopus Author ID 57214011688, ResearcherID AAZ-5229-2021, SPIN-код РИНЦ 6337-4978, https://orcid.org/0000-0003-2819-6001

Жижин Константин Юрьевич, чл.-корр. РАН, д.х.н., профессор кафедры неорганической химии им. А.Н. Реформатского, Институт тонких химических технологий им. М.В. Ломоносова ФГБОУ ВО «МИРЭА – Российский технологический университет» (119571, Россия, Москва, пр-т Вернадского, 86); заместитель директора по научной работе, Институт общей и неорганической химии им. Н.С. Курнакова Российской академии наук (119991, Россия, Москва, Ленинский пр-т, 31). E-mail: kyuzhizhin@igic.ras.ru. Scopus Author ID 6701495620, ResearcherID C-5681-2013, SPIN-код РИНЦ 4605-4065, https://orcid.org/0000-0002-4475-124X

Кузнецов Николай Тимофеевич, академик РАН, д.х.н., заведующий лабораторией, Институт общей и неорганической химии им. Н.С. Курнакова Российской академии наук (119991, Россия, Москва, Ленинский пр-т, 31). E-mail: ntkuz@igic.ras.ru. Scopus Author ID 56857205300, ResearcherID S-1129-2016, SPIN-код РИНЦ 3876-6006, https://orcid.org/0000-0002-0131-6387

The article was submitted: June 15, 2022; approved after reviewing: June 24, 2022; accepted for publication: September 15, 2022.

Translated from Russian into English by H. Moshkov
Edited for English language and spelling by Thomas Beavitt

CHEMISTRY AND TECHNOLOGY OF INORGANIC MATERIALS

ХИМИЯ И ТЕХНОЛОГИЯ НЕОРГАНИЧЕСКИХ МАТЕРИАЛОВ

ISSN 2686-7575 (Online)

https://doi.org/10.32362/2410-6593-2022-17-5-439-449

UDC 666.3.015.4

RESEARCH ARTICLE

Effect of activating additives on the cold sintering process of $(MnFeCoNiCu)_3O_4$ high-entropy ceramics

Andrey V. Smirnov[1,✉], Yuri D. Ivakin[1,2], Maxim V. Kornyushin[1], Anastasia A. Kholodkova[1,2], Alexander A. Vasin[1], Sofia Ayudinyan[3], Hasmik V. Kirakosyan[3]

[1]Mobile Solutions Engineering Center, MIREA – Russian Technological University, Moscow, 119454 Russia
[2]Faculty of Chemistry, M.V. Lomonosov Moscow State University, Moscow, 119991 Russia
[3]A.B. Nalbandyan Institute of Chemical Physics, National Academy of Sciences, Yerevan, 0014 Armenia
[✉]Corresponding author, e-mail: smirnov_av@mirea.ru

Abstract

Objectives. *To obtain experimental data on the effect of activating additive type on the cold sintering process of $(MnFeCoNiCu)_3O_4$ high-entropy ceramic. The following substances were used as activating additives: ammonium acetate (CH_3COONH_4), acetic acid (CH_3COOH), ammonium chloride (NH_4Cl), potassium fluoride dihydrate ($KF{\cdot}2H_2O$), lithium fluoride (LiF), sodium fluoride (NaF), and sodium hydroxide (NaOH).*

Methods. *Synthesis of the initial powder by low-temperature self-propagating method; investigation of the powder particles size distribution by laser diffraction method; analysis of the particle shape and compacted sample microstructure by scanning electron microscopy; investigation of the phase composition by X-ray phase analysis; high-entropy ceramic sample consolidation by cold sintering process. The density of the initial powder and the relative density of cold sintered samples were determined by the Archimedes method.*

Results. *Samples with a relative density of over 0.70 were obtained using distilled water, CH_3COONH_4 and NaOH during cold sintering at 300°C, with a holding time of 30 min and pressure 315 MPa.*

Conclusions. *For the first time, the effect of the type of activating additive on the relative density of high-entropy ceramics $(MnFeCoNiCu)_3O_4$ samples obtained by cold sintering process has been experimentally demonstrated. The samples microstructures have pronounced differences: 20 wt % distilled water does not lead to grain growth, with only their compaction to 0.71 relative density observed; however, the addition of 0.1 wt % CH_3COONH_4 and NaOH increases the average grain size when reaching similar relative densities (0.70 and 0.71, respectively). X-ray diffraction analysis showed that the cold sintering process does not lead to a change in the phase composition of the initial $(MnFeCoNiCu)_3O_4$ powder, confirming the preservation of the high-entropy structure.*

Keywords: *high-entropy ceramics, oxide ceramics, cold sintering process, sintering, phase composition*

For citation: Smirnov A.V., Ivakin Yu.D., Kornyushin M.V., Kholodkova A.A., Vasin A.A., Ayudinyan S., Kirakosyan H.V. Effect of activating additives on the cold sintering process of $(MnFeCoNiCu)_3O_4$ high-entropy ceramics. *Tonk. Khim. Tekhnol. = Fine Chem. Technol.* 2022;17(5):439–449 (Russ., Eng.). https://doi.org/10.32362/2410-6593-2022-17-5-439-449

НАУЧНАЯ СТАТЬЯ

Влияние активирующих добавок на процесс холодного спекания высокоэнтропийной керамики $(MnFeCoNiCu)_3O_4$

А.В. Смирнов[1,✉], Ю.Д. Ивакин[1,2], М.В. Корнюшин[1], А.А. Холодкова[1,2], А.А. Васин[1], С. Аюдинян[3], А.В. Киракосян[3]

[1]Инжиниринговый центр мобильных решений, МИРЭА – Российский технологический университет, Москва, 119454 Россия
[2]Химический факультет, Московский государственный университет им. М.В. Ломоносова, Москва, 119234 Россия
[3]Институт химической физики им. А.Б. Налбандяна, Ереван, 0014 Армения
[✉]Автор для переписки, e-mail: smirnov_av@mirea.ru

Аннотация

Цели. *Получение экспериментальных данных о влиянии вида активирующей добавки на процесс холодного спекания высокоэнтропийной керамики состава $(MnFeCoNiCu)_3O_4$. В качестве активирующих добавок были использованы: ацетат аммония (CH_3COONH_4), уксусная кислота (CH_3COOH), аммоний хлористый (NH_4Cl), калий фтористый 2-х водный $(KF{\cdot}2H_2O)$, литий фтористый (LiF), натрий фтористый (NaF), гидроксид натрия (NaOH).*
Методы. *Синтез исходного порошка методом низкотемпературного самораспространяющегося синтеза; исследование гранулометрического состава порошка методом лазерной дифракции; анализ формы частиц и микроструктуры скомпактированных образцов методом сканирующей электронной микроскопии; анализ фазового состава методом рентгенофазового анализа; консолидация образцов высокоэнтропийной керамики методом холодного спекания; плотность исходного порошка и относительная плотность образцов керамики холодного спекания определялись методом Архимеда.*
Результаты. *Образцы с относительной плотностью свыше 0.70 получены с применением дистиллированной воды, CH_3COONH_4 и NaOH в процессе холодного спекания при температуре 300°C, времени выдержки 30 мин и давлении прессования 315 МПа.*

Выводы. *Впервые экспериментально показано влияние вида активирующей добавки на относительную плотность образцов высокоэнтропийной керамики $(MnFeCoNiCu)_3O_4$, полученных с помощью процесса холодного спекания. Микроструктуры образцов имеют выраженные отличия: 20 мас. % дистиллированной воды не приводит к росту зерен, наблюдается только их уплотнение до 0.71 относительной плотности; при добавлении 0.1 мас. % CH_3COONH_4 и NaOH наблюдается рост среднего размера зерен при достижении близких показателей относительной плотности (0.70 и 0.71 соответственно). Рентгенодифракционный анализ показал, что процесс холодного спекания порошка $(MnFeCoNiCu)_3O_4$ не приводит к изменению фазового состава исходного порошка, что свидетельствует о сохранении высокоэнтропийной структуры.*

Ключевые слова: *высокоэнтропийная керамика, оксидная керамика, процесс холодного спекания, спекание, фазовый состав*

Для цитирования: Смирнов А.В., Ивакин Ю.Д., Корнюшин М.В., Холодкова А.А., Васин А.А., Аюдинян С., Киракосян А.В. Влияние активирующих добавок на процесс холодного спекания высокоэнтропийной керамики $(MnFeCoNiCu)_3O_4$. *Тонкие химические технологии*. 2022;17(5):439–449. https://doi.org/10.32362/2410-6593-2022-17-5-439-449

INTRODUCTION

High-entropy materials were first described in 2004 as innovative metallic disordered multicomponent alloys having promising applications [1]. The number of combinations of composition components that can be covered using this approach is almost limitless, and so far a very limited number of options have been explored. However, several high-entropy alloys have previously been shown to have exceptional mechanical and performance properties that are superior to conventional alloys [2]. Later, in 2015, entropy stabilization in a mixture of oxides was demonstrated, and the first samples of the so-called high-entropy ceramics were obtained. It has been shown that high-entropy ceramic systems have promising properties for a wide range of applications: thermal barrier coatings, thermoelectrics, catalysts, batteries, and wear-resistant coatings [3]. In recent years, several high-entropy oxide systems have been studied, such as ferrimagnetic $(CoCrFeMnNi)_3O_4$ [4, 5] and ferromagnetic $(CoCrFeMnZn)_3O_4$ and $(CoCrFeNiZn)_3O_4$ [6]; perovskites with rare earth elements ($La(CoCrFeMnNi)O_3$), which exhibit a complex magnetic state with a predominance of antiferromagnetic interactions [7]. It has been found that a high-entropy oxide ceramic material with a rock-salt type structure (MgCoNiCuZn)O exhibits long-range magnetic order despite the structural disorder of randomly distributed magnetic ions. It is assumed that similar magnetic properties can be realized in high-entropy oxide ceramic materials with different types of crystal lattice and different compositions of elements, in particular, in the $(MnFeCoNiCu)_3O_4$ system [8].

When studying the properties of the above-described promising high-entropy oxide ceramic materials, one of the main arising problems is how to preserve the high-entropy structure of the initial powder materials during their sintering. High sintering temperatures (usually more than 1000°C) lead to disruption of the high-entropy structure as a result of the phase transformations, evaporation and chemical reactions, as well as the decomposition of high-entropy phases [3]. For stable production of high-entropy ceramic samples, it is necessary to use consolidation methods at temperatures not exceeding the synthesis temperature of initial high-entropy ceramic powders, which are within the range of 350–750°C [3, 9].

The cold sintering process (CSP), an innovative ceramic sintering method that uses a liquid phase, compression-molding pressure and temperatures below 550°C, is under active study and development [10, 11]. It has been found that the participation in CSP of a liquid phase (most often water or aqueous solutions of acids and alkalis) can significantly reduce the sintering temperatures of oxide ceramic materials down to the range of 200–400°C and lower, in some cases even to room temperature [12]. In addition, some materials, such as ZnO, can be compacted to more than 90% of their theoretical density in less than 15 min at temperatures below 300°C [13]. The scheme of the CSP is shown in Fig. 1.

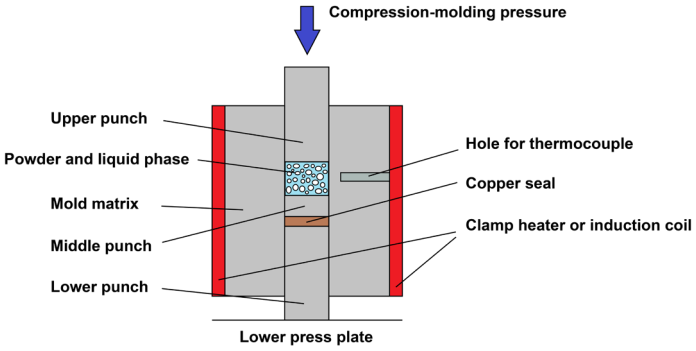

Fig. 1. Scheme of the cold sintering process.

The main CSP parameters are: pressing force; temperature in the mold; time of exposure under the action of a given pressure and temperature; activating additive type and concentration; liquid phase concentration; ceramic powder material properties (its solubility, particle size and granulometric composition (Fig. 2) [14]. These parameters are selected for each specific material experimentally. The mechanism or mechanisms of the CSP are under study. To date, three mechanisms of mass transfer in the CSP are proposed in the literature: dissolution–precipitation [11]; mass transfer due to surface diffusion in a layer with a high content of defects formed as a result of dissociative adsorption of water by oxide particles [13]; mass transfer due to surface spreading and coalescence of particles owing to the appearance of solid-phase mobility of the oxide structure as a result of the exchange of water molecules between the medium and the forms of water bound in the structure of oxide particles [15].

The choice of additives for CSP activation is based on theories concerning the process mechanism. These can be additives that increase the oxide particles solubility in an aqueous medium due to a change in pH. The addition of NaOH increases the aqueous solution pH, creating an alkaline environment. Acetic acid reduces the solution pH and promotes the dissolution of oxides in the acidic environment. When adsorbed on oxide particles, the acid proton increases the content of hydroxyl groups (bound forms of water in the structure of oxides) in them to increase structural mobility [16]. Ammonium acetate or ammonium chloride added to water also create an acidic environment due to hydrolysis when the temperature rises. In addition, studies on CSP have shown that the acetate ion is able to diffuse into the volume of oxide particles and exchange with the medium thus causing an increase in structural mobility [16, 17]. The addition of fluorides during hydrolysis leads to the formation of HF, which can increase the solubility of oxides also due to the formation of fluoride complexes [18]. Currently, there is an absence in the CSP literature of works about the effect of activating additives on the composition $(MnFeCoNiCu)_3O_4$, as well as a lack of works on high-entropy ceramics in general.

In [19], the fundamental possibility of obtaining samples of high-entropy ceramics $(MnFeCoNiCu)_3O_4$ by CSP using 20 wt % of distilled water as a liquid phase was experimentally shown for the first time. Ceramic samples with a porosity of 28–31% were obtained at 300°C, holding times of 3, 30, and 60 min and a compression-molding pressure of 315 MPa.

The purpose of this study is to obtain new experimental data on the effect of the activating additive type on the CSP of high-entropy ceramics $(MnFeCoNiCu)_3O_4$. The influence of the activating additive type was evaluated by the samples relative density. The densest samples were subjected to analysis of the microstructure and phase composition.

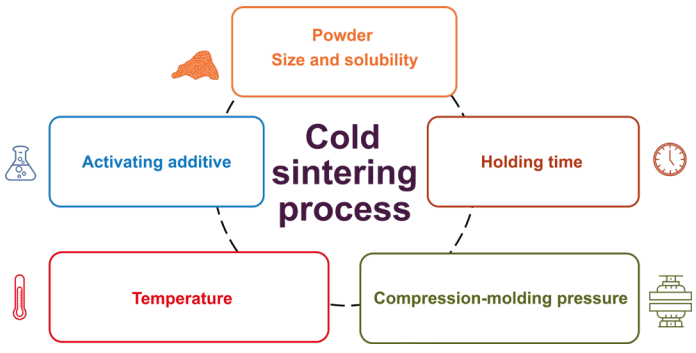

Fig. 2. Main parameters of the cold sintering process [14].

MATERIALS AND METHODS

The powder of high-entropy oxide ceramic material $(MnFeCoNiCu)_3O_4$ synthesized by low-temperature self-propagating synthesis (or bulk combustion) in air from an equimolar mixture of Mn, Fe, Co, Ni, and Cu metal nitrates was used as a starting material. To prepare a mixture of precursors, metal nitrate hydrates $(Me(NO_3)_n)$ (*Sigma-Aldrich*, USA) were dissolved together with organic fuel (citric acid) in own-made deionized water to obtain a saturated solution. The homogeneous mixture was poured into a quartz glass beaker and heated on an electric heater. After the evaporation of water, a viscous liquid (sol, then gel) was formed, which spontaneously

ignited at a temperature above 200°C (so-called bulk combustion accompanied by gas evolution and smoke). To monitor the reaction in various thermal conditions, we used measurements with a chromel-alumel thermocouple (*NPP "Etalon,"* Russia). The maximum synthesis temperature was about 450°C. After cooling, the synthesis product was removed from the beaker and ground in an agate mortar.

The CSP was carried out in a steel mold with induction heating (Fig. 3a). The mold assembly contained three punches: upper, middle and lower (11 mm in diameter). A mixture of $(MnFeCoNiCu)_3O_4$ powder with a liquid phase was located between the upper and middle punches, while a copper sealing ring was placed between the middle and lower punches (Fig. 3b). The seal was used to prevent the mixture from being squeezed out of the gaps in the mold during compression 0.4 g of $(MnFeCoNiCu)_3O_4$ powder and 0.08 mL of water (20 wt %) were mixed in a bowl under thorough stirring immediately before placing into the mold. The thermocouple was fixed in the mold in a cavity next to the sample. The mold with the induction heater was installed along the hydraulic press axis. The powder shrinkage in the mold was controlled by measuring the axial displacement of the hydraulic press lower platform by using a mechanical dial indicator (with a division value of 10 μm) (*VladPromash*, Russia) mounted on the hydraulic press frame.

The following modes of the cold baking process were used: baking temperature—250 and 300°C, time of heating to baking temperature—20 min, and holding time—30 min. The modes were chosen on the basis of the results of [19]. In all the experiments, the amount of the liquid phase was 20 wt %: distilled water or an aqueous solution of 0.1 wt % of an activating additive. The following substances were used as activating additives: ammonium acetate (CH_3COONH_4) (*Khimprom-M*, Russia), acetic acid (CH_3COOH) (*RKhZ "NORDIKS,"* Russia), ammonium chloride (NH_4Cl) (*Khimprom-M*, Russia), potassium fluoride dihydrate ($KF{\cdot}2H_2O$) (*RKhZ "Nordiks,"* Russia), lithium fluoride (LiF) (*Alfa Aesar*, USA), sodium fluoride (NaF) (*Alfa Aesar*, USA), and sodium hydroxide (NaOH) (*Alfa Aesar*, USA). All the reagents were of purissimum or analytical quality.

Characterization of the initial powder by particle size distribution was carried out using a laser particle size analyzer LS 13 320 MW (*Beckman Coulter*, USA). Before measuring the granulometric composition, the initial powder sample was deagglomerated by placing it in a glass tube with water and subjecting it to ultrasound in an ultrasonic bath at a power of 60 W. The density of the initial powder and the relative density of samples of cold-sintered ceramics were estimated according to the Archimedes method. The morphology of the initial powder and the microstructure of the ceramic samples were studied by scanning electron microscopy (SEM) using a JSM-6390 LA microscope (*JEO*, Tokyo, Japan). The average grain size of the ceramic samples was determined by the analysis of SEM images of the samples fractures. The diameter of samples with a distinct contour was measured. In the end, the results of the measurements contain both the sizes of rare particles and the sizes of their dense aggregates. Phase analysis of the synthesized powder and ground ceramic samples

(a) (b)

Fig. 3. (a) Steel mold with induction heater on hydraulic press; (b) mold parts.

of cold production was performed on an XRD-6000 X-ray diffractometer (*Shimadzu*, Kyoto, Japan) with CuKα radiation in the range of $10° \le 2\theta \le 70°$ at a step of $2\theta = 0.02°$. The samples diffraction patterns were compared with the data of PDF-2 database [20].

RESULTS AND DISCUSSION

A micrograph of the initial $(MnFeCoNiCu)_3O_4$ powder after synthesis is shown in Fig. 4. As typical for powders obtained by low-temperature self-propagating synthesis (bulk combustion), the powder consists of large particles of porous agglomerates. An analysis of the granulometric composition (Table 1) confirmed the presence of predominantly large agglomerates with a modal diameter d_M = 45.9 μm. After ultrasonic treatment, the average particle size decreased by about half, that is, the use of ultrasonics led to the destruction of a considerable amount of large agglomerates and aggregates. The pycnometric density of the powder as measured by the Archimedes method was 5.14 g/cm^3.

As a result of a series of CSP experiments of $(MnFeCoNiCu)_3O_4$ powder it was found that the relative density of samples ≥0.70 can only be achieved using distilled water or aqueous solutions of CH_3COONH_4 and NaOH (Table 2). When applying a compression-molding pressure of 315 MPa, a holding time of 30 min, a heating time of 20 min, and an additive concentration of 0.1 wt %, the highest relative density of the samples was consistently achieved at 300°C. The samples had sufficient transport strength for extraction from the mold, measurement of relative density by the Archimedes method, and subsequent measurements of electrical and magnetic properties. (The results of studies on the physical properties of samples of high-entropy ceramics will be presented in a separate publication.) It is possible that the process temperature could be reduced by increasing the concentration of effective activating additives (CH_3COONH_4 and NaOH) while maintaining relative density values above 0.70. However, under such experimental conditions, an increase in the CSP temperature is impossible due to the strong adhesion of the sample to punches at 350°C [19].

The densest CSP (Fig. 5) obtained using water and aqueous solutions of CH_3COONH_4 and NaOH, were studied by SEM and X-ray diffraction analysis. An analysis of the microstructures of samples (Fig. 6) obtained at different compositions of the liquid phase and identical CSP conditions indicates a noticeable effect of activating additives CH_3COONH_4 and NaOH. When using

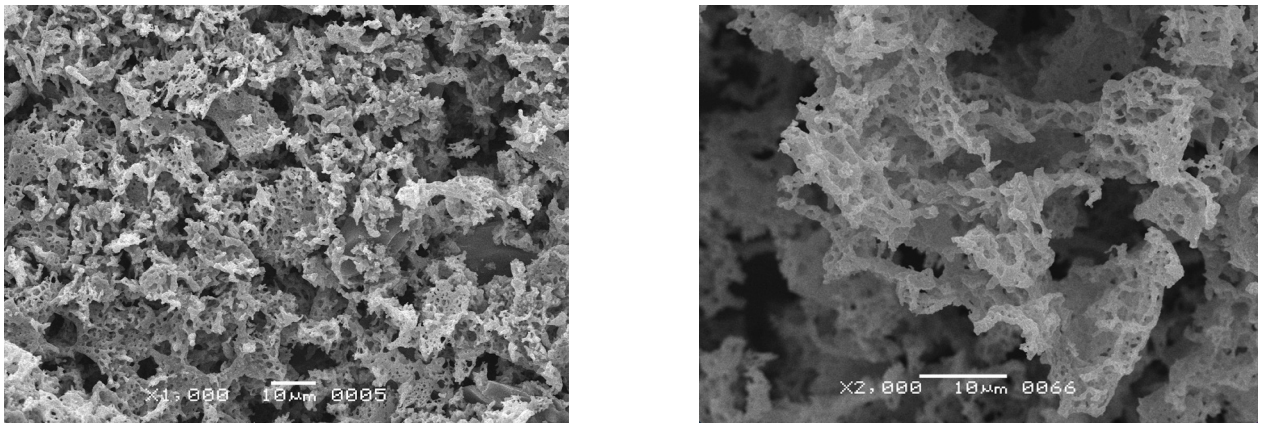

Fig. 4. SEM image of the $(MnFeCoNiCu)_3O_4$ powder.

Table 1. Results of the granulometric composition measurement for $(MnFeCoNiCu)_3O_4$ powder

No.	Conditions	d_M, μm	d_{10}, μm	d_{50}, μm	d_{90}, μm	S_{sp}, * cm^2/cm^3
1	Without ultrasonic treatment	45.9	8.9	32.0	73.8	3466
2	After ultrasonic treatment	20.4	6.0	18.1	36.4	5145

* S_{sp} is the specific surface area.

Table 2. Effect of activating additives on the relative density of cold-sintered samples

Activating additive	Temperature, °C	Cold sintering modes*	Relative density
H_2O	250	P = 315 MPa t = 30 min	0.69
	300		0.71
CH_3COONH_4	250		0.68
	300		0.70
CH_3COOH	250		0.65
	300		0.67
NH_4Cl	250		0.64
	300		0.65
$KF·2H_2$	250		0.54
	300		0.55
LiF	250		0.60
	300		0.59
NaF	250		0.63
	300		0.64
NaOH	250		0.70
	300		0.71

* P is the compression-molding pressure; t is the holding time.

distilled water, there is a change in the morphology of the initial powder particles, the formation of grains, their compaction, and a slight increase in size (Fig. 6a). It can be concluded that the presence of 20 wt % of distilled water and a mechanical pressure of 315 MPa are sufficient to initiate the CSP of a powder of the composition $(MnFeCoNiCu)_3O_4$ at a temperature of 300°C for 30 min. When adding 0.1 wt % CH_3COONH_4 (Fig. 6b) and NaOH (Fig. 6c), a pronounced grain growth is observed upon reaching close values of relative density (0.70 and 0.71, respectively). The CSP proceeds more intensively in an aqueous medium containing CH_3COONH_4 and NaOH. In the case of a powder of the composition $(MnFeCoNiCu)_3O_4$ these activating additives initiate the dissolution of the powder particles surface and/or increase

Fig. 5. Cold-sintered ceramic sample from $(MnFeCoNiCu)_3O_4$ powder, relative density 0.71 (temperature 300°C, 0.1 wt % of NaOH).

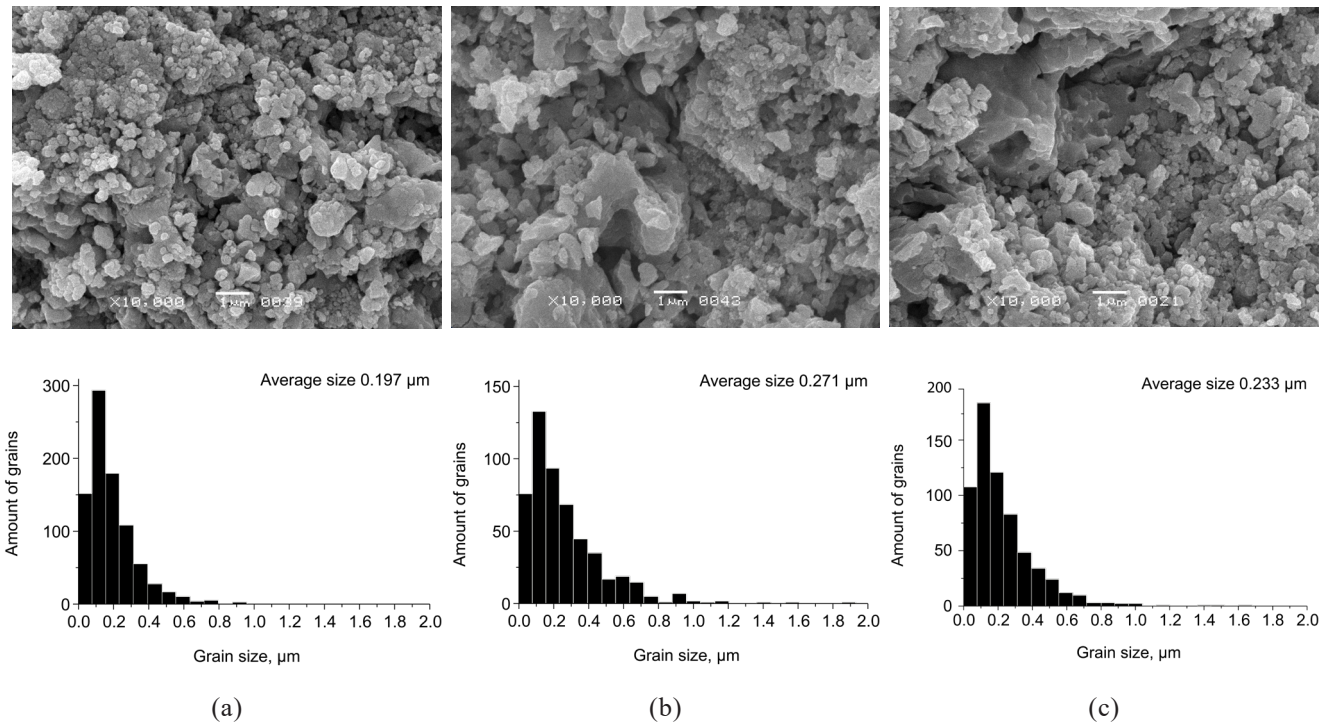

Fig. 6. Microstructure and particle size distribution histogram of cold-sintered $(MnFeCoNiCu)_3O_4$ ceramic samples obtained at different compositions of the liquid phase: (a) H_2O; (b) 0.1 wt % CH_3COONH_4; (c) 0.1 wt % NaOH. Temperature 300 °C, compression-molding pressure 315 MPa, dwell 30 min.

the number of defects in the surface layer of the particles of the powder material and, as a result, increase the solid-phase mobility of its crystal structure. For a detailed study of the effect of CH_3COONH_4 and NaOH on the microstructure and properties of high-entropy cold-sintering ceramics of the composition $(MnFeCoNiCu)_3O_4$, further studies of grain size distribution using SEM image analysis, characterization of the electrical and magnetic properties of samples depending on the activating additive concentration and process modes are planned.

Figure 7 shows the results of X-ray diffraction analysis of the phase composition of the initial powder (Fig. 7a) and cold sintering samples (Figs. 7b–7d). All diffraction patterns have identical reflection patterns corresponding to the phase with the spinel structure and additional reflections indicating the presence of a second phase with the rock salt structure. The presence of two phases distinguishes the high-entropy oxide ceramic $(MnFeCoNiCu)_3O_4$ studied in this work from the material of similar chemical composition described in [21], but having only one phase with a spinel structure. This fact is of considerable interest, since the properties of one- and two-phase high-entropy ceramics $(MnFeCoNiCu)_3O_4$ can vary significantly. In general, it can be stated that

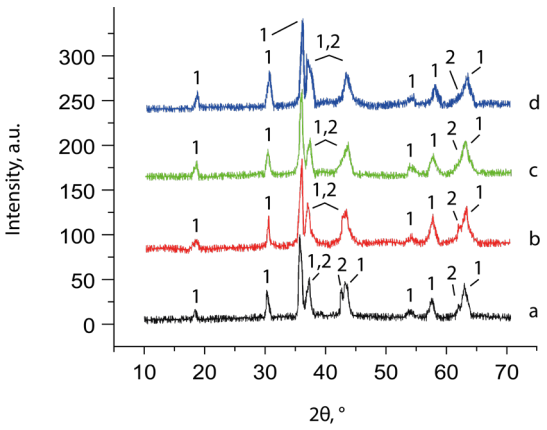

Fig. 7. XRD patterns of:
(a) initial powder $(MnFeCoNiCu)_3O_4$;
(b) cold-sintered sample, 0.1 wt % of NaOH;
(c) cold-sintered sample, 0.1 wt % of CH_3COONH_4;
(d) cold-sintered sample, H_2O.
Phase types indicated: 1—spinel; 2—rock salt. Temperature 300°C, compression-molding pressure 315 MPa, dwell 30 min.

the CSP of $(MnFeCoNiCu)_3O_4$ powder at 300°C using an aqueous medium with the addition of 0.1 wt % of CH_3COONH_4 and NaOH does not lead to a change in the initial powder phase composition. This indicates that the high-entropy structure has been preserved.

CONCLUSIONS

For the first time, the influence of the activating additive type on the relative density of samples of high-entropy ceramics $(MnFeCoNiCu)_3O_4$ obtained by the CSP is shown experimentally. Ceramic samples with a relative density of 0.70–0.71 were obtained using 20 wt % of distilled water or an aqueous solution of 0.1 wt % of CH_3COONH_4 or NaOH as a liquid medium. Samples of high-entropy ceramic material were obtained at a temperature of 300°C, a holding time of 30 min, and a compression-molding pressure of 315 MPa. The microstructures of the samples have pronounced differences: 20 wt % of distilled water does not lead to a pronounced growth of grains, only their compaction to 0.71 relative density is observed. When adding 0.1 wt % of CH_3COONH_4 and NaOH, a noticeable grain growth is observed upon reaching close values of relative density (0.70 and 0.71, respectively). For a more detailed study of this effect, further studies on the grain size distribution and physical properties of samples depending on the activating additive concentration and process modes are necessary. X-ray diffraction analysis showed that the CSP of $(MnFeCoNiCu)_3O_4$ powder at a temperature of 300°C and using an aqueous medium with the addition of 0.1 wt % of CH_3COONH_4 and NaOH does not lead to a change in the phase composition of the initial powder, which indicates the preservation of the high entropy structure.

Acknowledgments

The study was supported by the Ministry of Science and Higher Education of the Russian Federation, Agreement No. 075-15-2021-974 of September 28, 2021. The applied research was conducted on the topic of "Development of technological methods for reducing the sintering temperature of high-entropy ceramic materials based on transition metal oxides." The work was carried out with the use of equipment of the Joint Educational and Scientific Center for Collective Use at the MIREA – Russian Technological University and the Center for Collective Use "High-Tech Technologies of Mechanical Engineering" at the Moscow Polytechnic University.

Also, the work was supported by the Science Committee of the Ministry of Education, Science, Culture and Sports of the Republic of Armenia, the research project No. 20TTWS-2F040.

Authors' contributions

A.V. Smirnov – research conceptualization and writing the text of the article;

Yu.D. Ivakin – research conceptualization, selection of activating additives, microstructure analysis, and editing the text of the article;

M.V. Kornyushin – conducting research and data curation;

A.A. Kholodkova – analysis of X-ray diffractograms and editing the text of the article;

A.A. Vasin – visualization and editing the text of the article;

S. Aydinyan – initial powder synthesis and editing the text of the article;

A.V. Kirakosyan – initial powder synthesis and editing the text of the article.

The authors declare no conflict of interest.

REFERENCES

1. Yeh J.-W., Chen S.-K., Lin S.-J., Gan J.-Y., Chin T.-S., Shun T.-T., *et al*. Nanostructured High-Entropy Alloys with Multiple Principal Elements: Novel Alloy Design Concepts and Outcomes. *Adv. Eng. Mater.* 2004;6(5):299–303. https://doi.org/10.1002/adem.200300567

2. George E.P., Raabe D., Ritchie R.O. High-entropy alloys. *Nat. Rev. Mater*. 2019;4(8):515–34. https://doi.org/10.1038/s41578-019-0121-4

3. Oses C., Toher C., Curtarolo S. High-entropy ceramics. *Nat. Rev. Mater*. 2020;5(4):295–309. https://doi.org/10.1038/s41578-019-0170-8

4. Dąbrowa J., Stygar M., Mikuła A., Knapik A., Mroczka K., Tejchman W., *et al*. Synthesis and microstructure of the $(Co,Cr,Fe,Mn,Ni)_3O_4$ high entropy oxide characterized by spinel structure. *Mater. Lett*. 2018;216:32–6. https://doi.org/10.1016/j.matlet.2017.12.148

5. Mao A., Quan F., Xiang H.-Z., Zhang Z.-G., Kuramoto K., Xia A.-L. Facile synthesis and ferrimagnetic property of spinel $(CoCrFeMnNi)_3O_4$ high-entropy oxide nanocrystalline powder. *J. Mol. Struct*. 2019;1194:11–18. https://doi.org/10.1016/j.molstruc.2019.05.073

6. Mao A., Xiang H.-Z., Zhang Z.-G., Kuramoto K., Zhang H., Jia Y. A new class of spinel high-entropy oxides with controllable magnetic properties. *J. Magn. Magn. Mater*. 2020;497:165884. https://doi.org/10.1016/j.jmmm.2019.165884

7. Witte R., Sarkar A., Kruk R., Eggert B., Brand R.A., Wende H., *et al*. High-entropy oxides: An emerging prospect for magnetic rare-earth transition metal perovskites. *Phys. Rev. Mater*. 201913;3(3):034406. https://doi.org/10.1103/PhysRevMaterials.3.034406

8. Jimenez-Segura M.P., Takayama T., Bérardan D., Hoser A., Reehuis M., Takagi H., *et al*. Long-range magnetic ordering in rocksalt-type high-entropy oxides. *Appl. Phys. Lett*. 2019;114(12):122401. https://doi.org/10.1063/1.5091787

9. Dai S., Li M., Wang X., Zhu H., Zhao Y., Wu Z. Fabrication and magnetic property of novel $(Co,Zn,Fe,Mn,Ni)_3O_4$ high-entropy spinel oxide. *J. Magn. Magn. Mater*. 2021;536:168123. https://doi.org/10.1016/j.jmmm.2021.168123

10. Bordia R.K., Kang S.L., Olevsky E.A. Current understanding and future research directions at the onset of the next century of sintering science and technology. *J. Am. Ceram. Soc*. 2017;100(6):2314–2352. https://doi.org/10.1111/jace.14919

11. Guo J., Floyd R., Lowum S., Maria J.-P., Herisson de Beauvoir T., Seo J.-H., Randall C.A. Cold Sintering: Progress, Challenges, and Future Opportunities. *Annu. Rev. Mater. Res*. 2019;49(1):275–295. https://doi.org/10.1146/annurev-matsci-070218-010041

12. Maria J.-P., Kang X., Floyd R.D., Dickey E.C., Guo H., Guo J., *et al*. Cold sintering: Current status and prospects. *J. Mater. Res*. 2017;32(17):3205–3218. https://doi.org/10.1557/jmr.2017.262

13. Gonzalez-Julian J., Neuhaus K., Bernemann M., Pereira da Silva J., Laptev A., Bram M., *et al*. Unveiling the mechanisms of cold sintering of ZnO at 250 °C by varying applied stress and characterizing grain boundaries by Kelvin Probe Force Microscopy. *Acta Mater*. 2018;144(1):116–128. https://doi.org/10.1016/j.actamat.2017.10.055

14. Galotta A., Sglavo V.M. The cold sintering process: A review on processing features, densification mechanisms and perspectives. *J. Eur. Ceram. Soc*. 2021;41(16):1–17. https://doi.org/10.1016/j.jeurceramsoc.2021.09.024

15. Ivakin Y., Smirnov A., Kholodkova A., Vasin A., Kormilicin M., Kornyushin M., *et al*. Comparative Study of Cold Sintering Process and Autoclave Thermo-Vapor Treatment on a ZnO Sample. *Crystals*. 2021;11(1):71. https://doi.org/10.3390/cryst11010071

16. Ivakin Yu.D., Smirnov A.V., Kormilitsin M.N., Kholodkova A.A., Vasin A.A., Kornyushin M.V., Tarasovskii V.P., Rybal'chenko V.V. Effect of Mechanical Pressure on the Recrystallization of Zinc Oxide in a Water Fluid Medium under Cold Sintering. *Russ. J. Phys. Chem. B.* 2021;15(8):1228–1250. https://doi.org/10.1134/S1990793121080054

17. Ivakin Y.D., Smirnov A.V., Kurmysheva A.Yu., Kharlanov A.N., Solís Pinargote N.W., Smirnov A., *et al*. The Role of the Activator Additives Introduction Method in the Cold Sintering Process of ZnO Ceramics: CSP/SPS Approach. *Materials.* 2021;14(21):6680. https://doi.org/10.3390/ma14216680

18. Nakajima T., Žemva B., Tressaud A. *Advanced Inorganic Fluorides: Synthesis, Characterization and Applications*. Elsevier; 2000. 701 p. https://doi.org/10.1016/B978-0-444-72002-3.X5000-5

19. Smirnov A.V., *et al*. The Cold Sintering Process of High-Entropy Ceramics $(MnFeCoNiCu)_3O_4$. *Int. J. Mech. Eng*. 2021;6(3):1–6.

20. Gates-Rector S., Blanton T. The Powder Diffraction File: A Quality Materials Characterization Database. *Powder Diffr*. 2019;34(4):352–360. https://doi.org/10.1017/S0885715619000812

21. Wang D., Liu Z., Du S., Zhang Y., Li H., Xiao Z., *et al*. Low-temperature synthesis of small-sized high-entropy oxides for water oxidation. *J. Mater. Chem. A.* 2019;7(42):24211–24216. https://doi.org/10.1039/C9TA08740K

About the authors:

Andrey V. Smirnov, Cand. Sci. (Eng.), Head of the Department of Advanced Materials Technologies of the Mobile Solutions Engineering Center, MIREA – Russian Technological University (78, Vernadskogo pr., Moscow, 119454, Russia). E-mail: smirnov_av@mirea.ru. ResearcherID J-2763-2017, Scopus Author ID 56970389000, RSCI SPIN-code 2919-9250, https://orcid.org/0000-0002-4415-5747

Yuri D. Ivakin, Cand. Sci. (Chem.), Senior Researcher, Department of Physical Chemistry, Faculty of Chemistry, Lomonosov Moscow State University (1-3, Kolmogorova ul., Moscow, 119234, Russia). E-mail: yu.ivakin@mail.ru. ResearcherID N-9483-2013, Scopus Author ID 6603058433, RSCI SPIN-code 7337-4173, https://orcid.org/0000-0002-8416-3071

Maxim V. Kornyushin, Engineer, Laboratory of Ceramic and Composite Materials of the Mobile Solutions Engineering Center, MIREA – Russian Technological University (78, Vernadskogo pr., Moscow, 119454, Russia). E-mail: kornyushin@mirea.ru. Scopus Author ID 57219230569, RSCI SPIN-code 7995-3408, https://orcid.org/0000-0001-6104-7716

Anastasia A. Kholodkova, Cand. Sci. (Chem.), Junior Researcher, Department of Physical Chemistry, Faculty of Chemistry, Lomonosov Moscow State University (1-3, Kolmogorova ul., Moscow, 119234, Russia). E-mail: anakholo@gmail.com. ResearcherID M-2169-2016, Scopus Author ID 56530861400, RSCI SPIN-code 7256-7784, https://orcid.org/0000-0002-9627-2355

Alexander A. Vasin, Cand. Sci. (Eng.), Leading Researcher, Laboratory of Ceramic and Composite Materials of the Engineering Center for Mobile Solutions, MIREA – Russian Technological University (78, Vernadskogo pr., Moscow, 119454, Russia). E-mail: alexandrvasin123@gmail.com. ResearcherID K-3214-2015, Scopus Author ID 57211840246, RSCI SPIN-code 3864-9132, https://orcid.org/0000-0002-9501-2316

Sofia Aydinyan, Cand. Sci. (Chem.), Senior Researcher, A.B. Nalbandyan Institute of Chemical Physics (5/2, P. Sevak ul., Yerevan, 0014, Armenia). E-mail: sofiyaaydinyan25@gmail.com. Scopus Author ID 24479551800, https://orcid.org/0000-0001-6530-6308

Hasmik V. Kirakosyan, Cand. Sci. (Chem.), Junior Researcher, A.B. Nalbandyan Institute of Chemical Physics (5/2, P. Sevak ul., Yerevan, 0014, Armenia). E-mail: hasmik-kirakosyan@list.ru. Scopus Author ID 56925595700, https://orcid.org/0000-0003-1103-7952

Об авторах:

Смирнов Андрей Владимирович, к.т.н., заведующий отделением технологий перспективных материалов Инжинирингового центра мобильных решений, ФГБОУ ВО «МИРЭА – Российский технологический университет» (119454, Россия, Москва, пр-т Вернадского, д. 78). E-mail: smirnov_av@mirea.ru. ResearcherID J-2763-2017, Scopus Author ID 56970389000, SPIN-код РИНЦ 2919-9250, https://orcid.org/0000-0002-4415-5747

Ивакин Юрий Дмитриевич, к.х.н., старший научный сотрудник кафедры физической химии, Химический факультет, ФГБОУ ВО «Московский государственный университет им. М.В. Ломоносова» (119234, Россия, Москва, ул. Колмогорова, 1, стр. 3). E-mail: yu.ivakin@mail.ru. ResearcherID N-9483-2013, Scopus Author ID 6603058433, SPIN-код РИНЦ 7337-4173, https://orcid.org/0000-0002-8416-3071

Корнюшин Максим Витальевич, инженер лаборатории керамических и композиционных материалов Инжинирингового центра мобильных решений, ФГБОУ ВО «МИРЭА – Российский технологический университет» (119454, Россия, Москва, пр-т Вернадского, д. 78). E-mail: kornyushin@mirea.ru. Scopus Author ID 57219230569, SPIN-код РИНЦ 7995-3408, https://orcid.org/0000-0001-6104-7716

Холодкова Анастасия Андреевна, к.х.н., младший научный сотрудник кафедры физической химии, Химический факультет, ФГБОУ ВО «Московский государственный университет им. М.В. Ломоносова» (119234, Россия, Москва, ул. Колмогорова, 1, стр. 3). E-mail: anakholo@gmail.com. ResearcherID M-2169-2016, Scopus Author ID 56530861400, SPIN-код РИНЦ 7256-7784, https://orcid.org/0000-0002-9627-2355

Васин Александр Александрович, к.т.н., ведущий научный сотрудник лаборатории керамических и композиционных материалов Инжинирингового центра мобильных решений, ФГБОУ ВО «МИРЭА – Российский технологический университет» (119454, Россия, Москва, пр-т Вернадского, д. 78). E-mail: alexandrvasin123@gmail.com. Researcher ID K-3214-2015, Scopus Author ID 57211840246, SPIN-код РИНЦ 3864-9132, https://orcid.org/0000-0002-9501-2316

София Айдинян, к.х.н., старший научный сотрудник, Институт химической физики им. А.Б. Налбандяна (0014, Армения, Ереван, ул. П. Севака, д. 5/2). E-mail: sofiyaaydinyan25@gmail.com. Scopus Author ID 24479551800, https://orcid.org/0000-0001-6530-6308

Асмик В. Киракосян, к.х.н., младший научный сотрудник, Институт химической физики им. А.Б. Налбандяна (0014, Армения, Ереван, ул. П. Севака, д. 5/2). E-mail: hasmik-kirakosyan@list.ru. Scopus Author ID 56925595700, https://orcid.org/0000-0003-1103-7952

The article was submitted: April 19, 2022; approved after reviewing: July 08, 2022; accepted for publication: September 16, 2022.

Translated from Russian into English by M. Povorin
Edited for English language and spelling by Thomas Beavitt

ERRATUM

ИСПРАВЛЕНИЯ

ISSN 2686-7575 (Online)

https://doi.org/10.32362/2410-6593-2022-17-5-450-451

Erratum to the article: “Bifunctional gallium cation chelators”

Anna G. Polivanova, Inna N. Solovieva, Dmitrii O. Botev, Danil Y. Yuriev, Alyona N. Mylnikova, Maxim S. Oshchepkov

Tonkie Khimicheskie Tekhnologii = Fine Chemical Technologies. 2022;17(2):107–130 (Russ., Eng.).

Page 126, in ***Acknowledgments*** instead of

Acknowledgments

The presented work was supported by the Ministry of Science and Higher Education of the Russian Federation within the framework of the state task (project FSSM-2020-0004) “Development of the basics for obtaining and studying the interaction with the body of new multifunctional nanosized macromolecular systems for the targeted delivery of drugs, diagnostics and radiopharmaceuticals to combat the main socially significant diseases, including theranostics.

should read:

Acknowledgments

The presented work was supported by the Ministry of Science and Higher Education of the Russian Federation within the framework of the state task (project FSSM-2020-0004) “Development of the basics for obtaining and studying the interaction with the body of new multifunctional nanosized macromolecular systems for the targeted delivery of drugs, diagnostics and radiopharmaceuticals to combat the main socially significant diseases, including theranostics. The authors are grateful to M.I. Semchukova and G.A. Antonov for their help in preparing the materials of the article.

The original article can be found under https://doi.org/10.32362/2410-6593-2022-17-2-107-130

Исправление к статье «Бифункциональные хелаторы к катиону галлия»

А.Г. Поливанова, И.Н. Соловьёва, Д.О. Ботев, Д.Ю. Юрьев, А.Н. Мыльникова, М.С. Ощепков

Тонкие химические технологии = Fine Chemical Technologies. 2022;17(2):107–130 (Russ., Eng.).

На странице 126 в разделе ***Благодарности*** вместо

Благодарности

Представленная работа поддержана Министерством науки и высшего образования Российской Федерации в рамках государственного задания (проект FSSM-2020-0004) «Разработка основ получения и изучение взаимодействия с организмом новых мультифункциональных наноразмерных макромолекулярных систем адресной доставки лекарственных веществ, диагностических и радиофармпрепаратов для борьбы с основными социально значимыми заболеваниями, в том числе методами тераностики».

Acknowledgments

The presented work was supported by the Ministry of Science and Higher Education of the Russian Federation within the framework of the state task (project FSSM-2020-0004) “Development of the basics for obtaining and studying the interaction with the body of new multifunctional nanosized macromolecular systems for the targeted delivery of drugs, diagnostics and radiopharmaceuticals to combat the main socially significant diseases, including theranostics.

следует читать:

Благодарности

Представленная работа поддержана Министерством науки и высшего образования Российской Федерации в рамках государственного задания (проект FSSM-2020-0004) «Разработка основ получения и изучение взаимодействия с организмом новых мультифункциональных наноразмерных макромолекулярных систем адресной доставки лекарственных веществ, диагностических и радиофармпрепаратов для борьбы с основными социально значимыми заболеваниями, в том числе методами тераностики». Авторский коллектив выражает благодарность Семчуковой М.И. и Антонову Г.А. за помощь в подготовке материалов статьи.

Acknowledgments

The presented work was supported by the Ministry of Science and Higher Education of the Russian Federation within the framework of the state task (project FSSM-2020-0004) “Development of the basics for obtaining and studying the interaction with the body of new multifunctional nanosized macromolecular systems for the targeted delivery of drugs, diagnostics and radiopharmaceuticals to combat the main socially significant diseases, including theranostics. The authors are grateful to M.I. Semchukova and G.A. Antonov for their help in preparing the materials of the article.

Оригинальная статья может быть найдена https://doi.org/10.32362/2410-6593-2022-17-2-107-130

MIREA – Russian Technological University
78, Vernadskogo pr., Moscow, 119454, Russian Federation.
Publication date *October 31, 2022.*
Not for sale

МИРЭА – Российский технологический университет
119454, РФ, Москва, пр-т Вернадского, д. 78.
Дата опубликования *31.10.2022.*
Не для продажи

www.finechem-mirea.ru